1982

Coherence studies of geomagnetic fluctuations in the frequency range .05 to 10 Hz.

Fisher, Joseph Timothy.

Monterey, California. Naval Postgraduate School

http://hdl.handle.net/10945/20094

NAVAL POSTGRADUATE SCHOOL
Monterey, California

THESIS

COHERENCE STUDIES OF GEOMAGNETIC FLUCTUATIONS IN THE FREQUENCY RANGE .05 TO 10 HZ

by

Joseph Timothy Fisher

December 1982

Thesis Advisor: Otto Heinz

Approved for public release; distribution unlimited

SECURITY CLASSIFICATION OF THIS PAGE (When Data Entered)

REPORT DOCUMENTATION PAGE		READ INSTRUCTIONS BEFORE COMPLETING FORM
1. REPORT NUMBER	2. GOVT ACCESSION NO.	3. RECIPIENT'S CATALOG NUMBER
4. TITLE (and Subtitle) Coherence Studies of Goemagnetic Fluctuations in the Frequency Range .05 to 10 Hz		5. TYPE OF REPORT & PERIOD COVERED Master's Thesis December 1982
		6. PERFORMING ORG. REPORT NUMBER
7. AUTHOR(s) Joseph Timothy Fisher		8. CONTRACT OR GRANT NUMBER(s)
9. PERFORMING ORGANIZATION NAME AND ADDRESS Naval Postgraduate School Monterey, California 93940		10. PROGRAM ELEMENT, PROJECT, TASK AREA & WORK UNIT NUMBERS
11. CONTROLLING OFFICE NAME AND ADDRESS Naval Postgraduate School Monterey, California 93940		12. REPORT DATE December 1982
		13. NUMBER OF PAGES 170
14. MONITORING AGENCY NAME & ADDRESS (if different from Controlling Office)		15. SECURITY CLASS. (of this report)
		15a. DECLASSIFICATION/DOWNGRADING SCHEDULE
16. DISTRIBUTION STATEMENT (of this Report) Approved for public release; distribution unlimited		
17. DISTRIBUTION STATEMENT (of the abstract entered in Block 20, if different from Report)		
18. SUPPLEMENTARY NOTES		
19. KEY WORDS (Continue on reverse side if necessary and identify by block number) Coherence Geomagnetic Fluctuations		
20. ABSTRACT (Continue on reverse side if necessary and identify by block number) Fluctuations in the horizontal component of the earth's magnetic field were measured at a land site (La Mesa) and on the floor of Monterey Bay at a depth of 70 meters. The measurements span a 19-hour period (August 17/18, 1982). Assuming a circular polarization basis set, analysis was conducted to determine the coherence between the two sites in the frequency range .05-10 Hz. Preliminary analysis		

DD FORM 1 JAN 73 1473 EDITION OF 1 NOV 65 IS OBSOLETE
S/N 0102-014-6601

SECURITY CLASSIFICATION OF THIS PAGE (When Data Entered)

indicates a high degree of coherence from .05-.4 Hz. Also, a study of the polarization of the micropulsation field at each site was conducted in terms of Stokes parameters.

Coherence Studies of Geomagnetic Fluctuations in the Frequency Range .05 to 10Hz

by

Joseph Timothy Fisher
Lieutenant Commander, United States Navy
B.A., University of South Florida, 1972

Submitted in partial fulfillment of the
requirements for the degree of

MASTER OF SCIENCE IN PHYSICS

from the

NAVAL POSTGRADUATE SCHOOL
December 1982

ABSTRACT

Fluctuations in the horizontal component of the earth's magnetic field were measured at a land site (La Mesa) and on the floor of Monterey Bay at a depth of 70 meters. The measurements span a 19-hour period (August 17/18, 1982). Assuming a circular polarization basis set, analysis was conducted to determine the coherence between the two sites in the frequency range .05-10 Hz. Preliminary analysis indicates a high degree of coherence from .05-.4 Hz. Also, a study of the polarization of the micropulsation field at each site was conducted in terms of Stokes parameters.

TABLE OF CONTENTS

LIST OF FIGURES

ACKNOWLEDGMENTS

Special thanks to Dr. Otto Heinz for his patience and faith and to Dr. Michael Thomas for his assistance. Appreciation to Mr. Roger Hilleary and Mr. Edwin Donnellan of the W. R. Church Computer Center for their time and expert help.

I. INTRODUCTION

This thesis research is part of an ongoing effort being conducted by the Naval Postgraduate School to obtain a long-term data base of ELF electromagnetic noise on the ocean floor. The result of this project should be a better understanding and interpretation of that noise and its sources.

Magnetic noise is important to the geophysicist and to the Navy. Magnetic techniques are applied in exploration for minerals, the prediction of communications propagation and to the modeling of the sphere on which we live. Geomagnetic studies are of interest to the Navy for their application to submarine detection, submarine communications and to mine warfare.

The objective of this thesis within the broader context of the overall project was to design and validate a computer code that would facilitate data manipulation and analysis. To that end, the present computer code calculates for two sites (one on the ocean floor, the other on land), the individual site's power spectral densities and Stokes parameters 0, 1, 2 and 3 for two of the individual site's orthogonal components in the horizontal plane. The code also computes the coherence of these two orthogonal components and their phase difference. Lastly, the program computes the right and left circular polarization power

spectral densities of the sites and the coherence between the seafloor and land-based sites.

As discussed, the present code applies only to two sites and two orthogonal geomagnetic components at each site. However, extension to several sites and/or components should be an easy undertaking due to the style of the present program.

II. BACKGROUND

A. THE MAIN GEOMAGNETIC FIELD

Historical observation and modern measurement demonstrate that the principal source of the geomagnetic field (approximately 50,000 nanoteslas) is beneath the surface of the earth. An easy-to-picture causal interpretation of this phenomenon is painted by imagining the earth with a dipole magnet near its center as pictured in Figure 2.1. The magnet axis is tilted at an angle of 11.5 degrees from the earth's rotation axis. This model provides a prediction accuracy to a few percent of the measured geomagnetic field. Figures accurate to less than one percent of the earth's measured field can be obtained using more sophisticated models [Ref. 1].

The generally accepted physical process for the generation of the geomagnetic field is that of the self-sustaining dynamo [Ref. 2]. Figure 2.2 presents a simple picture of such a dynamo. The physical requirements of this theory are mostly met in the interior of the earth. For example, the earth's center is a large conducting system. Additionally, we can assume that the earth's molten core is of a differential rotational nature with turbulent upwelling.

Energy sources for such a dynamo are most likely available in the earth's core due to a number of processes. This

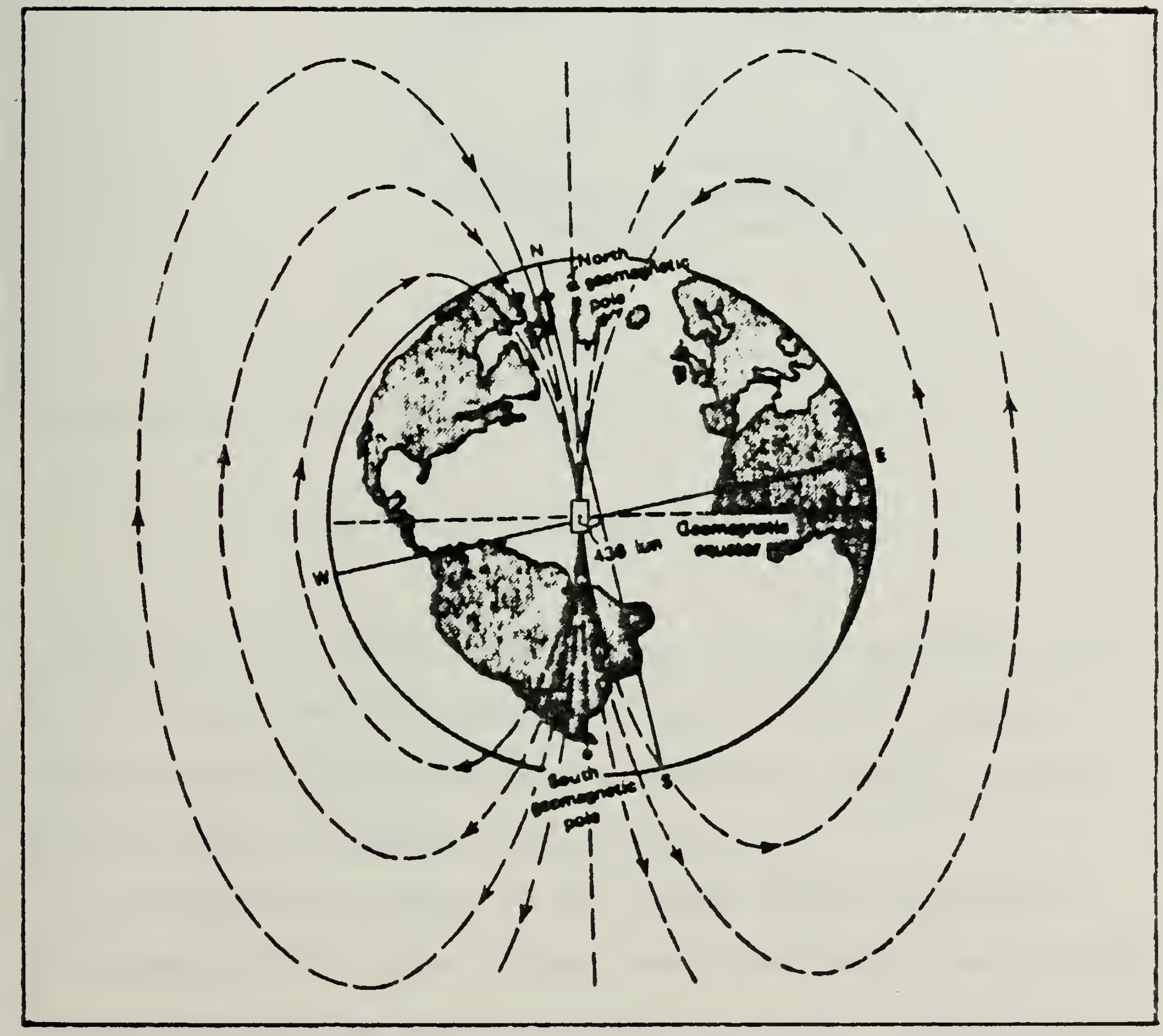

Figure 2.1 Eccentric Dipole Model of Geomagnetic Field

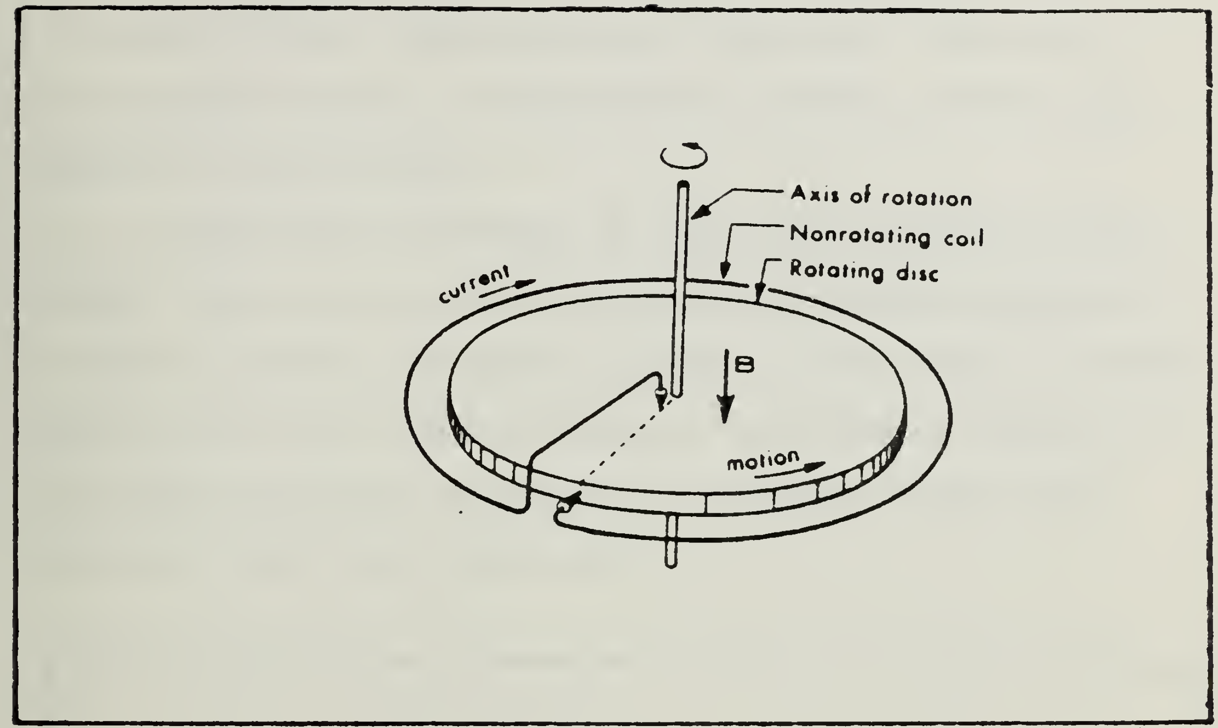

Figure 2.2 Simple Disk Dynamo

all boils down to mean that the motion of a conductor, such as the earth's molten core, in a magnetic field produces a current which in turn produces a magnetic field in support of the original magnetic field [Ref. 3].

A simplified picture of the dynamo theory originates by assuming that in the distant past a magnetic "seed" field was captured by the earth's conductive core. The differential rotation of this core "winds up" the field into an intense azimuthal field, such as would happen to a twisted rubber band. Turbulent upwelling of the core tends to

carry this azimuthal field outward, converting it to a toroidal helical field within an associated azimuthal circulating current. This current in turn generates the earth's dipolar field.

An additional advantage of the self-sustaining dynamo theory lies in its ability to explain the well-documented reversals of the geomagnetic field. It has been postulated that two or more coupled "dynamos" as shown in Figure 2.3 can cause reversals of the main geomagnetic field over geologic time scales [Ref. 4].

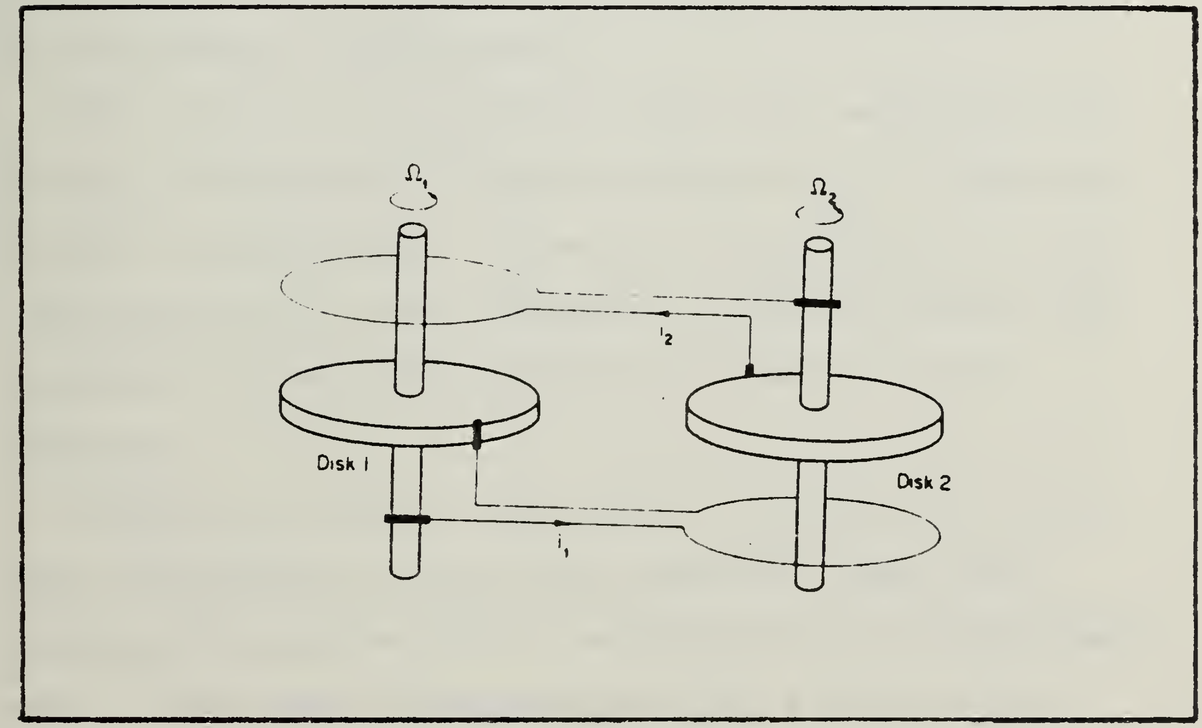

Figure 2.3 Twin Disk Dynamo

B. GEOMAGNETIC FLUCTUATIONS

The geomagnetic field changes with time. The changes in the field have periods ranging from fractions of seconds to thousands of years. The very slow variations (periods of years or more) are not of interest here but are known as secular variations and are thought to be geologic in origin.

The geomagnetic field changes of interest here are those fluctuations that occur over the period of a day or less. It is customary to view the magnetic field as the stable main field with these comparatively rapid fluctuations superimposed on it. Figure 2.4 presents the spectrum of the superimposed fluctuations.

The fluctuations (Figure 2.4) that are superimposed on the main field range in intensity from .05 to 50 nanoteslas and have various causes. Some major contributors to these fluctuations are in the ionospheric currents overhead and in magnetic storms which probably originate in solar eruptions.

Finally, arriving at the point of interest here, are those disturbances to the earth's magnetic field that propagate through the earth's magnetosphere as hydrodynamic waves. These small perturbations cover a wide range in amplitude and duration and are known as micropulsations. Figure 2.5 presents a graphical display of these disturbances. Micropulsations are thought to be the result of fluctuations

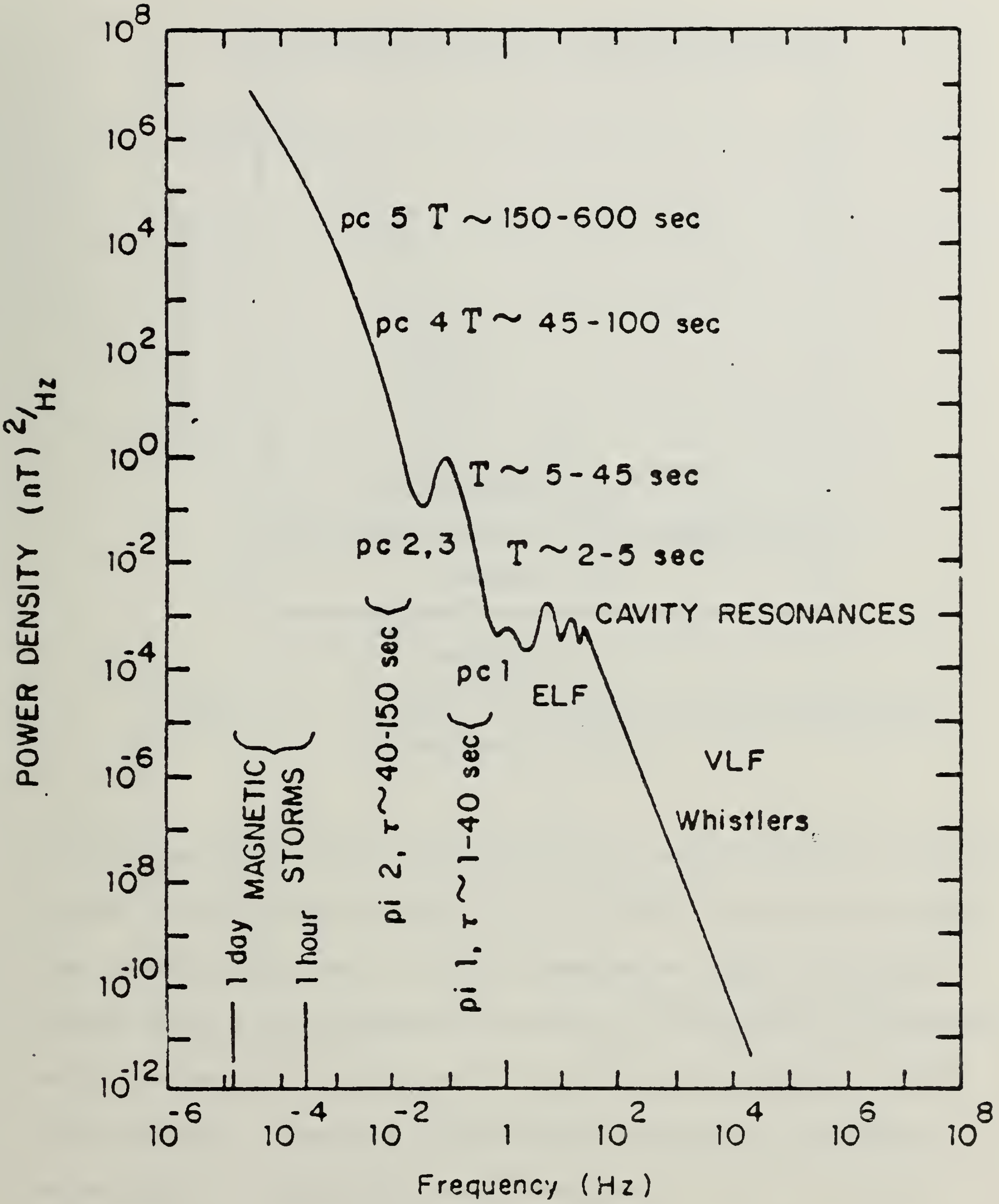

Figure 2.4 Power Spectrum of Geomagnetic Disturbances Observed on the Surface of the Earth.

[Claudis, Davidson, and Newkirk, 1971]

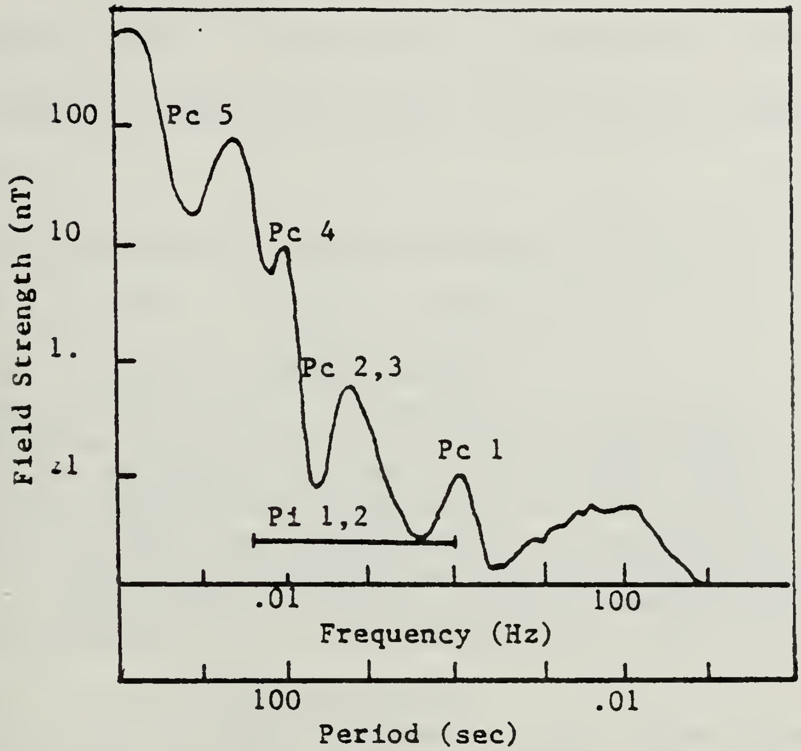

Figure 2.5 Field Strength of Micropulsations [Campbell, 1966]

in the incident solar wind affecting wave-particle interaction in the magnetosphere [Ref. 5]. As they propagate through the conductive layers of the atmosphere, they are transformed into electromagnetic waves via ionospheric currents, which we detect at the earth's surface as magnetic field fluctuations. There are two major categories of micropulsations: continuous and irregular.

Smoothly varying, periodic pulsations are classified as (Pc) micropulsations. Their distinct periodicity is indicative of a resonance inside the magnetospheric cavity. One model proposed to explain this occurrence of smooth, periodic

pulses is that the resonance is a result of an oscillatory hydromagnetic wave. This wave is associated with groups of ions which "bounce" back and forth in the magnetosphere [Ref. 6].

These continuous micropulsations are further classified according to their periods as follows:

1. Pc1: (0.15-5 second period)
   Known as "Pearls," these micropulsations are generated by the cyclotron instability of the energetic protons. They have been positively correlated with solar disturbances and occur during daylight hours in the auroral zone and during night and early morning hours in the midlatitudes. Their average amplitude is approximately 0.05-0.1 nanotesla [Ref. 7].

2. Pc2: (5-10 second period)
   This is a diurnal phenomenon that shows some positive correlation with solar activity and the seasons. They usually decrease in their period as magnetic activity increases. Their average amplitude is 0.1-1 nanotesla.

3. Pc3: (10-45 second period)
   This micropulsation is similar to Pc2 pulsations except for the difference in period.

4. Pc4: (45-150 second period)
   Sunspot activity appears to have an effect on Pc4 pulsations. The Pc4 pulsations also change their period seasonally with an average amplitude of 5-10 nanotesla.

5. Pc5: (150-600 second period)
   These large-scale pulsations typically occur during morning and evening with amplitudes of 10-100 nanotesla. Their duration shows a strong geomagnetic latitude dependence.

Irregular (Pi) micropulsations appear to be associated with polar magnetic disturbances and are observed during night-time hours. The theory is that these micropulsations

arise from disturbances of the ionosphere due to particle bombardment from the magnetosphere. Increased solar radiation levels also appear to have an effect on their existence. Irregular micropulsations are classified as follows:

1. Pi1: (1-40 second period)
   These pulsations have a small amplitude and usually occur at night and early morning. They vary in intensity from 0.01-0.1 nanotesla. They demonstrate a positive correlation with auroral disturbances.

2. Pi2: (40-150 second period)
   Pi2 pulsation amplitude range is on the order of 1-5 nanotesla. They usually occur during the early evening hours but may continue throughout the night. The periods of these pulsations decreases with increasing magnetic activity.

The Pc5 and Pc4 micropulsations last several hours. However, the Pc3-1 micropulsations and irregular pulsations have a maximum duration of approximately one hour but may cease after only a few minutes [Ref. 8]. Above 3 Hz, the most pronounced field variations are the earth ionosphere cavity resonances of Schumann resonances [Ref. 9].

C. OCEAN WAVE EFFECTS

In addition to all of the geomagnetic fluctuations discussed above, if working in the ocean environment, one must take into account hydrodynamically induced magnetic fluctuations. These fluctuations are internally produced resulting from the movement of a conductor (seawater) in an external magnetic field. The effects of waves have been calculated [Ref. 10] and are pictured in Figure 2.6.

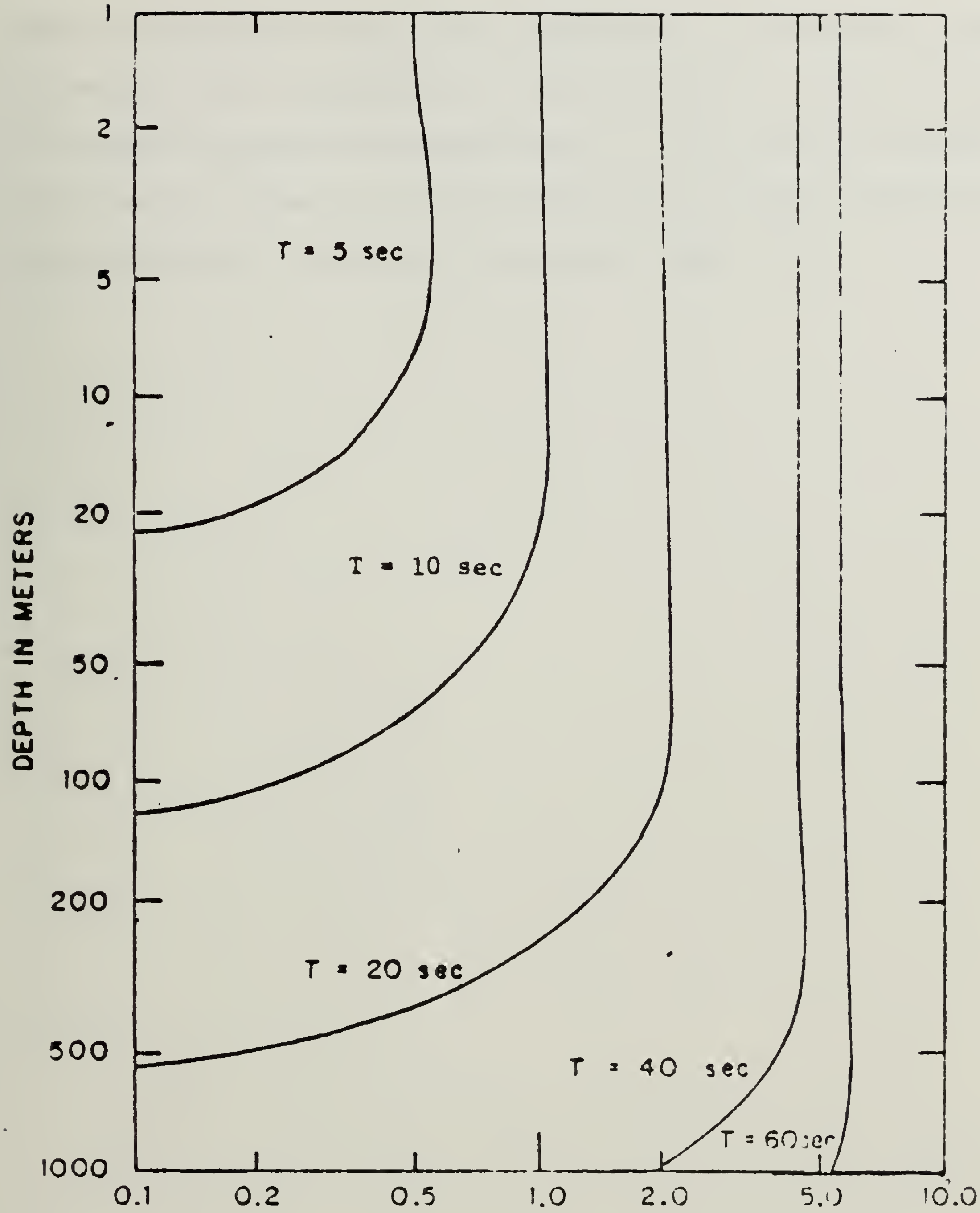

Figure 2.6 Induced Magnetic Field per Meter Amplitude of the Surface Wave

[Weaver, 1965]

Weaver's equations have been modified to incorporate bottom reflection and transmission with the result that the effect of bottom decreased the magnitude of the induced magnetic field by less than 3 dB for frequencies greater than 0.16 Hz in water depths less than 500 meters [Ref. 11].

III. COLLECTION SYSTEM

A. DATA COLLECTION SYSTEM

The data acquisition system is illustrated in Figure 3.1. Major components consist of:

(1) coil antenna sensors (2)
(2) preamplifiers (2)
(3) signal conditioners (2)
(4) pulse code modulation system (1)
(5) radio transmitter (1)
(6) radio receiver (1)
(7) tape recorder (1)

For the work reported in this paper, two systems consisting of components (1) through (5) were deployed. They were similar in most respects with the major exception that the ocean equipment was enclosed in watertight glass spheres. A thorough description of the data acquisition system is given in Reference 12.

1. Coil Antenna Sensors

Each coil antenna sensor consists of two continuously wound coils which are constructed of about 5460 turns of 18-gauge copper magnet wire. Glass spheres are used to maintain the watertight integrity of the coils and all other immersed equipment for the ocean configuration. See Figure 3.2 for the ocean system. The coils are mounted orthogonally

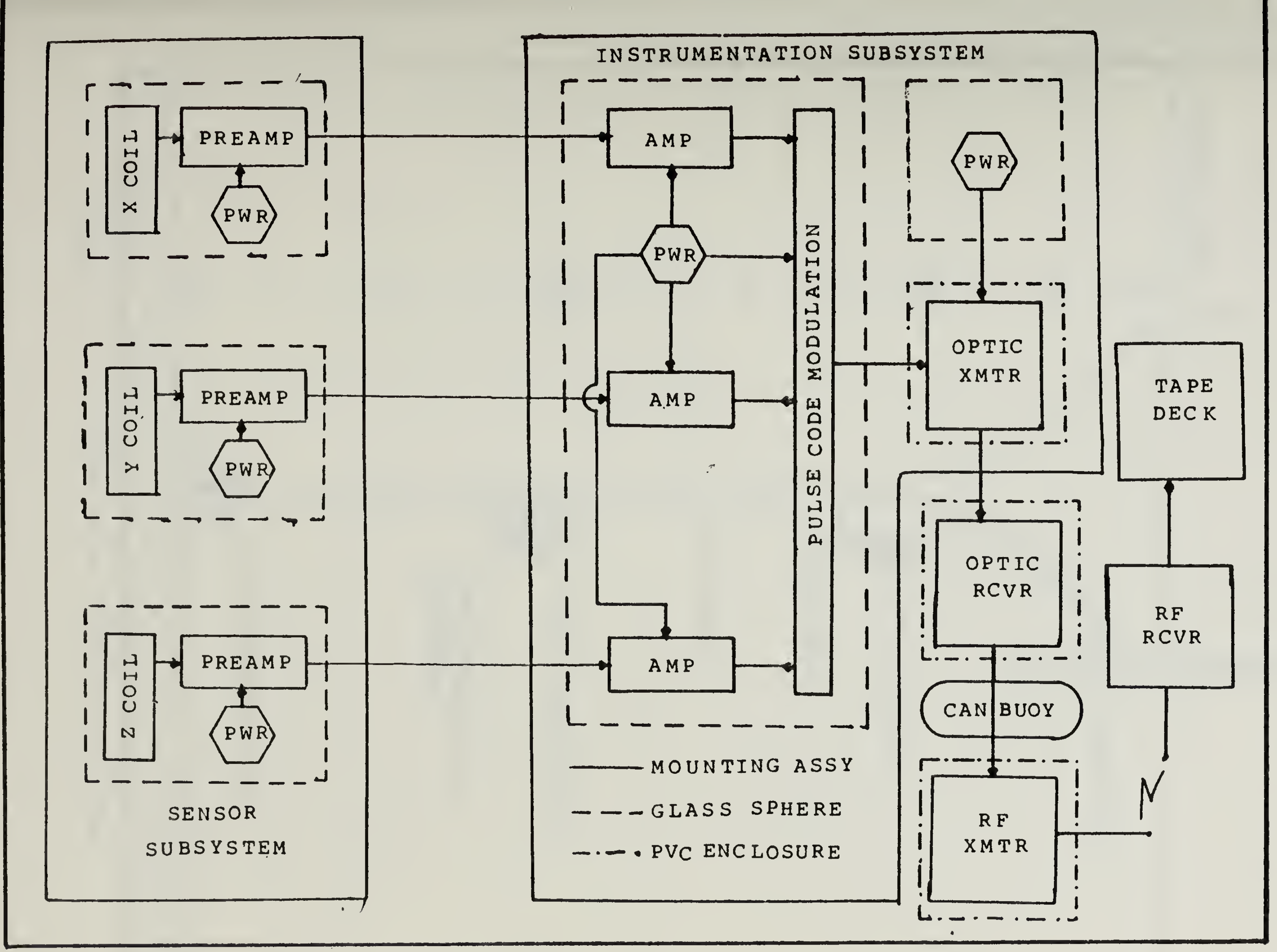

Figure 3.1 Data Collection System

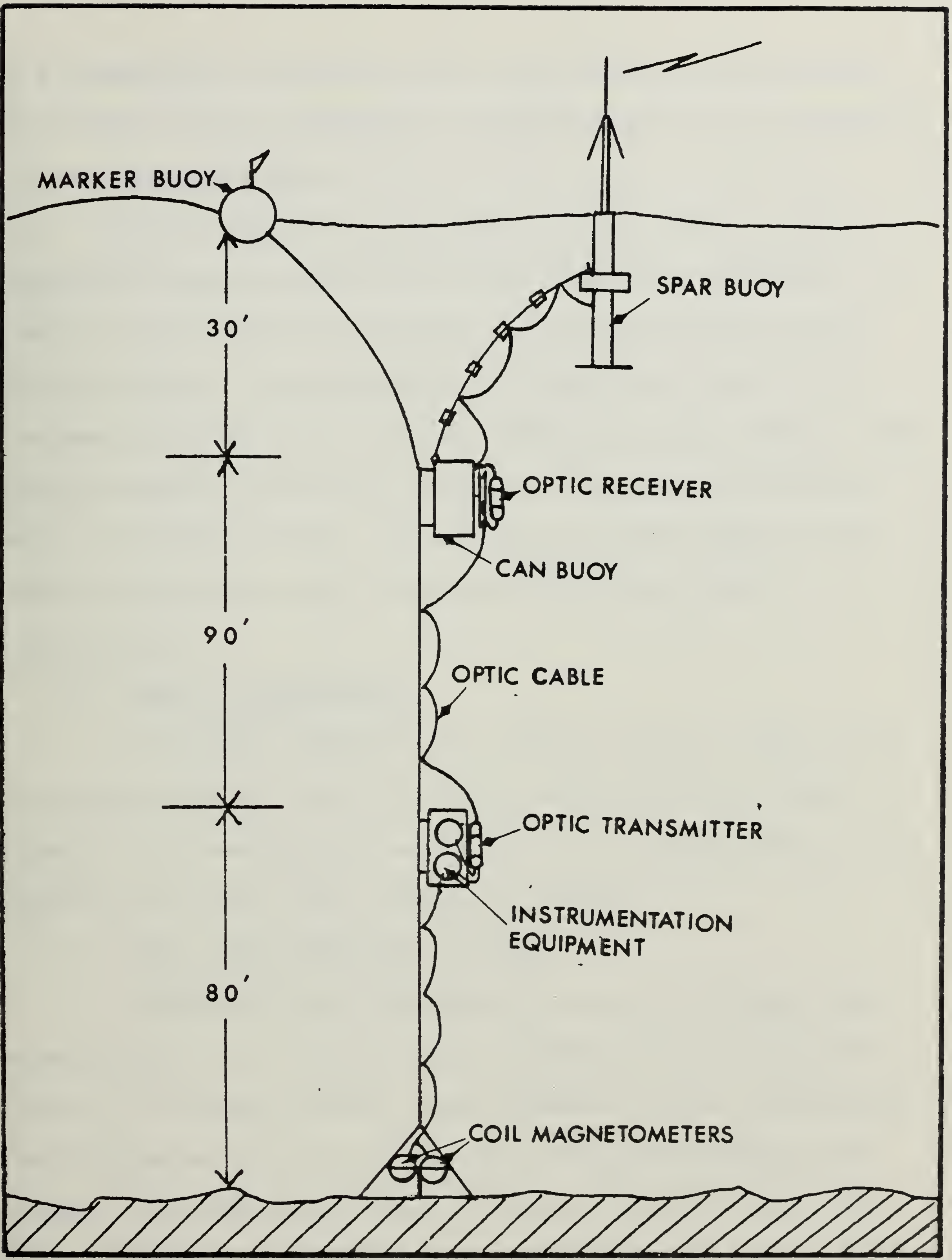

Figure 3.2 Ocean Data Collection System

in a nonmagnetic frame with each coil having a resistance of 120 ohms and an inductance of approximately 9.31 Henries.

2. Preamplifiers

The preamplifiers are model 13-10A low-noise ELF amplifiers manufactured by Dr. Alan Philips. The final stage of the amplifier contains an active low-pass filter which provides a sharp cutoff for frequencies above 20 Hz. Frequencies above 10 Hz are not examined in this paper. The overall amplifier gain for inputs of less than 2.5 millivolts is 60 dB in power. The purpose of the filter is to remove 60 Hz noise and to prefilter the data before digitization.

3. Signal Conditioners

The signal conditioners receive analog signals from the preamplifiers, amplify them by about 30 dB and limit signals with peak amplitudes of 7.5 volts (modifiable) from entering the pulse code modulation system.

4. Pulse Code Modulation System

The pulse code modulation system was designed and manufactured by Dr. Robert Lowe, Lowecom, Inc. The system offers a 15-channel analog input capability with selectable sampling rates of 2, 4, 8, 16, 32, 64 and 128 samples per second. The PCM system uses a crystal oscillator and integrated circuitry to develop the clocking pulses, a 16-channel analog multiplexer, a 16-channel, 12-bit analog-to-digital converter as the basis for the pulse coding. The crystal

clock oscillator loses 1 bit in 1 million. The clock pulse gates the analog multiplexer, the analog-to-digital converter and additional circuitry that form the pulse code words. The PCM output is organized in frames with each frame headed by a synchronization word which is followed by the pulse-coded samples from PCM channels 1 through 15.

5. Transmission and Recording

After encoding, the data is transmitted via VHF radio to a Naval Postgraduate School located receiver and recorded on an instrumentation tape recorder. For the data of this paper, a sample rate of 32 samples per second was used.

B. DATA ANALYSIS EQUIPMENT

1. Analysis Hardware

The PCM data is fed into a PCM decoder which places the decoded PCM onto a 9-track 800 BPI computer tape. This computer tape is read into the Naval Postgraduate School IBM 3033 computer for manipulation and analysis.

2. Data Analysis Software

The IBM 3033 is used to convert the data to usable form and then to perform any operations on the data as desired. At present the computer code is written in Fortran IV and converts the digital data to voltage, Fast Fourier transforms the data, calculates power spectral densities, determines Stokes parameters 0 through 3 and provides phase and coherence figures. Appendix A contains test verification

of the code. Appendix B contains the code that prepares data from one site for storage in the IBM 3033 Mass Storage System for later recall and comparison with another site. Appendix C contains the code that prepares and manipulates the code from a second site, retrieves from the Mass Storage System that data previously prepared and manipulates the two data sets simultaneously.

IV. COMPUTER CODE

A. INTRODUCTION

As mentioned earlier, one of the intentions of this effort was to develop a code that would permit the comparison and/or simultaneous geomagnetic analysis of two different sites. The present data collection system provides for the recording of transmitted data from those sites onto different tracks of the instrumentation tape recorder. Since only one track of that analog tape can be placed on one digital computer tape, a means of storing one channel had to be devised. As can be seen by a quick review of Appendices B and C, the present technique that allows this simultaneous manipulation of data from two sites is to read the computer tape from one site and to process that data to the point where it is ready for analysis. These results are then stored in the IBM 3033. Subsequently, the same routine (with modifications to fit the parameters of the second site) are applied to data read from the second site computer tape. Now both sets of data are in the same form and ready for manipulation.

B. DATA ANALYSIS SOFTWARE

The two programs (one for each of two sites) are essentially the same with the exception that one program, program B, is a short version of the other, program A. Thus, the next paragraphs will discuss in detail the longer program.

This description fits equally well to program B except that program B ends after applying the system transfer functions and placing these results in the Mass Storage System.

1. The Main Program

The main program is divided into sections which perform the following functions:

* Data input
* Fourier analysis of time series data
* Application of system transfer function. Note: At this point, program B reads the data into the Mass Storage System and ends. Program A, at this point, retrieves that same data from Mass Storage.
* Data averaging
* Calculation and plotting of:

  (1) power spectral densities of the individual site geomagnetic orthogonal components.

  (2) orthogonal component coherence of the geomagnetic field of one site.

  (3) Stokes parameters 0 through 3 of the individual site orthogonal components.

  (4) single site right and left circular polarization power spectral densities.

  (5) single plane coherence of right and left circular polarization between sites.

a. Data Input

The data is read into the IBM 3033 via the subroutine "read" which was written by Tim Stanton of the Naval Postgraduate School. The "read" subroutine reads the PCM data from the computer tape and converts it into an

integer from 0 to 4095. The main program than converts this integer to voltage. See Appendix B or C.

b. Fourier Analysis

The next section of the code utilizes a subroutine developed at the Naval Postgraduate School and called "fourt." "Fourt" Fast Fourier transforms the voltage data from the time domain to the frequency domain. See Appendix A for validation of this routine.

c. Transfer Functions

After the Fast Fourier transform, the program applies the transfer functions for the system. Development of the transfer functions is contained in Reference 12. The transfer functions are applied up to 10 Hz as straight line functions. The data is now in nanoteslas.

d. Power Spectral Density

This quantity is computed by multiplying the previously calculated spectral density summation by the observation period and dividing by the number of data groups (typically 20) that the computer tape was segmented into, providing an average power.

e. Coherence

The next steps of the program determined for one site the geomagnetic orthogonal components Stokes parameters 0, 1, 2, and 3, and the phase of the components and their coherence. Next, right and left circular polarization

parameters are computed for the individual sites followed by calculation of the coherence of these parameters between the two sites.

C. PARAMETER THEORY

1. Stokes Parameters

A useful tool for determining the state of polarization of a wave are the Stokes parameters 0, 1, 2, and 3 [Ref. 13].

Two linearly polarized plane waves with field vectors in the directions of $\hat{\varepsilon}_1$ and $\hat{\varepsilon}_2$ can be described as:

$$\vec{E}_1 = \hat{\varepsilon}_1 E_1 e^{(i \vec{k}\cdot\vec{x} - i\omega t)}$$

$$\vec{E}_2 = \hat{\varepsilon}_2 E_2 e^{(i \vec{k}\cdot\vec{x} - i\omega t)}$$

These waves can be combined to give a general plane wave propagating in the direction $\vec{k} = k\hat{n}$:

$$\vec{E}(\vec{x},t) = (\hat{\varepsilon}_1 E_1 + \hat{\varepsilon}_2 E_2) e^{(i \vec{k}\cdot\vec{x} - i\omega t)} \qquad (1)$$

If E_1 and E_2 have the same phase, (1) represents a linearly polarized wave with its polarization vector making an angle $\theta = \tan^{-1}(E_2/E_1)$ with E_1 and with a magnitude $E = \sqrt{E_1^2 + E_2^2}$.

If E_1 and E_2 have different phases, the wave (1) is elliptically polarized.

In the simplest case, circular polarization, E_1 and E_2 have the same amplitude but differ in phase by 90°. The wave (1) is then:

$$\vec{E}\ (\vec{x},t) = E_o\ (\hat{\varepsilon}_1 \pm \hat{\varepsilon}_2)\ e^{(\vec{k}\cdot\vec{x}\ -\ i\omega t)} \tag{2}$$

Then the components of (2) are:

$$\begin{aligned} E_x\ (\vec{x},t) &= E_o \cos\ (kz - \omega t) \\ E_y\ (\vec{x},t) &= E_o \sin\ (kz - \omega t) \end{aligned} \tag{3}$$

Thus, at a fixed point in space, the fields (3) are swept around circularly at the frequency ω. For $(\vec{\varepsilon}_1 + i\vec{\varepsilon}_2)$, the rotation is counterclockwise if the observer is facing the oncoming wave. This wave is described as having positive helicity. $(\vec{\varepsilon}_1 - i\vec{\varepsilon}_2)$ has negative helicity or is rotating clockwise when looking into the wave.

The two circularly polarized waves (2) form an equally acceptable set of basis fields for description of a general state of polarization by introducing the complex orthogonal unit vectors:

$$\vec{\varepsilon}_{\pm} = \frac{1}{\sqrt{2}} (\hat{\varepsilon}_1 \pm i\hat{\varepsilon}_2)$$

such that

$$\hat{\varepsilon}^*_{\pm} \cdot \hat{\varepsilon}_{\mp} = 0$$

$$\hat{\varepsilon}^*_{\pm} \cdot \hat{\varepsilon}_3 = 0$$

$$\hat{\varepsilon}^*_{\pm} \cdot \hat{\varepsilon}_{\pm} = 1$$

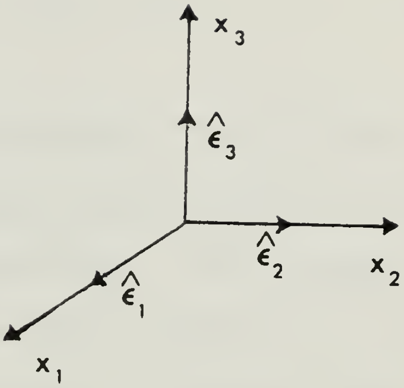

Then a general representation of (1) is:

$$\vec{E}\ (\vec{x},t) = (E_+\ \vec{\varepsilon}_+ + E_-\ \vec{\varepsilon})\ e^{(i\ \vec{k}\cdot\vec{x}\ -\ i\omega t)} \qquad (4)$$

where E_+ and E_- are complex amplitudes. If E_+ and E_- have different amplitudes but the same phase, (4) is an elliptically polarized wave with principal axes of the ellipse in the plane defined by $\hat{\varepsilon}_1$ and $\hat{\varepsilon}_2$.

Thus, the polarization content of a plane wave is known if it can be written in the form (1) or (4) with known coefficients (E_1, E_2) or (E_+, E_-). Conversely, how can we determine from observations on a wave the state of its polarization? The answer lies in the use of the four Stokes parameters. Their measurement or calculation determines the state of polarization of a wave.

For a wave propagating in the z direction, the scalar products:

$$\hat{\varepsilon}_1 \cdot \vec{E}, \hat{\varepsilon}_2 \cdot \vec{E}, \hat{\varepsilon}_+^* \cdot \vec{E}, \hat{\varepsilon}_-^* \cdot \vec{E}$$

are the amplitudes of radiation respectively, with linear polarization in the x direction, linear polarization in the y direction, positive and negative helicity. The squares of these amplitudes provide a measure of the intensity of each type of polarization. Phase information is obtained from cross products. If we assume the scalar coefficients of (1) and (4) to be a magnitude times a phase factor:

$$E_1 = a_1 e^{i\delta_1}, E_2 = a_2 e^{i\delta_2}$$

$$E_+ = a_- e^{i\delta +}, E_- = a e^{i\delta -}$$

and use the circular polarization basis $(\hat{\varepsilon}_+, \hat{\varepsilon}_-)$, we have:

$$S_o = |\hat{\varepsilon}_+ \cdot E|^2 + |\hat{\varepsilon}_- \cdot E|^2 = a_+^2 + a_-^2$$

$$S_1 = 2\mathrm{Re}[(\hat{\varepsilon}_+ \cdot E_+)^* (\hat{\varepsilon}_- \cdot E)] = 2a_+ a_- \cos(\delta_- - \delta_+)$$

$$S_2 = 2\mathrm{Im}[(\hat{\varepsilon}_+ \cdot E_+)^* (\hat{\varepsilon}_- \cdot E_-)] = 2a_+ a_- \sin(\delta_- - \delta_+)$$

$$S_3 = |\hat{\varepsilon}_+ \cdot E|^2 - |\hat{\varepsilon}_- \cdot E|^2 = a_+^2 - a_-^2$$

2. Coherence

If a plane wave of frequency ν is propagating in the z direction, it has components:

$$E_x(t) = a_1(t)e^{i\phi_1(t) - i2\pi\nu t}$$

$$E_y(t) = a_2(t)e^{i\phi_2(t) - i2\pi\nu t}$$

that are mutually orthogonal and at right angles to the direction of propagation [Ref. 13]. Then the complex degree of coherence can be written as:

$$\mu_{xy} = \frac{J_{xy}}{\sqrt{J_{xx}}\,\sqrt{J_{yy}}}$$

where J_{xx},... are the elements of the coherency matrix

$$\vec{J} = \begin{vmatrix} E_x E_x^* & E_x E_y^* \\ E_y E_x^* & E_y E_y^* \end{vmatrix} = \begin{vmatrix} a_1 & a_1 a_2 e^{i\phi_1 - i\phi_2} \\ a_1 a_2 e^{i\phi_1 - i\phi_2} & a_2 \end{vmatrix}$$

The complex factor μ_{xy} is the complex degree of coherence and is a measure of the correlation between components of the field vector in the x and y directions.

D. SOFTWARE TESTING

The basis set for the code calculations is that of a circularly polarized wave. Thus a circularly polarized wave was chosen as the test input. The wave was created by generating a 4 Hz sine wave for sites A and B x coil input and 4 Hz cosine wave for sites A and B y coil input. The results of this test are valid only at the input frequency as a measure of the code veracity. One of the characteristics of any FFT routine is that small residuals are created throughout the spectrum of interest. These residuals are primarily caused by the finite observation time. These small-valued artifacts will be carried throughout all subsequent parameter calculations and will appear in the test plots. This inclusion of unexpected values at frequencies other than the test input of 4 Hz should be considered as the result of the artificiality of the single value test input. Input of real world data that covers a full spectrum of values obscures the "FOURT" routine propensity to create these artifacts.

1. Sites A and B Orthogonal Component Power Spectral Density Test

Spectral density is defined as:

$$S_x = \frac{1}{N} \sum_{1}^{n} (x_i)(x_i)^*$$

for site A x coil where x is the Fourier Transform of some

input to the x coil. It follows that the average power spectral density is:

$$PSD_{xa} = \frac{Time}{N} \sum_{1}^{n} (X_a)(X_a)^* = S_{xa} \cdot Time$$

where time is the observation time. Thus, for the test inputs of sine 4 Hz into the x coils at sites A and B and the cosine 4 Hz into the y coils, we expect and obtain (see Figures A.1, A.2, A.11, A.12) a peak magnitude of .5 at 4 Hz at each site.

2. <u>Sites A and B Orthogonal Component Coherence Test</u>

Coherence as defined above is:

$$\mu_{xya} = \left| \frac{S_{xya}}{\sqrt{S_{xa}}\ \sqrt{S_{ya}}} \right|$$

for two orthogonal components where S_{xya} is defined by:

$$S_{xya} = \frac{Time}{N} \sum_{1}^{n} (X_a)(Y_a)^*$$

With X and Y our transformed inputs and considering the same inputs, we expect to see a coherence of magnitude 1 at a frequency of 4 Hz and its harmonics. Figures A.8 and A.18 demonstrate the validity of the coherence calculations of

the code. Also the value of 1 for the test case coherence at frequencies other than 4 Hz is a manifestation of the residual effect discussed above.

3. Sites A and B Stokes Parameter 1 Test

Using the definitions developed in preceding paragraphs, Stokes 1 is:

$$S_{1a} = 2a_{+}a_{-}\sin(\delta_{-} - \delta_{+}) = 2[S_x - S_y] = 0$$

for $S_x = S_y$ as is the case for this test input and as is shown in Figures A.4 and A.13.

4. Sites A and B Stokes Parameter 2 Test

Again using definitions developed in the preceding paragraphs, Stokes parameter 2 is:

$$S_{2a} = 2a_{+}a_{-}\sin(\delta_{-} - \delta_{+}) = 0 \text{ for } (\delta_{-} - \delta_{+}) = 0$$

Figures A.5 and A.15 validate the code for this calculation.

5. Sites A and B Stokes Parameter 3 Test

Stokes 3 is:

$$S_{3a} = a_{+}^{2} - a_{-}^{2} = -(.707)^{2} -(.707)^{2} = -1$$

Figures A.6 and A.16 validate the code for this calculation.

6. Sites A and B Stokes Parameter 0 Test

Stokes 0 is:

$$S_{oa} = a_+^2 + a_-^2 = 2 \; [S_{xa} = S_{xb}] = 2$$

(See Figures A.3 and A.13.)

7. Sites A and B Phase Difference of x and y Test

The phase difference of sine 4 Hz versus cosine 4 Hz is 90° or 1.57 radians. (See Figures A.7 and A.17.)

8. Sites A and B Two Orthogonal Component Power Spectral Density with Right and Left Circular Polarization Basis Set Test

The development of the spectral densities for this case is similar to the development of spectral density for a single component. Starting with the cross spectra density definition for right and left circular polarization

$$BP_{xya} = (X + iY) \qquad \text{(right polarized)}$$

$$BM_{xya} = (X - iY) \qquad \text{(left polarized)}$$

It follows that the spectral density is:

$$SP_{xya} = \frac{1}{N} \sum_1^n (BP_{xya})(BP_{xya})^* \qquad \text{(right polarized)}$$

$$SM_{xya} = \frac{1}{N} \sum_1^n (BM_{xya})(BM_{xya})^* \qquad \text{(left polarized)}$$

The power spectral densities will be:

$$SP_{xya} = \frac{Time}{N} \sum_{1}^{n} SP_{xya}$$

$$SM_{xya} = \frac{Time}{N} \sum_{1}^{n} SM_{xya}$$

where the time is the observation time. Examples of this calculation with a test input of 4 Hz right circularly polarized wave are in Figures A.9, A.10, A.19 and A.20.

9. Coherence of Sites A and B Right and Left Circular Polarization Basis Set Test

Right and left circular polarizations are:

$$COP = \frac{SP_{abxy}}{\sqrt{SP_a}\ \sqrt{SM_b}} \qquad \text{(right polarization)}$$

$$COM = \frac{SM_{abxy}}{\sqrt{SM_a}\ \sqrt{SM_b}} \qquad \text{(left polarization)}$$

where SP_{abxy} and SM_{abxy} are the cross spectra densities of the two orthogonal components at the sites A and B.

$$SP_{abxy} = \frac{Time}{N} \sum_{n}^{n} (BP_{xya})(BP_{xya}) \qquad \text{(right polarization)}$$

$$SM_{abxy} = \frac{Time}{N} \sum_{1}^{n} (BM_{xya})(BM_{xyb}) \qquad \text{(left polarization)}$$

The test case of sine 4 Hz as the xa and xb inputs versus cosine 4 Hz as the ya and yb inputs yields a coherence of 0 for left circular polarization and 1 for right circular polarization. (See Figures A.20 and A.21.)

V. ANALYSIS

Preliminary, "eyeball" analysis was conducted on data collected over a period from 1122 local 17 Aug 82 to 0639 local 18 Aug 82. The timeframes inspected within this window were:

TIME (local)	DATE
1122-1254	17 Aug 82
1301-1408	17 Aug 82
2028-2200	17 Aug 82
0121-0251	18 Aug 82
0259-0431	18 Aug 82
0507-0639	18 Aug 82

Original intentions were to collect data over a full 24-hour period. However, the batteries at the Monterey Bay site went dead after 20 hours. Of the 20 hours of collected data, eight hours appeared dominated by system noise and were not included in the analysis. However, the remaining data of approximately eight hours spans a 24-hour period and provides evidence of some obvious trends that lend themselves to the cursory analysis conducted here. Representative plots of the calculated parameters are in Appendix D. Technical Report NPS 61-83-005 contains a complete set of plots of the calculations that span the full 20 hours of data collection. This complete set of plots was used in the analysis that follows.

A. POWER SPECTRAL DENSITIES

Both sites exhibit a marked decrease in power spectral density with frequency. There is an obvious exception to this observation at 4 Hz at the land site. The sharp peak at 4 Hz is attributed to 60 Hz aliasing which is a result of the Fast Fourier Transform (FFT) subroutine. Fast Fourier algorithm construction is such that data being transformed may be convolved back onto itself [Ref. 15]. This convolution is routinely avoided by using a sample rate that is twice the upper frequency of the domain of interest. A sample rate of 32 samples per second was used in this experiment and should have precluded aliasing of the frequency of 60 Hz, especially when combined with the amplifier filter cutoff of 20 Hz. However, the 60 Hz component of the magnetic field was measured and found to be 4 nanotesla/Hz which is 10^5 higher than magnetic noise data [Ref. 16]. The 20 Hz filter cannot completely filter out signals of this magnitude. Thus the 4 Hz signal is a result of aliasing of the strong ambient 60 Hz signal.

B. STOKES PARAMETERS

All Stokes parameters demonstrate reasonable agreement. That is, Stokes 0 is obviously $a_+^2 + a_-^2$ and Stokes 3 is obviously $a_+^2 - a_-^2$ as shown in Figures D.3, D.6, D.13 and D.16.

1. Ocean Site

The ocean site Stokes 2 and 3 parameters exhibit a time dependence. That is, in the early a.m. hours the large magnitude of Stokes 2 is the noticeable feature. This magnitude decreases at sunrise and through the day until it reasserts itself after sunset. A review of Stokes parameters 2 and 3 over the total observation time (see Technical Report NPS-61-83-005) indicates that this falloff is independent of frequency. The increase in magnitude of Stokes 2 after sunset is also independent of frequency with the exception of some very discrete spectral components.

2. Land Site

The land site Stokes 2 and 3 parameters show a time dependence with a shorter cycle. That is, the magnitude of Stokes 2 is large near sunset, followed by its decrease during the morning hours. The early afternoon hours reflect an increase in Stokes 2 until after sunset. Figures 5.1 through 5.4 show the decreased magnitude of Stokes parameters 2 and 3 for the morning hours.

C. X AND Y COIL PHASE DIFFERENCE

1. Ocean Site

The use of Stokes parameters in the calculation of the phase difference dictates that changes in the time series averaged Stokes parameters should be evident in the x and y component phase difference. This is the case as

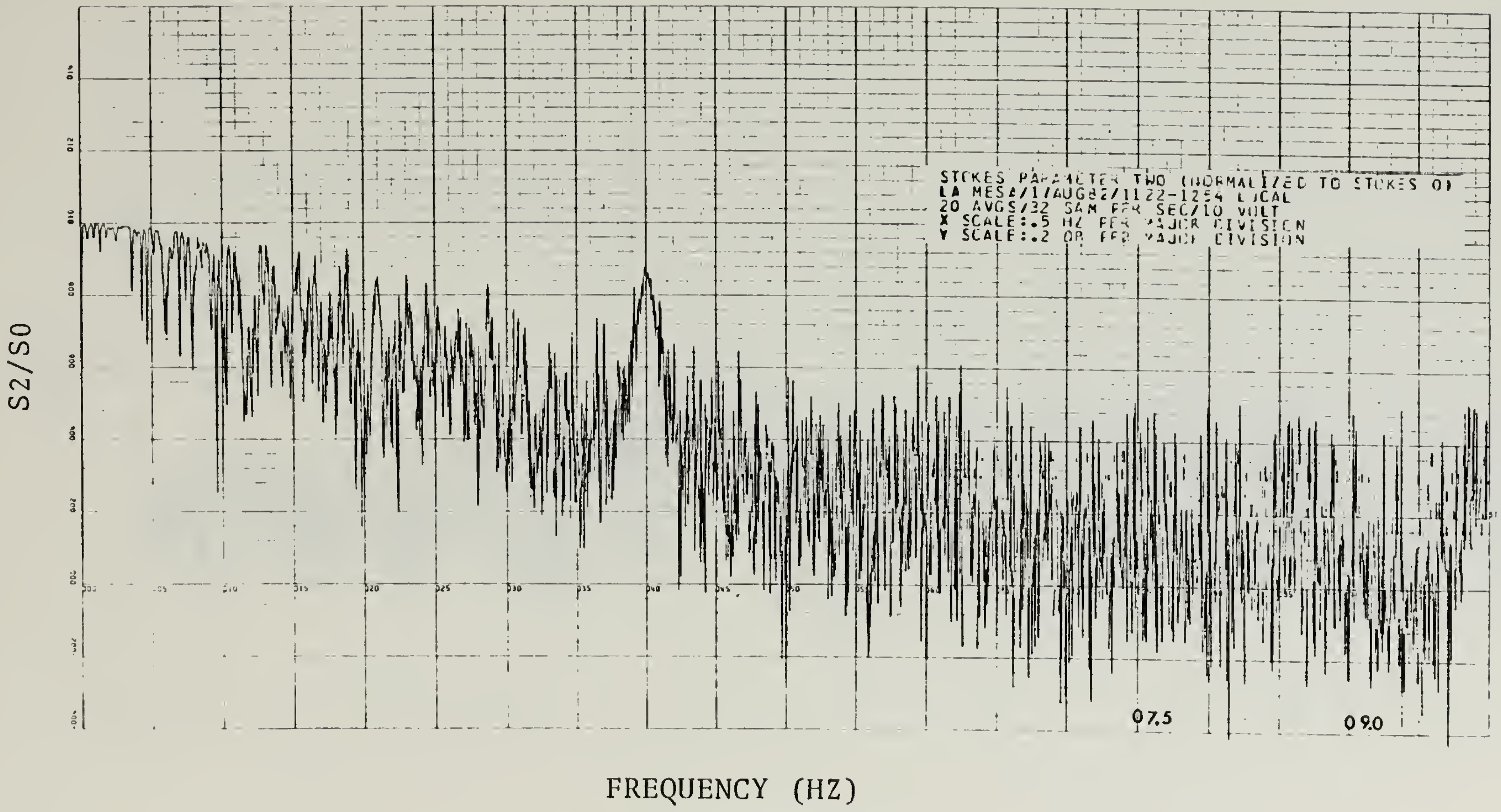

Figure 5.1 Stokes Parameter 2, La Mesa, 1122-1254 Local, 17 Aug. 82

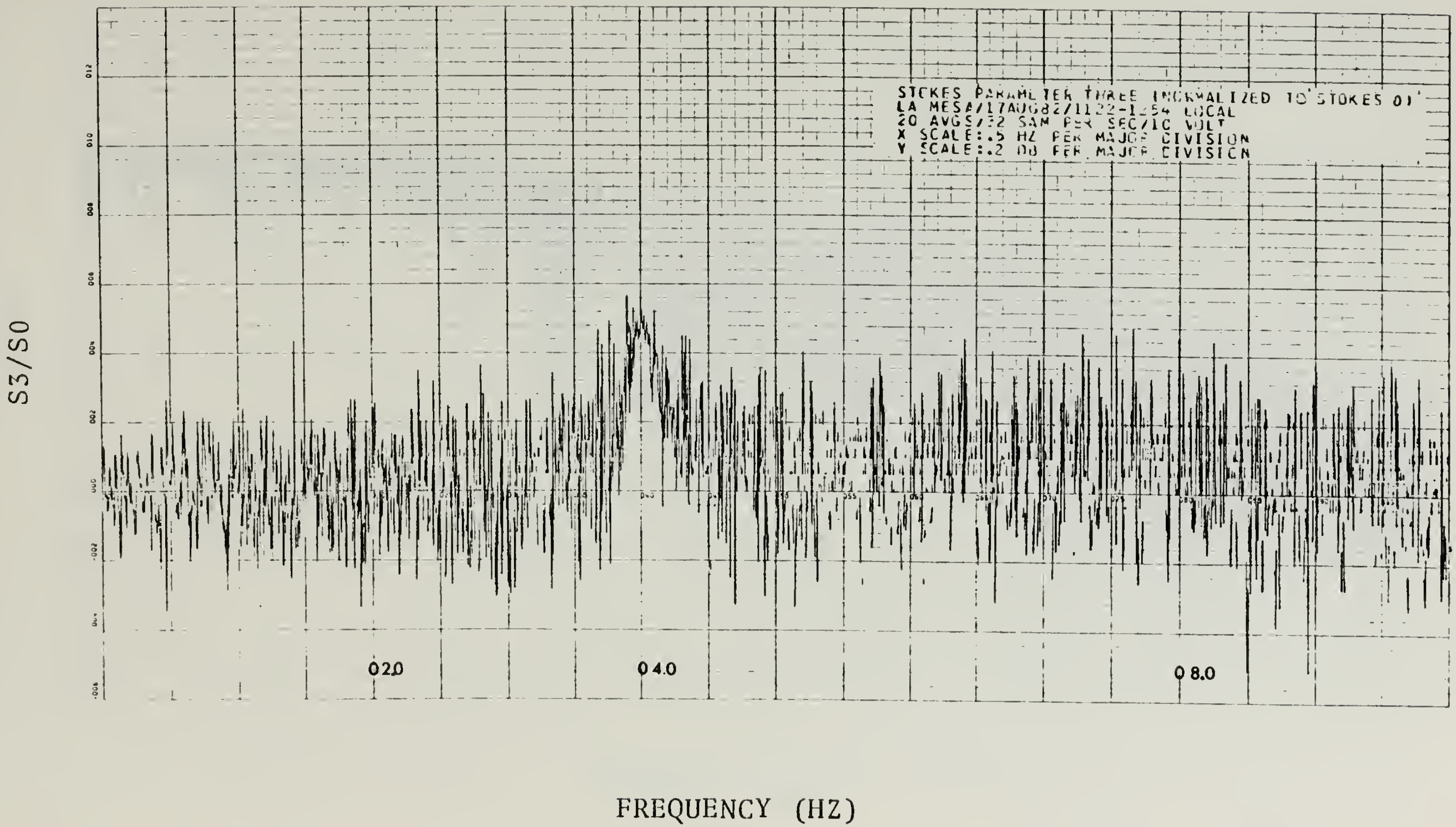

Figure 5.2 Stokes Parameter 3, La Mesa, 1122-1254 Local, 17 Aug. 82

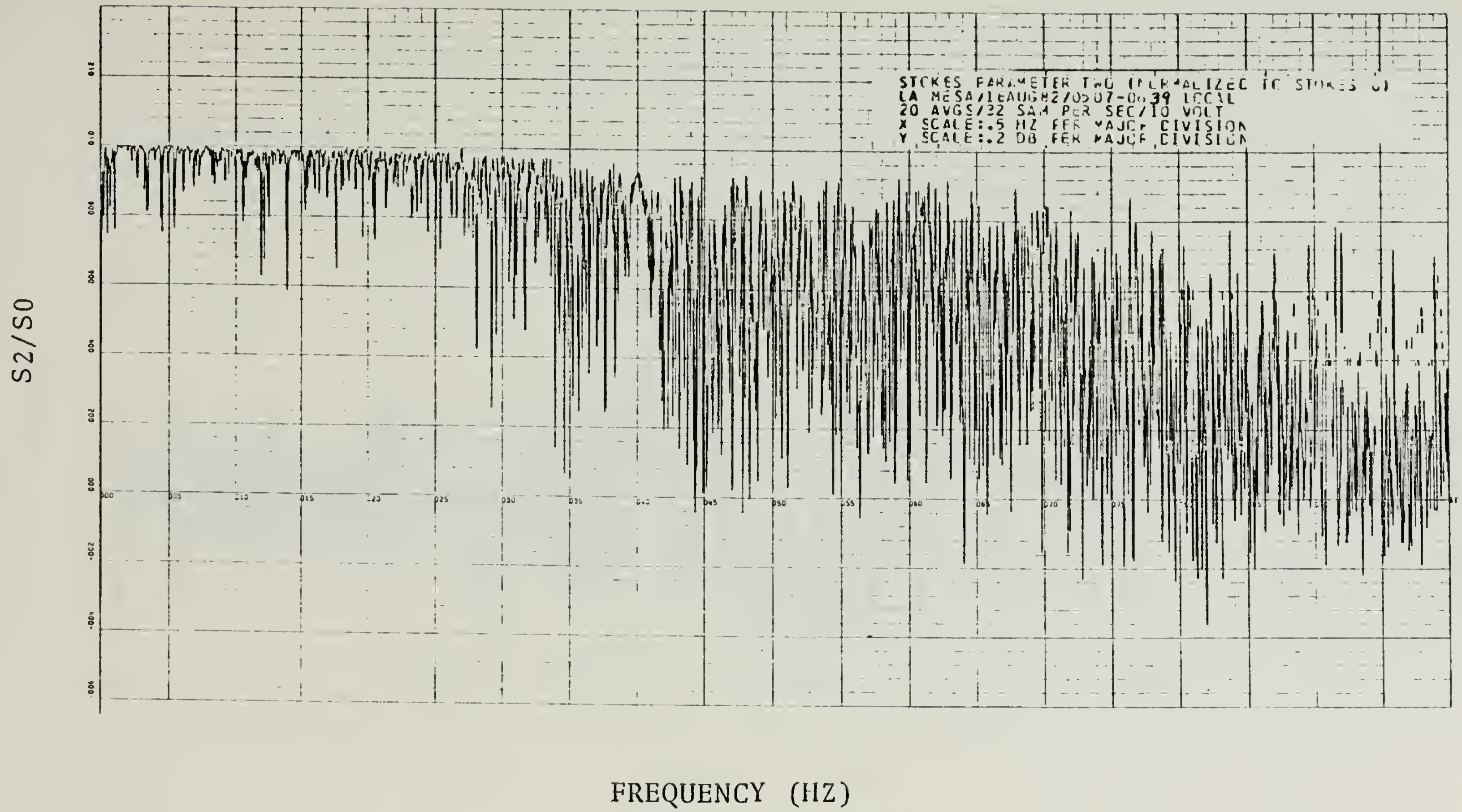

Figure 5.3 Stokes Parameter 2, La Mesa, 0507-0639 Local, 18 Aug. 82

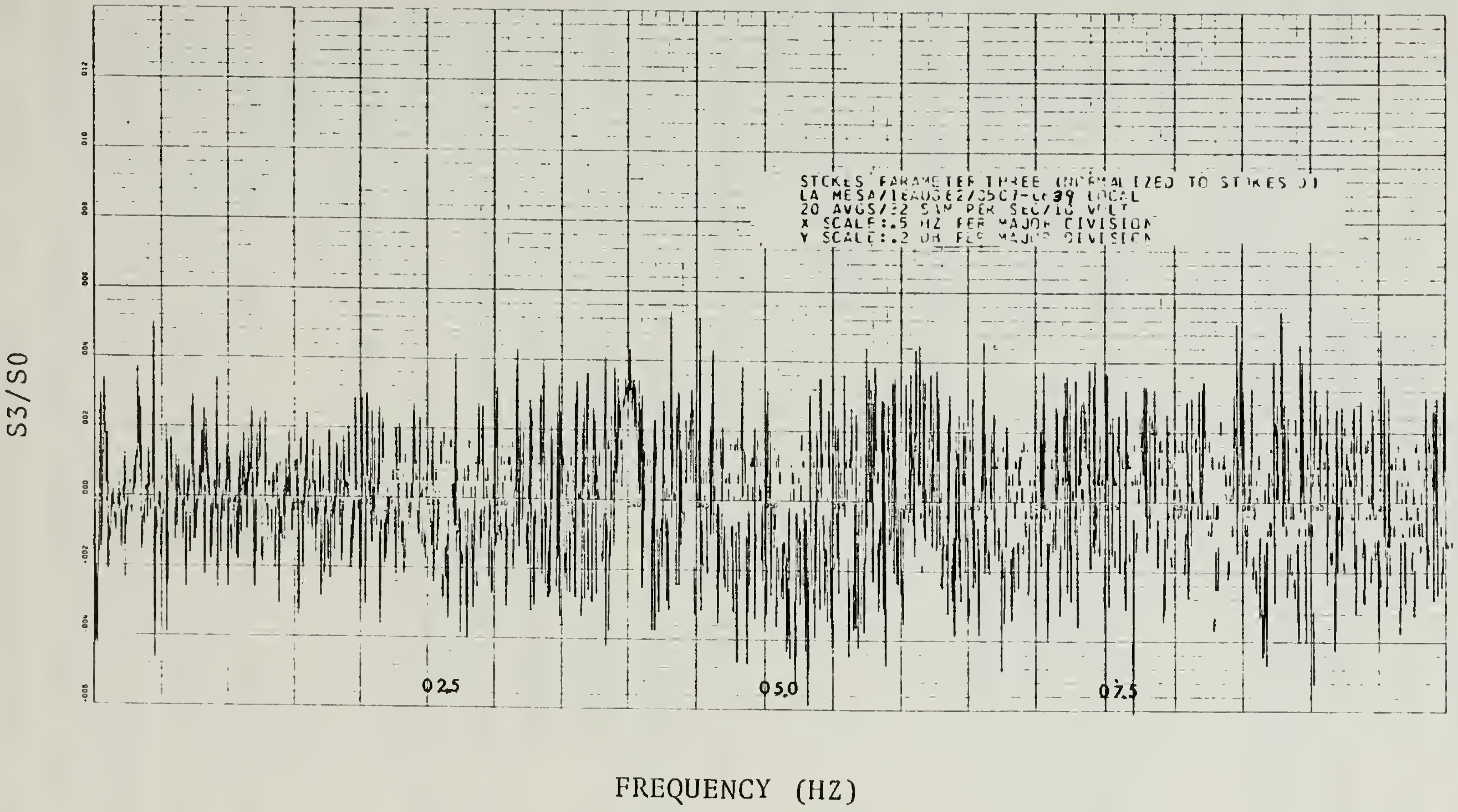

Figure 5.4 Stokes Parameter 3, La Mesa, 0507-0639 Local, 18 Aug. 82

shown in Figures D.7 and D.17. The phase difference from sunset to sunrise shows a definite decrease with an "eyeball" average of .2 to .4 radians. Daylight hours show a difference ranging from .5 to .3 radians with the greatest difference near local noon.

2. Land Site

The land site phase difference reflects its Stokes parameters with a difference of about .3 radians in the higher frequencies at all hours and a difference of .1 radians during the daylight hours.

D. X AND Y COIL COHERENCE

1. Ocean Site

Time dependence is again a strong factor with high degrees of coherence in the ocean site x and y coils being greatest during hours of darkness and diminishing at sunrise. Figures 5.5 and 5.6 are examples of this phenomenon. The exception to this observation is at local noon when the coherence of the ocean coils is again very high but diminishes before and after the noon time data.

2. Land Site

The land site x and y coil coherence reflects the previous parameter cycle time dependence. There is a high degree of coherence in the lower frequencies at sunrise that is followed by diminishing coherence in the higher frequencies. Local noon shows an improved coherence at

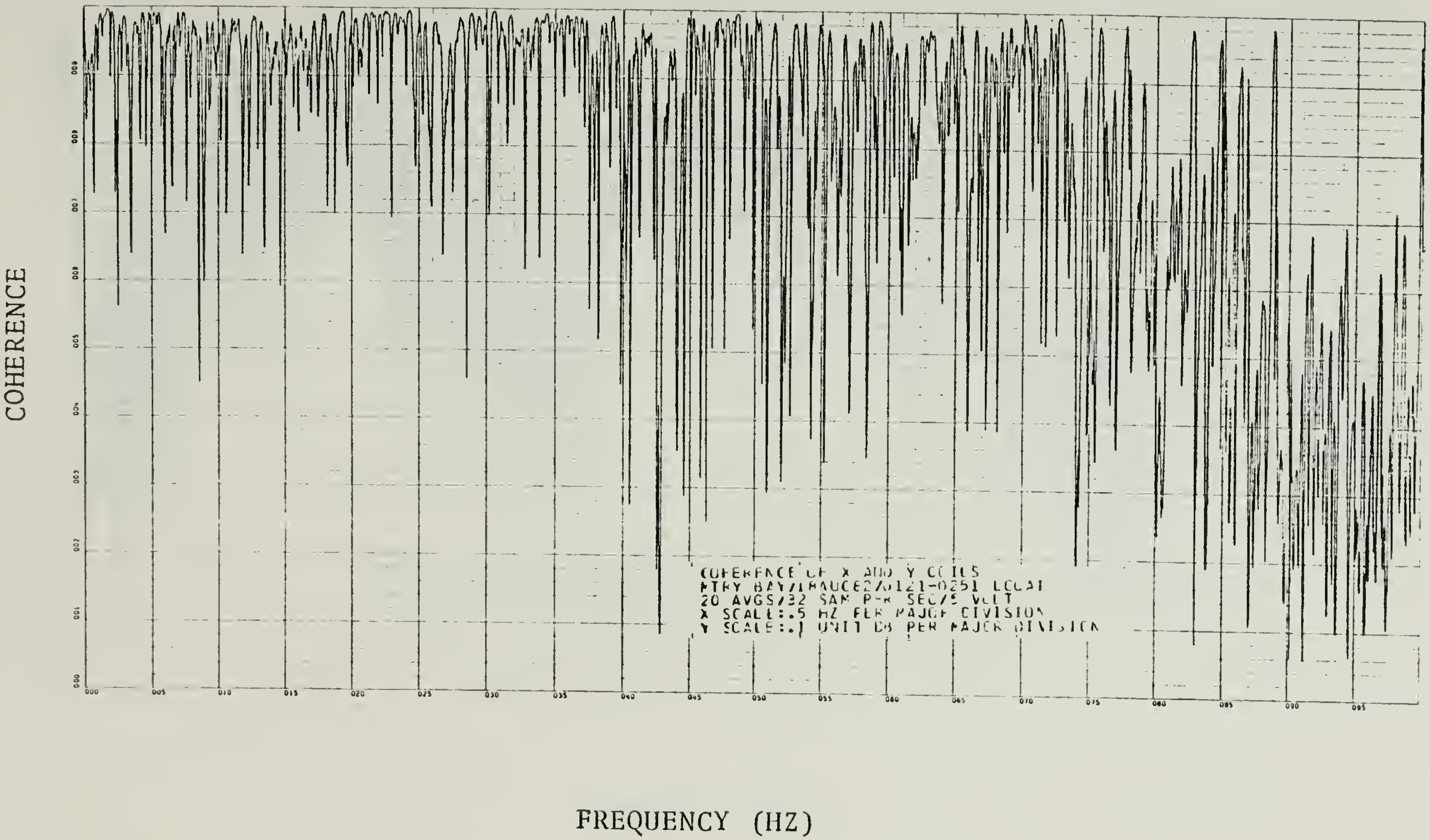

Figure 5.5 Coherence of x and y Coils, Mtry Bay, 18 Aug. 82, 0121-0251 Local

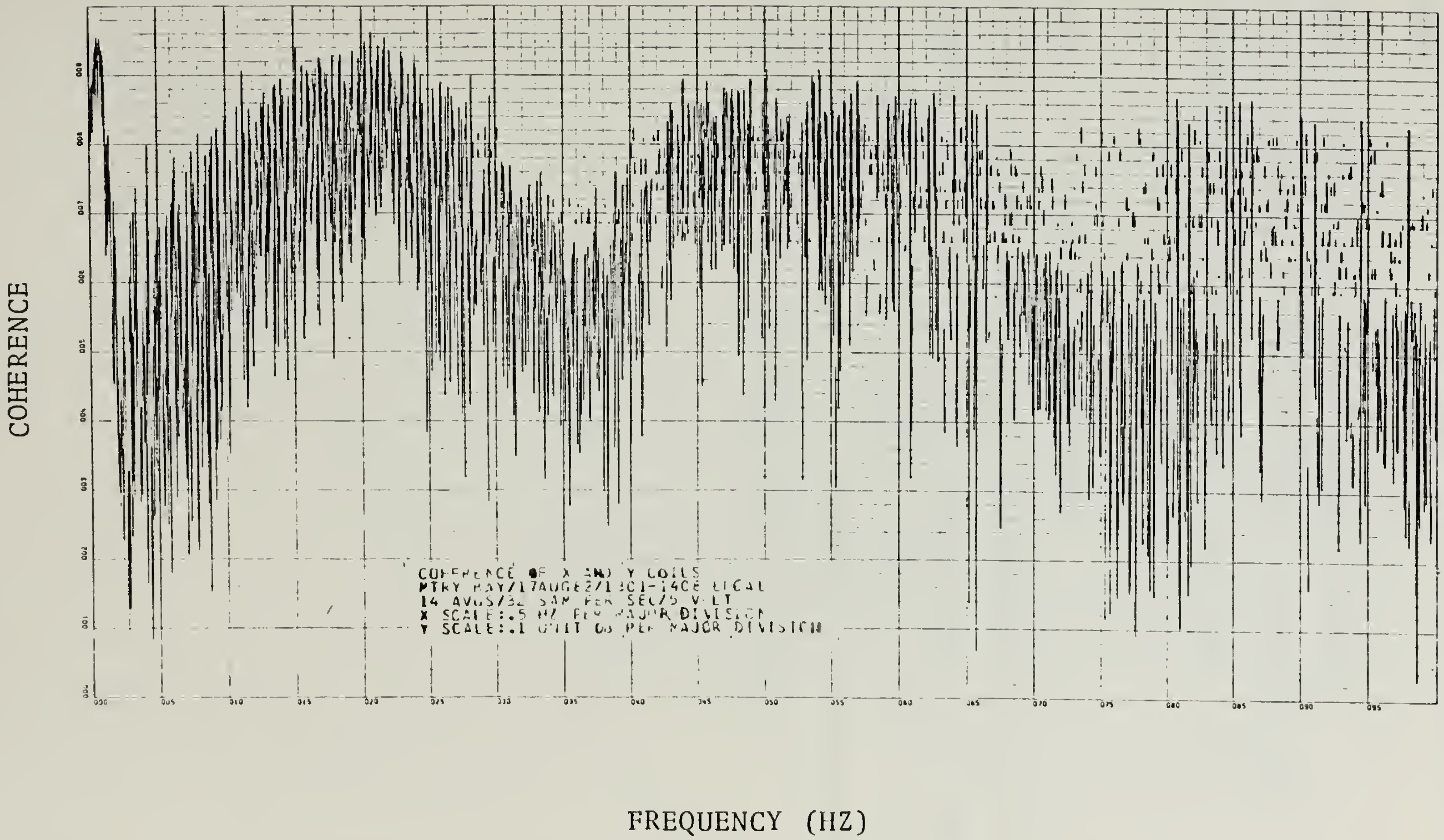

Figure 5.6 Coherence of x and y Coils, Mtry Bay, 18 Aug. 82, 1301-1408 Local

these frequencies but is followed by a degraded coherence after sunset.

E. CIRCULAR POLARIZATION POWER SPECTRAL DENSITY

There is no marked contrast between right and left circular polarization power spectral densities. Both calculations provide similar results.

F. COHERENCE OF CIRCULAR POLARIZATION

No preference for right versus left circular polarization is discernable. The most obvious trend is that of a high degree of coherence in the frequency range .05 Hz to .4 Hz as shown in Figures 5.7 and 5.8. Generally, coherence of the two sites decreases thereafter with frequency.

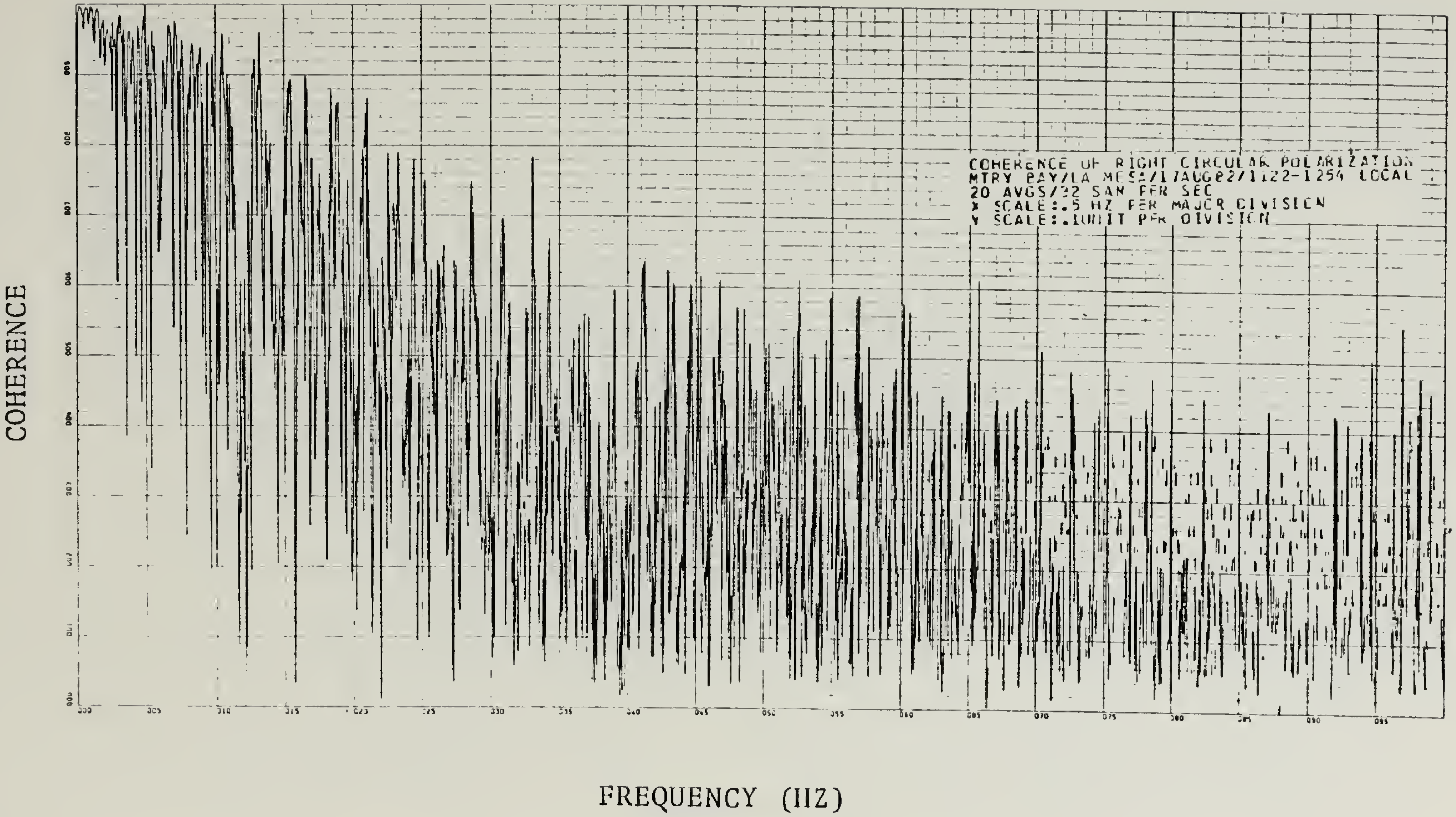

Figure 5.7 Coherence of Right Circular Polarization Monterey Bay/La Mesa 1122-1254 Local, 17 Aug. 82

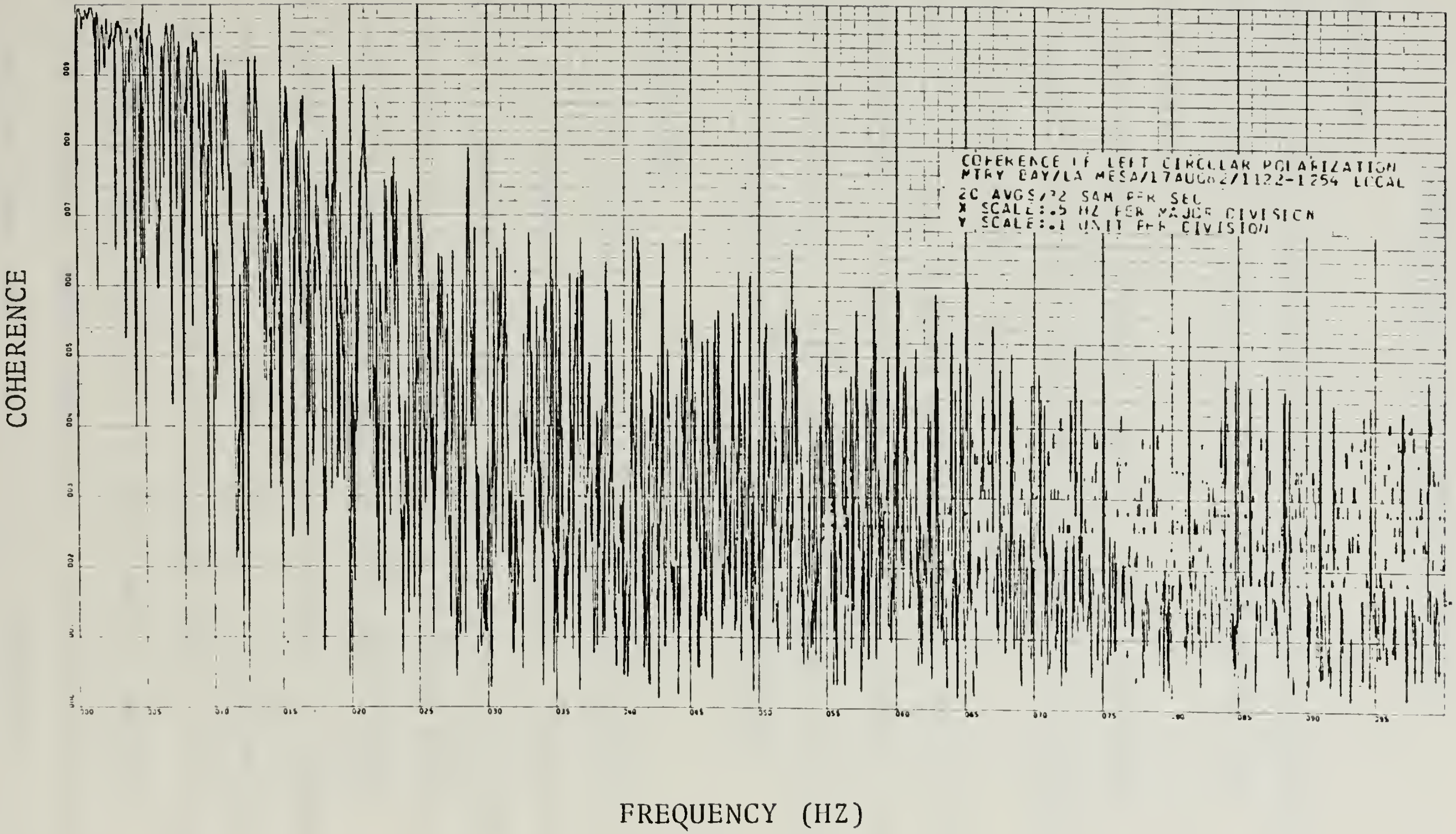

Figure 5.8 Coherence of Left Circular Polarization Monterey Bay/La Mesa 1122-1254 Local, 17 Aug. 82

VI. CONCLUSIONS AND RECOMMENDATIONS

A. CONCLUSIONS

In view of the limited data base and the preliminary state of the analysis, only tentative conclusions are possible at this point.

(1) In the frequency range .05 to .4 Hz, the ocean and land data exhibit a high degree of coherence. At higher frequencies the coherence rapidly diminishes.

(2) Both polarized and unpolarized signals were observed with a preponderance of high degrees of polarization occurring at the lower frequencies. The nature of the polarization appears to be a function of both time and frequency.

B. RECOMMENDATIONS

The first and obvious recommendation is to collect more data. This is already in the planning stage. The second and also obvious recommendation is to conduct a more thorough analysis of the data on hand. This also is already being planned. More concrete recommendations concern data processing.

One 90-minute real time data tape requires 12 computer cylinders of storage space. Thus, for the approximately eight hours of data computed and analyzed here, 72 cylinders of storage were used. This is too much and is mostly a matter of the computer code employed. A little work can provide a program that would require less computer storage

space. This will be a real necessity as a data base of weeks or months is compiled for analysis. It is recommended that the present code by "streamlined" to use the IBM 3033 as a calculation "scratch pad." Then a few lines of "Computer Job Control Language" can be employed to store the calculations on a high-density tape for future use at the Naval Postgraduate School or anywhere in the world.

APPENDIX A

TEST PROGRAM

```
//JOEM1MB JOB (1592,0129),'FISHER SMC.1399',CLASS=C
//*MAIN ORG=NPGVM1.1592P,LINES=(60)
//*FORMAT PR,DDNAME=PLOT.SYSVECTR,DEST=LOCAL
// EXEC FRTXCLGP,PARM.LKED='LIST,MAP,XREF',REGION.GO=2700K
//SYSUT1    DD   UNIT=SYSDA,SPACE=(CYL,(8,8))
//SYSUT2    DD   UNIT=SYSDA,SPACE=(CYL,(8,8))
//SYSLIN    DD   SPACE=(6080,(80,30)),UNIT=SYSDA
//FORT.SYSIN DD DSN=MSS.SYS3.NONIMSL.SOURCE(FOURT),DISP=SHR
//     DD   *
C           A LARGE NUMBER OF ARRAYS ARE UTILIZED
C           WITH THE INTENTION OF MAINTAINING EACH
C           BIT OF ORIGINAL DATA OR CALCULATION,
C           READY FOR RECALL AT ANY TIME FOR FURTHER
C           COMPUTAITON. EQUIVALENT ARRAYS ARE EMPLOYED
C           BECAUSE THE PLOTTING ROUTINE 'DRAWP' IS
```

```
C          NOT ABLE TO HANDLE COMPLEX ARRAYS.
C          ARRAYS 'ITB','RTB','ALAB' AND 'TITLE' ARE
C          USED TO GENERATE THE VERSATEC PLOTTER OUTPUT.
C          OCEAN ARRAYS ARE INDICATED VIA THE SUFFIX
C          'O', AND LAND ARRAYS ARE INDICATED WITH 'L'.
      COMPLEX*8 XXO(8192),YYO(8192),
     C CSO(8192),COO(8192),ZXO(8192),
     C CRO(8192),CTO(8192),CUO(8192),
     C CVO(8192),CWO(8192),CPO(8192),
     C ZYO(8192),COMOL(8192),COL(8192),
     C CUL(8192),CVL(8192),CWL(8192),
     C COPOL(8192),XXL(8192),YYL(8192),ZXL(8192),
     C ZYL(8192),CSL(8192),BPO(8192),
     C BMO(8192),BPL(8192),BML(8192),
     C SPOL(8192),SMOL(8192),SPO(8192),
     C SPL(8192),SMO(8192),CTL(8192),
```

```
C CPL(8192),CRL(8192),SML(8192)
  DIMENSION TIME(8192),FREQ(8192),
C WORK(16384),FRQ2(8192)
  INTEGER*4 ITB(12)/12*0/
  REAL*4    RTB(28)/28*0.0/,
C CROO(16384),CPOO(16384),CUOO(16384),
C COOO(16384),CTOO(16384),CVOO(16384),
C CWOO(16384),CTLL(16384),
C CPLL(16384),CRLL(16384),COLL(16384),
C CULL(16384),CVLL(16384),
C CWLL(16384),COMOLL(16384),COPOLL(16384),
C SPOO(16384),SPLL(16384),
C SMOO(16384),SMLL(16384)
  REAL ALAB(22)/'PDXO','PDYO','ST1O',
C 'ST2O','ST3O','STOO','PHA0',
C 'GAMC','PDXL','PDYL','ST1L','ST2L',
```

```
C 'STBL','STOL','PHAL','GAML',
C 'SPLO','SPLL','SMOO','SMLL','CPOL','CMOL'/
  REAL*8 TITLE(12)
  EQUIVALENCE(TITLE(1),RTB(5)),(CROO(1),
C CRO(1)),(CPOO(1),CPO(1)),
C (COOO(1),COO(1)),(CTOO(1),CTO(1)),(CUOO(1),CUO(1)),
C (CWOO(1),CWO(1)),(CVOO(1),CVO(1)),(CTLL(1),CTL(1)),
C (CPLL(1),CPL(1)),(CRLL(1),CRL(1)),(COLL(1),COL(1)),
C (CULL(1),CUL(1)),(CVLL(1),CVL(1)),(CWLL(1),CWL(1)),
C (COPOLL(1),COPOL(1)),(COMOLL(1),
C COMOL(1)),(SPOO(1),SPO(1)),
C (SPLL(1),SPL(1)),(SMOO(1),SMO(1)),(SMLL(1),SML(1))
  DATA XXO,YYO,CSO,COO,ZXO,ZYO,CRO,CTO,CUO,CVO,CWO,
C XXL,YYL,ZXL,ZYL,CSL,BPO,BMO,BPL,
C BML,SPOL,SMOL,SPO,SPL,SMO,
C SML,CTL,CRL,COL,CVL,COPOL,CWL,
```

```
C COPOL,COMOL/278528*(0.0,0.0)/
  DATA TIME,FREQ,FRQ2/24576*0.0/
  IFRAME=8192
  NR=30
  FNR=FLOAT(NR)
  P=0.0
  DO 70 L1=1,NR
C         THE DO LOOP ENDING WITH STATEMENT 70 ENABLES
C         THE PROGRAM TO PROCESS A LARGE AMOUNT OF DATA
C         BY REPEATING THE PROCESS IN BLOCKS.THE DATA
C         POINTS FROM EACH RUN THROUGH THE DO LOOP ARE
C         ADDED TOGETHER AND EVENTUALLY AVERAGED BY THE
C         NUMBER OF RUNS THROUGH THE DO LOOP. 'NR'
C         REPRESENTS THE NUMBER OF DATA SEQUENCES TO
C         BE AVERAGED. 1 SEQUENCE CURRENTLY EQUALS
C         8192 DATA POINTS FOR EACH CHANNEL OR 256
```

```
C           SECONDS OF DATA. FOR THIS TEST SINE AND
C           COSINE WAVES OF 4HZ WIL BE USED.
      DO 60 JJ=1,IFRAME
      XXO(JJ)=SIN(P*.785398163)
      YYO(JJ)=COS(P*.785398163)
      XXL(JJ)=SIN(P*.785398163)
      YYL(JJ)=COS(P*.785398163)
      P=P+1
   60 CONTINUE
C           THE FOLLOWING SECTION GENERATES THE TIME
C           AND FREQUENCY ARRAYS AND NORMALIZES
C           THE INPUT PCM DATA TO VOLTAGE FORM IN
C           PREPARATION FOR THE FAST FOURIER TRANSFORM
C           TO THE FREQUENCY DOMAIN.
      N=8192
      FN=FLOAT(N)
```

```
      DELTAT=1./32.
      T=FN*DELTAT
      DELTAF=1./T
      DO 20 J=1,N
      TIME(J)=DELTAT*FLOAT(J)
      FREQ(J)=DELTAF*FLOAT(J)
      FRQ2(J)=ALOG10(FREQ(J))
   20 CONTINUE
C         THE NEXT FOUR STATEMENTS PERFORM
C         AN FFT ON THE INPUT TIME SERIES
C         DATA.
      CALL FOURT(XXO,N,1,-1,0,WORK)
      CALL FOURT(YYO,N,1,-1,0,WORK)
      CALL FOURT(XXL,N,1,-1,0,WORK)
      CALL FOURT(YYL,N,1,-1,0,WORK)
      DO 40 K4=1,N
```

```
      XXO(K4)=XXO(K4)/FN
      YYO(K4)=YYO(K4)/FN
      XXL(K4)=XXL(K4)/FN
      YYL(K4)=YYL(K4)/FN
   40 CONTINUE
C          THE NEXT LOOP CALCULATES THE
C          UNNORMALIZED SPECTRAL DENSITIES
C          FOR SINGLE SITE ORTHOGONAL
C          COMPONENTS OF THE GEOMAGNETIC FIELD,
C          THE INDIVIDUAL SITE CROS SPECTRA
C          BETWEEN COMPONENTS, THE INDIVIDUAL
C          ORTHOGONAL COMPONENTS OF RIGHT AND
C          LEFT CIRCULARLY POLARIZED SPECTRA,
C          AND TWO SITE CROSS SPECTRA FOR RIGHT
C          AND LEFT CIRCULAR POLARIZATION.
      DO 30 II=1,N
```

```
ZXO(II)=ZXO(II)+(XXO(II)*CONJG(XXO(II)))

ZYO(II)=ZYO(II)+(YYO(II)*CONJG(YYO(II)))

CSO(II)=CSO(II)+(XXO(II)*CONJG(YYO(II)))

ZXL(II)=ZXL(II)+(XXL(II)*CONJG(XXL(II)))

ZYL(II)=ZYL(II)+(YYL(II)*CONJG(YYL(II)))

CSL(II)=CSL(II)+(XXL(II)*CONJG(YYL(II)))

BPO(II)=XXO(II)+((0.,1.)*YYO(II))

BMO(II)=XXO(II)-((0.,1.)*YYO(II))

BPL(II)=XXL(II)+((0.,1.)*YYL(II))

BML(II)=XXL(II)-((0.,1.)*YYL(II))

SPOL(II)=SPOL(II)+(BPO(II)*CONJG(BPL(II)))

SMOL(II)=SMOL(II)+(BMO(II)*CONJG(BML(II)))

SPO(II)=SPO(II)+(BPO(II)*CONJG(BPO(II)))

SPL(II)=SPL(II)+(BPL(II)*CONJG(BPL(II)))

SMO(II)=SMO(II)+(BMO(II)*CONJG(BMO(II)))

SML(II)=SML(II)+(BML(II)*CONJG(BML(II)))
```

```
  30  CONTINUE
  70  CONTINUE
C           THE NEXT LOOP NORMALIZES THE  ABOVE
C           SPECTRA AND CALCULATES POWER SPECTRAL
C           DENSITIES.
      DO 33 I3=1,N
      ZXO(I3)=ZXO(I3)*T/FNR
      ZYO(I3)=ZYO(I3)*T/FNR
      CSO(I3)=CSO(I3)*T/FNR
      ZXL(I3)=ZXL(I3)*T/FNR
      ZYL(I3)=ZYL(I3)*T/FNR
      CSL(I3)=CSL(I3)*T/FNR
      SPOL(I3)=SPOL(I3)*T/FNR
      SPO(I3)=SPO(I3)*T/FNR
      SPL(I3)=SPL(I3)*T/FNR
      SMO(I3)=SMO(I3)*T/FNR
```

```
      SML(I3)=SML(I3)*T/FNR
      SMOL(I3)=SMOL(I3)*T/FNR
   33 CONTINUE
C          THE NEXT LOOP CALCULATES STOKES
C          PARAMETERS 0 THROUGH 3 OF THE
C          INDIVIDUAL SITE ORTHOGONAL
C          COMPONENTS AND THE COHERENCE OF
C          THE PLANAR CIRCULAR POLARIZATION
C          PARAMETERS BETWEEN SITES.
      DO 44 I4=1,N
      CTO(I4)=(ZXO(I4)+ZYO(I4))*2./T
      CPO(I4)=(ZXO(I4)-ZYO(I4))*2./(T*CTO(I4))
      CRO(I4)=(4*CSO(I4))/(CTO(I4)*T)
      COO(I4)=CSO(I4)/(CSQRT(ZXO(I4))*CSQRT(ZYO(I4)))
      CWO(I4)=ATAN2(AIMAG(COO(I4)),REAL(COO(I4)))
      COO(I4)=CSQRT(COO(I4)*CONJG(COO(I4)))
```

```
CTO(I4)=4.3429448*CLOG(CTO(I4))

CUO(I4)=4.3429448*CLOG(ZXO(I4))

CVO(I4)=4.3429448*CLOG(ZYO(I4))

CTL(I4)=(ZXL(I4)+ZYL(I4))*2./T

CPL(I4)=(ZXL(I4)-ZYL(I4))*2./(T*CTL(I4))

CRL(I4)=(4*CSL(I4))/(CTL(I4)*T)

COL(I4)=CSL(I4)/(CSQRT(ZXL(I4))*CSQRT(ZYL(I4)))

CTL(I4)=4.3429448*CLOG(CTL(I4))

CUL(I4)=4.3429448*CLOG(ZXL(I4))

CVL(I4)=4.3429448*CLOG(ZYL(I4))

CWL(I4)=ATAN2(AIMAG(COL(I4)),REAL(COL(I4)))

COL(I4)=CSQRT(COL(I4)*CONJG(COL(I4)))

COPOL(I4)=SPOL(I4)/(CSQRT(SPO(I4))*CSQRT(SPL(I4)))

COPOL(I4)=CSQRT(COPOL(I4)*CONJG(COPOL(I4)))

COMOL(I4)=SMOL(I4)/(CSQRT(SMO(I4))*CSQRT(SML(I4)))

COMOL(I4)=CSQRT(COMOL(I4)*CONJG(COMOL(I4)))
```

```
      SPO(I4)=4.3429448*CLOG(SPO(I4))
      SPL(I4)=4.3429448*CLOG(SPL(I4))
      SMO(I4)=4.3429448*CLOG(SMO(I4))
      SML(I4)=4.3429448*CLOG(SML(I4))
   44 CONTINUE
C          VERSATEC PLOT OF CALCULATED QUANTITIES
      NPTS=10./DELTAF+1.
C          'NPTS' DETERMINES NUMBER OF POINTS
C          NECESSARY TO PLOT THE 0 TO 10 HERTZ RANGE.
      ITB(2)=0
      ITB(3)=20
      ITB(4)=10
      ITB(6)=1
      ITB(7)=1
      ITB(12)=1
      RTB(1)=0
```

```
RTB(2)=0
RTB(3)=ALAB(1)
READ(5,3000)TITLE
CALL DRAWP(NPTS,FRQ2,CUOO,ITB,RTB)
ITB(6)=1
RTB(3)=ALAB(2)
READ(5,3000)TITLE
CALL DRAWP(NPTS,FRQ2,CVOO,ITB,RTB)
ITB(6)=1
RTB(3)=ALAB(3)
READ(5,3000)TITLE
CALL DRAWP(NPTS,FREQ,CPOO,ITB,RTB)
ITB(6)=1
RTB(3)=ALAB(4)
READ(5,3000)TITLE
CALL DRAWP(NPTS,FREQ,CROO,ITB,RTB)
```

```
ITB(6)=1
RTB(3)=ALAB(5)
READ(5,3000)TITLE
CALL DRAWP(NPTS,FREQ,CROO(2),ITB,RTB)
ITB(6)=1
RTB(3)=ALAB(6)
READ(5,3000)TITLE
CALL DRAWP(NPTS,FRQ2,CTOO,ITB,RTB)
ITB(6)=1
RTB(3)=ALAB(7)
READ(5,3000)TITLE
CALL DRAWP(NPTS,FREQ,CWOO,ITB,RTB)
ITB(6)=1
RTB(3)=ALAB(8)
READ(5,3000)TITLE
CALL DRAWP(NPTS,FREQ,COOO,ITB,RTB)
```

```
ITB(6)=1
RTB(3)=ALAB(9)
READ(5,3000)TITLE
CALL DRAWP(NPTS,FRQ2,CULL,ITB,RTB)
ITB(6)=1
RTB(3)=ALAB(10)
READ(5,3000)TITLE
CALL DRAWP(NPTS,FRQ2,CVLL,ITB,RTB)
ITB(6)=1
RTB(3)=ALAB(11)
READ(5,3000)TITLE
CALL DRAWP(NPTS,FREQ,CPLL,ITB,RTB)
ITB(6)=1
RTB(3)=ALAB(12)
READ(5,3000)TITLE
CALL DRAWP(NPTS,FREQ,CRLL,ITB,RTB)
```

```
ITB(6)=1
RTB(3)=ALAB(13)
READ(5,3000) TITLE
CALL DRAWP(NPTS,FREQ,CRLL(2),ITB,RTB)
ITB(6)=1
RTB(3)=ALAB(14)
READ(5,3000) TITLE
CALL DRAWP(NPTS,FRQ2,CTLL,ITB,RTB)
ITB(6)=1
RTB(3)=ALAB(15)
READ(5,3000) TITLE
CALL DRAWP(NPTS,FREQ,CWLL,ITB,RTB)
ITB(6)=1
RTB(3)=ALAB(16)
READ(5,3000) TITLE
CALL DRAWP(NPTS,FREQ,COLL,ITB,RTB)
```

```
ITB(6)=1

RTB(3)=ALAB(17)

READ(5,3000) TITLE

CALL DRAWP(NPTS,FRQ2,SPOO,ITB,RTB)

ITB(6)=1

RTB(3)=ALAB(18)

READ(5,3000) TITLE

CALL DRAWP(NPTS,FRQ2,SPLL,ITB,RTB)

ITB(6)=1

RTB(3)=ALAB(19)

READ(5,3000) TITLE

CALL DRAWP(NPTS,FRQ2,SMOO,ITB,RTB)

ITB(6)=1

RTB(3)=ALAB(20)

READ(5,3000) TITLE

CALL DRAWP(NPTS,FRQ2,SMLL,ITB,RTB)
```

```
      ITB(6)=1
      RTB(3)=ALAB(21)
      READ(5,3000)TITLE
      CALL DRAWP(NPTS,FREQ,COPOLL,ITB,RTB)
      ITB(6)=1
      RTB(3)=ALAB(22)
      READ(5,3000)TITLE
      CALL DRAWP(NPTS,FREQ,COMOLL,ITB,RTB)
 3000 FORMAT(6A8)
      STOP
      END
/*
//GO.SYSIN DD *
TEST POWER SPECTRAL DENSITY OF SIN 4HZ
IN XXO,30 AVGS,(REF DB VS LOG FREQ)
TEST POWER SPECTRAL DENSITY OF COS 4HZ
```

```
IN YYO,30 AVGS,(REF DB VS LOG FREQ)

TEST STOKES 1/STOKES 0 OF SIN 4HZ

IN XXO AND COS 4HZ IN YYO,30 AVGS

TEST STOKES 2/STOKES 0 OF SIN 4HZ

IN XXO AND COS 4HZ IN YYO,30 AVGS

TEST STOKES 3/STOKES 0 OF SIN 4HZ

IN XXO AND COS 4HZ IN YYO,30 AVGS

TEST STOKES 0 OF SIN 4HZ IN XXO AND

COS 4HZ IN YYO,30 AVGS,(REF DB VS LOG)

TEST PHASE OF SIN 4HZ IN XXO

AND COS 4HZ IN YYO,30 AVGS

TEST COHER OF SIN 4HZ IN XXO

AND COS 4HZ IN YYO,30 AVGS

TEST POWER SPECTRAL DENSITY OF SIN 4HZ

IN XXL,30 AVGS,(REF DB VS LOG FREQ)

TEST POWER SPECTRAL DENSITY OF COS 4HZ
```

```
IN YYL,30 AVGS.(REF DB VS LOG FREQ)

TEST STOKES 1/STOKES 0 OF SIN 4HZ

IN XXL AND COS 4HZ IN YYL,30 AVGS

TEST STOKES 2/STOKES 0 OF SIN 4HZ

IN XXL AND COS 4HZ IN YYL,30 AVGS

TEST STOKES 3/STOKES 0 OF SIN 4HZ

IN XXL AND COS 4HZ IN YYL,30 AVGS

TEST STOKES 0 OF SIN 4HZ IN XXL AND

COS 4HZ IN YYL,30 AVGS,(REF DB VS LOG)

TEST PHASE OF SIN 4HZ IN XXL

AND COS 4HZ IN YYL,30 AVGS

TEST COHER CF SIN 4HZ IN XXL

AND COS 4HZ IN YYL,30 AVGS

TEST RT CIRC POLARIZATION PSD OF SIN 4HZ IN

XXO AND COS 4HZ IN YYO, (DB VS LOG),30 AVGS

TEST RT CIRC POLARIZATION PSD OF SIN 4HZ IN
```

```
XXL AND COS 4HZ IN YYL, (DB VS LOG),30 AVGS

TEST LEFT CIRC POLARIZATION PSD OF SIN 4HZ

IN XXO AND COS 4HZ IN YYO (DB VS LOG),30 AVGS

TEST LEFT CIRC POLARIZATION PSD OF SIN 4HZ

IN XXL AND COS 4HZ IN YYL (DB VS LOG),30 AVGS

TEST COHER RT CIRC POLARIZATION OF SIN 4HZ

IN XXO,XXL AND COS 4HZ IN YYO,YYL, 30 AVGS

TEST COHER LEFT CIRC POLARIZATION OF SIN 4HZ

IN XXO,XXL AND COS 4HZ IN YYO,YYL, 30 AVGS

/*

//
```

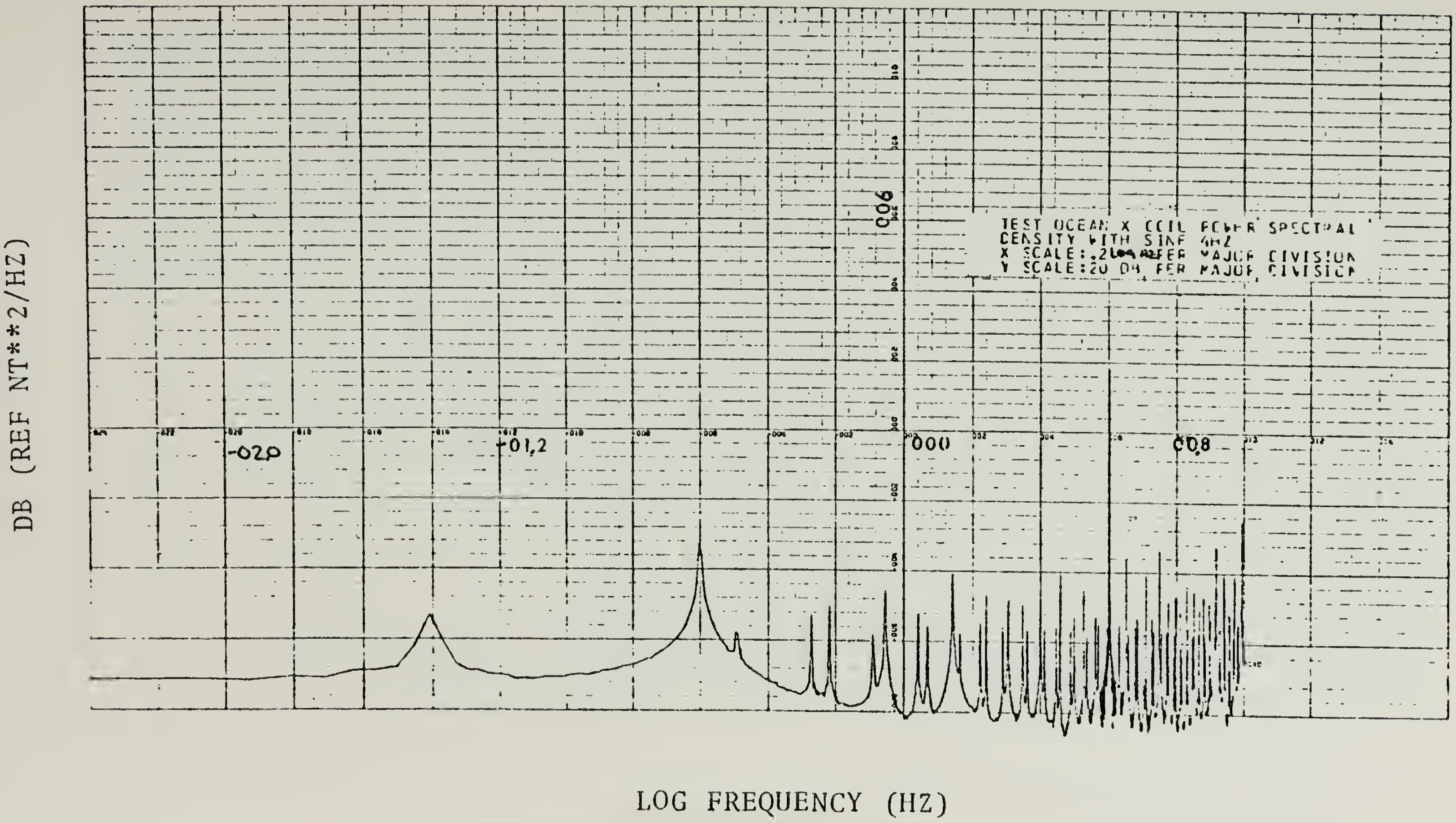

Figure A.1 Test Ocean x Coil Power Spectral Density

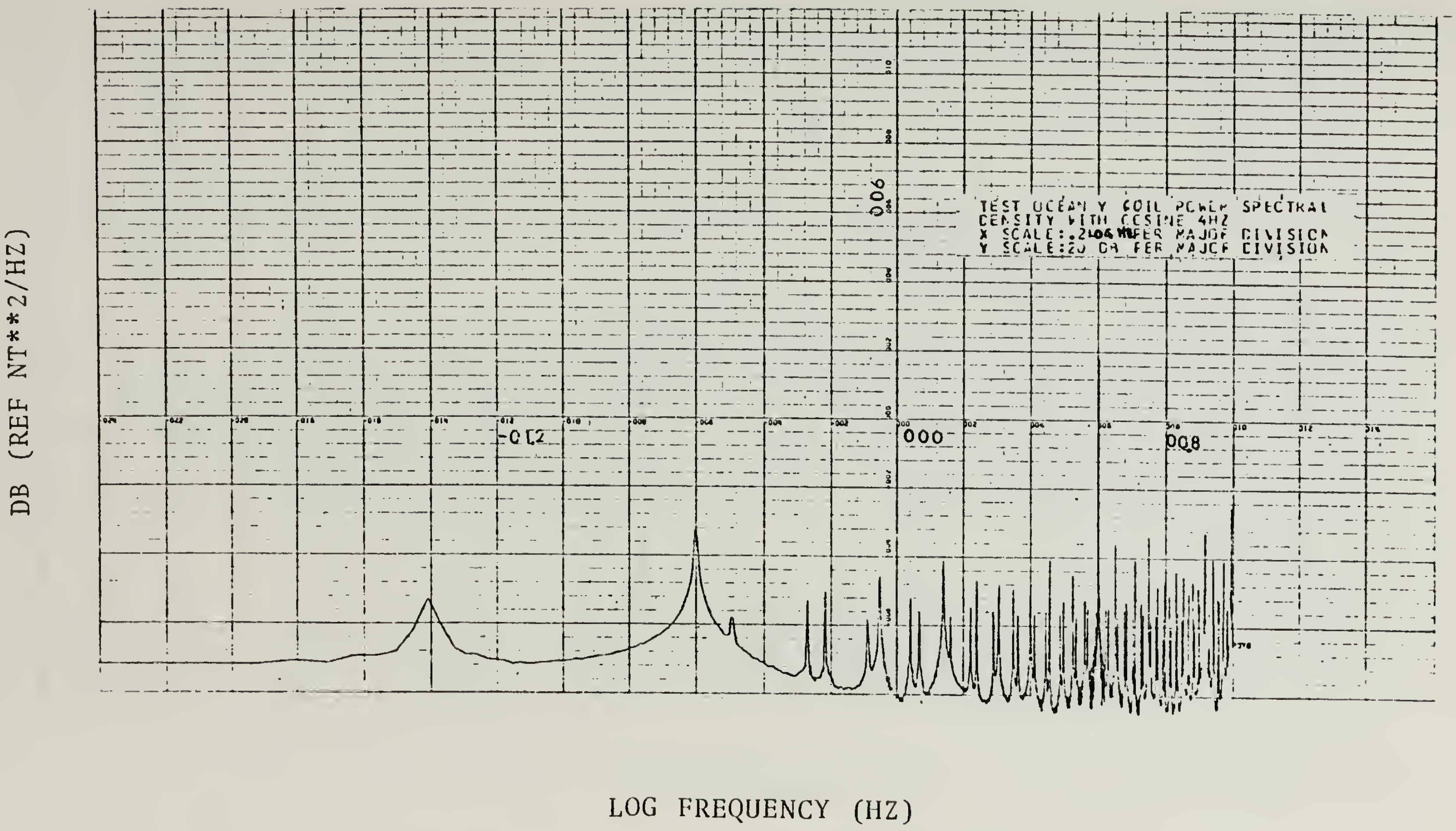

Figure A.2 Test Ocean y Coil Power Spectral Density

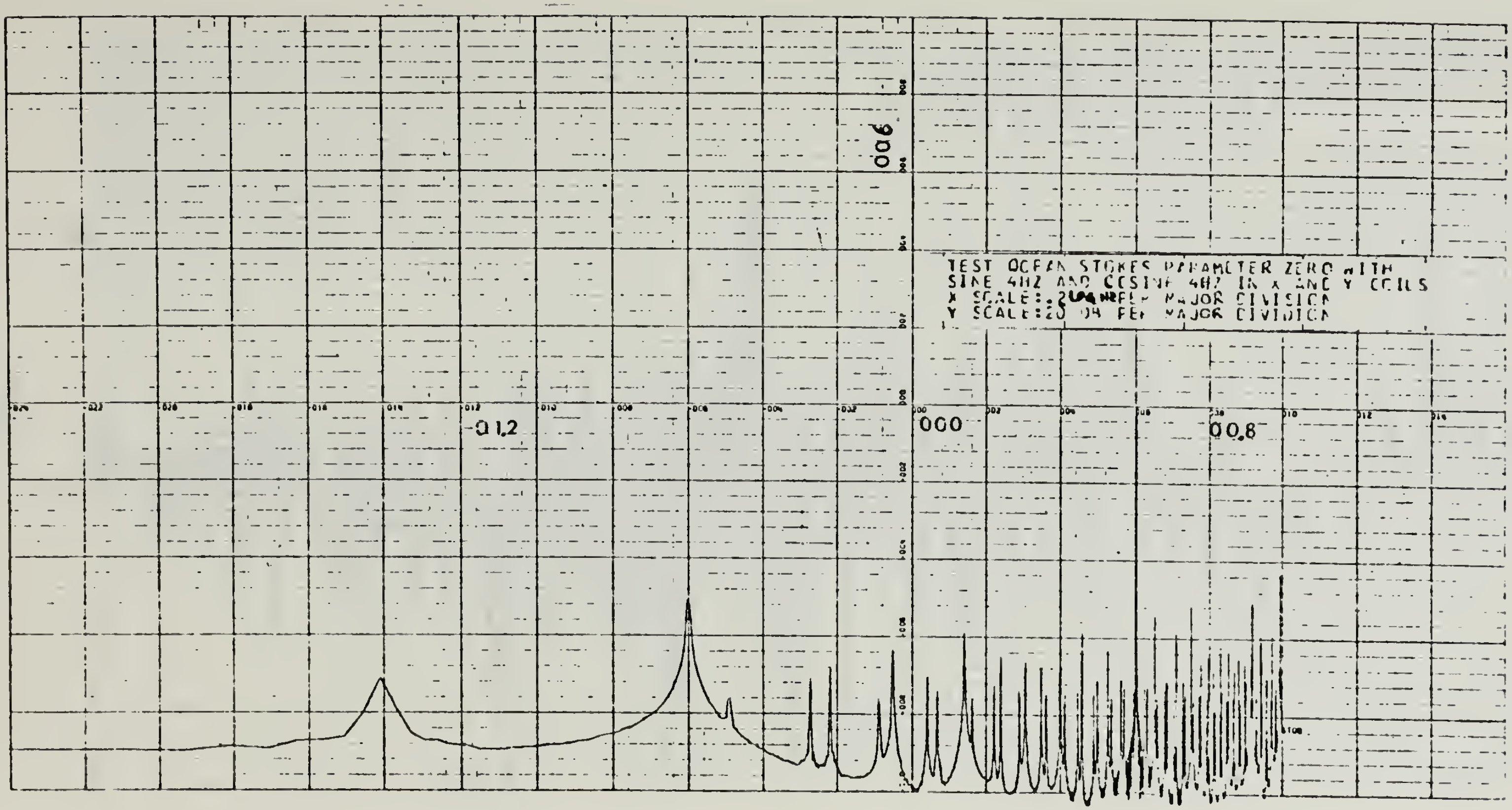

LOG FREQUQNCY (HZ)

Figure A.3 Test Ocean Stokes Parameter Zero

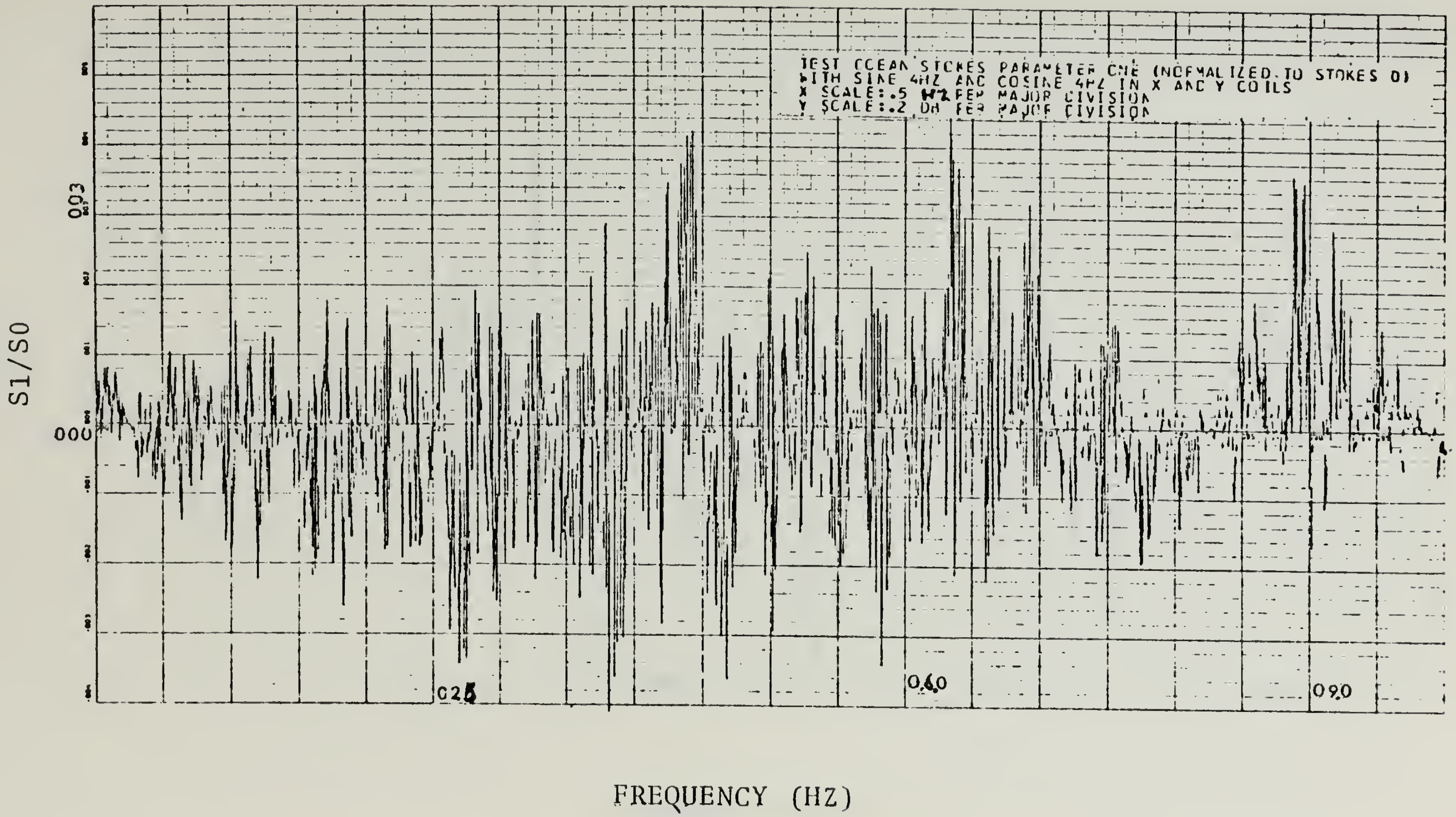

Figure A.4 Test Ocean Stokes Parameter One

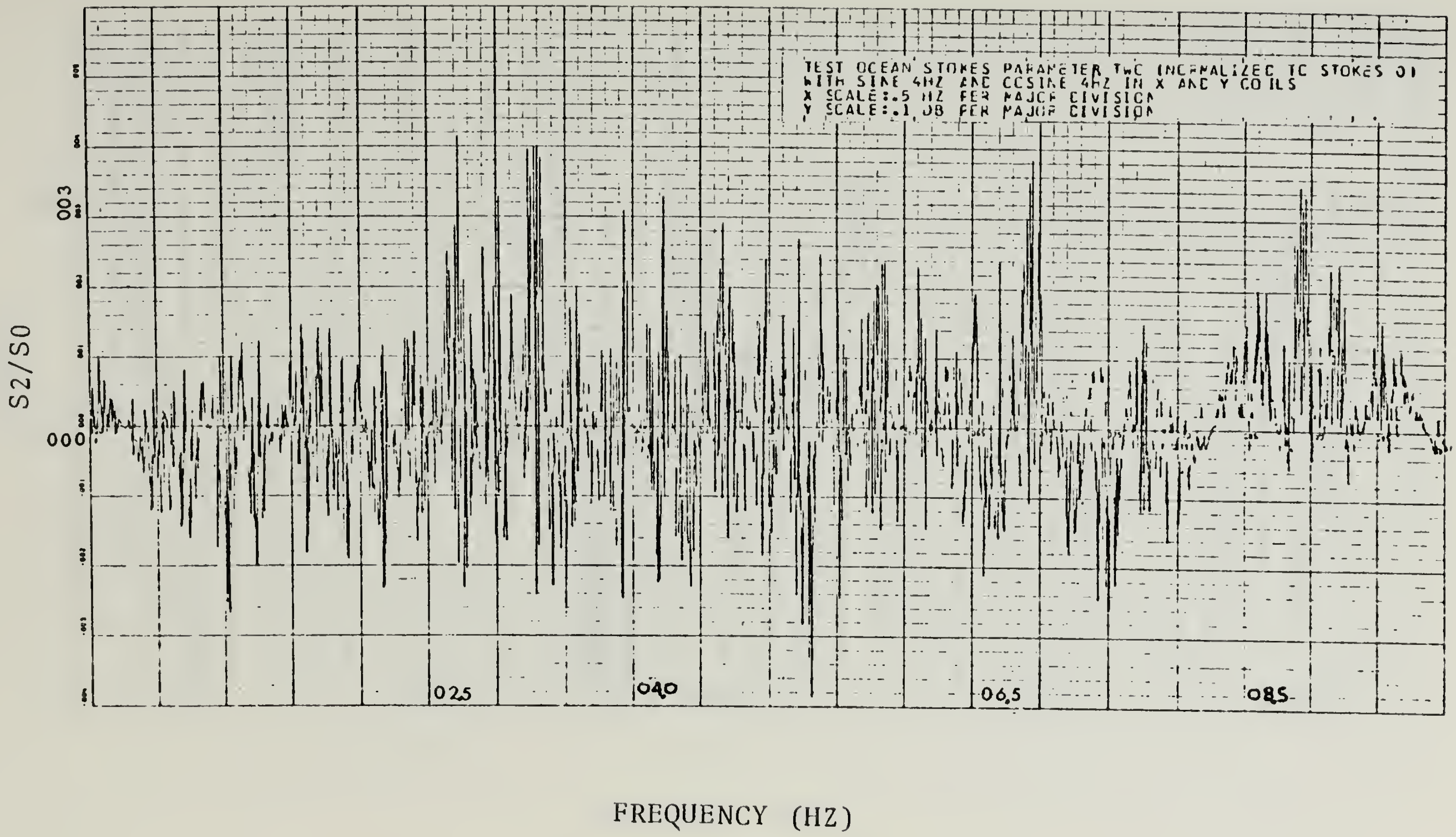

Figure A.5 Test Ocean Stokes Parameter Two

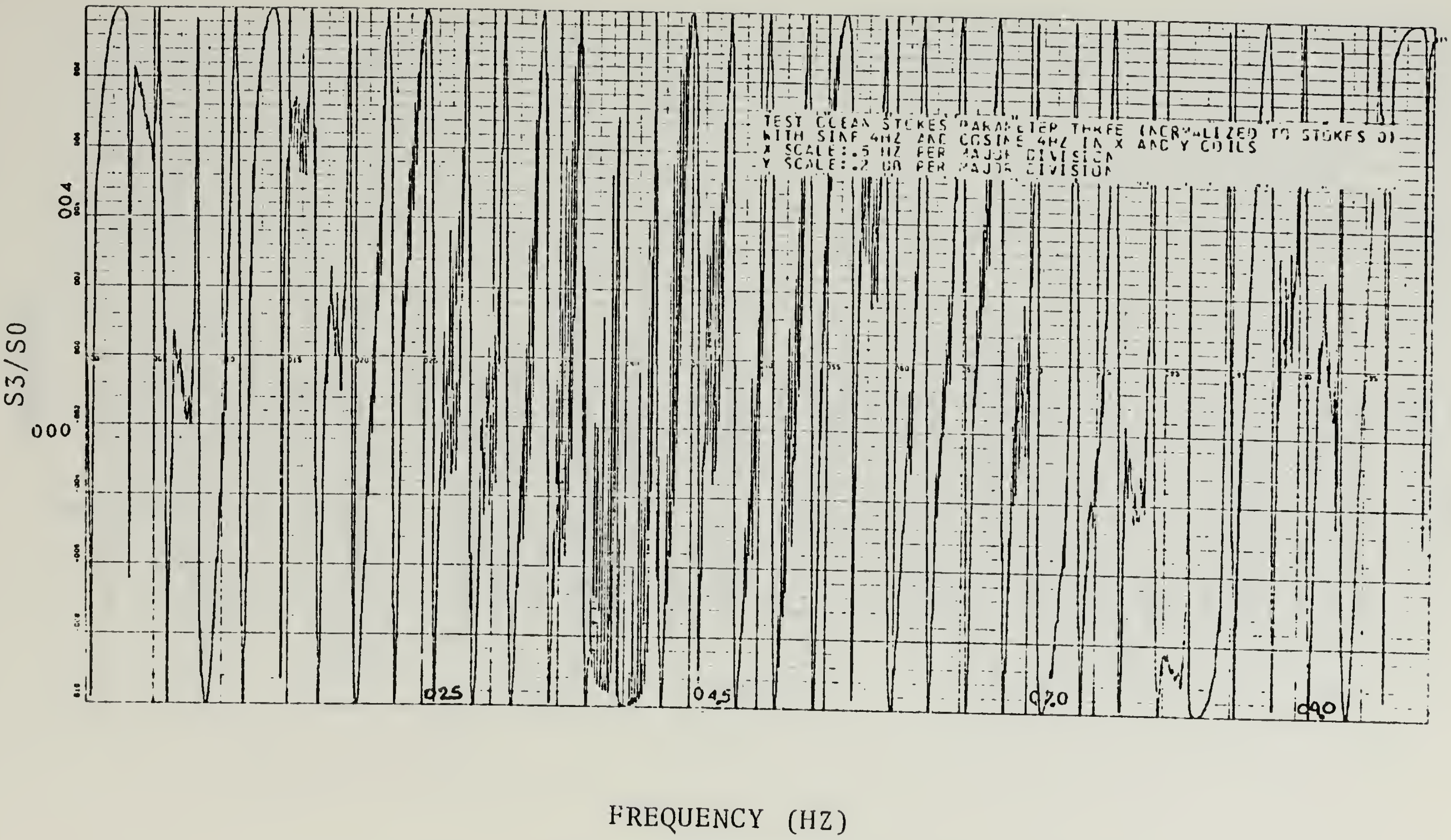

Figure A.6 Test Ocean Stokes Parameter Three

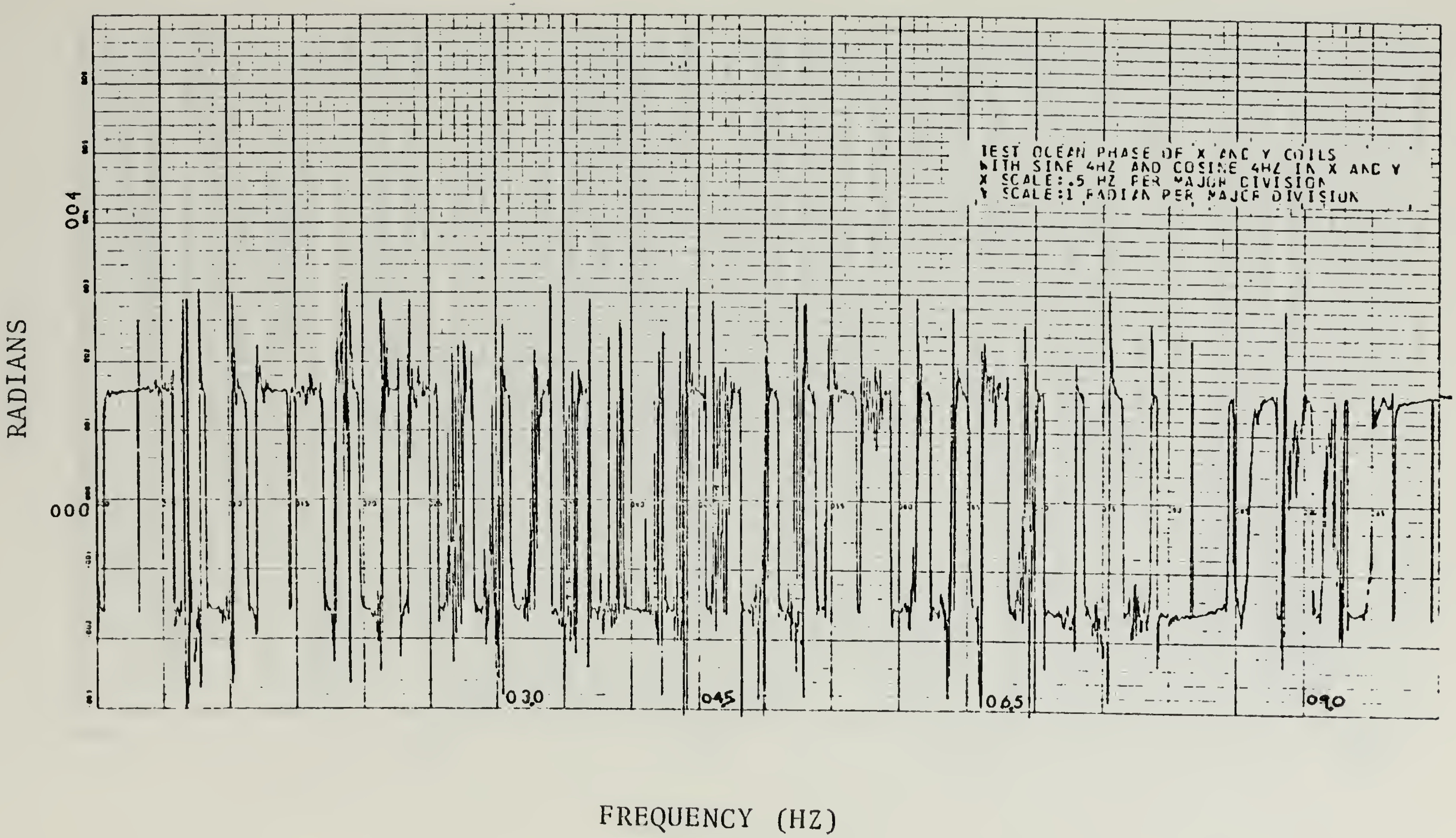

Figure A.7 Test Ocean Phase of x and y Coils

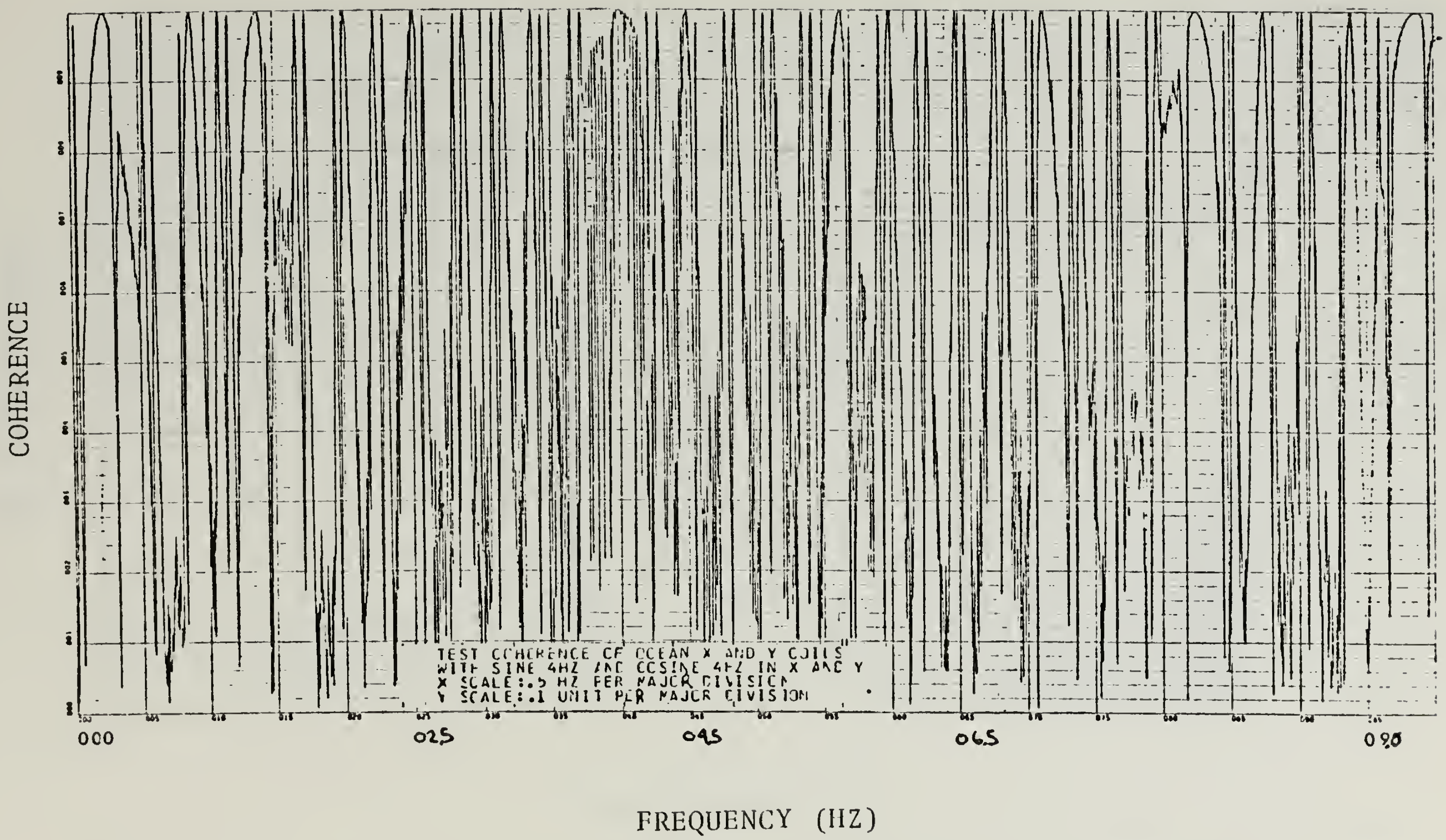

Figure A.8 Test Coherence of Ocean x and y Coils

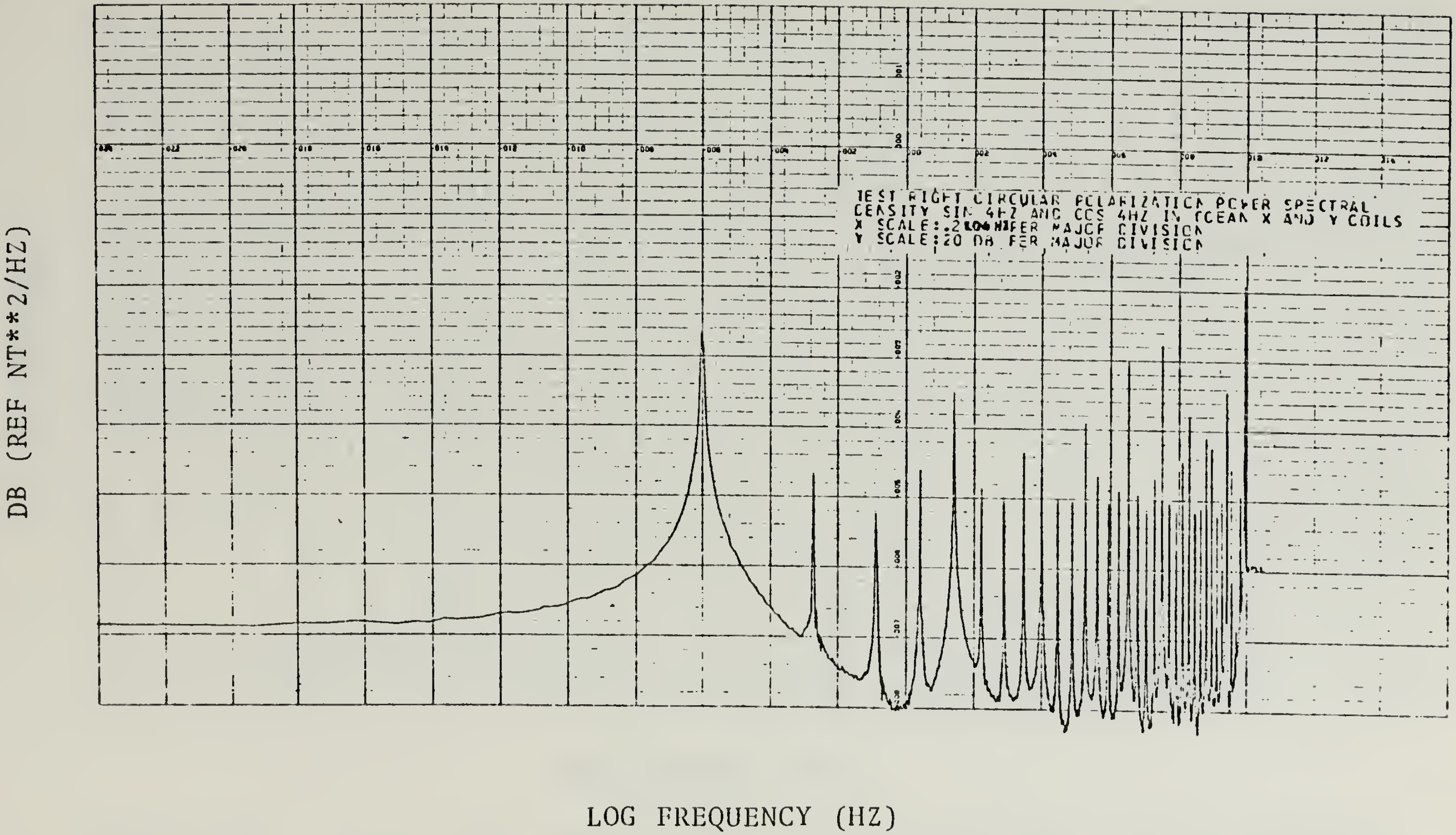

Figure A.9 Test Ocean Right Circular Polarization Power Spectral Density

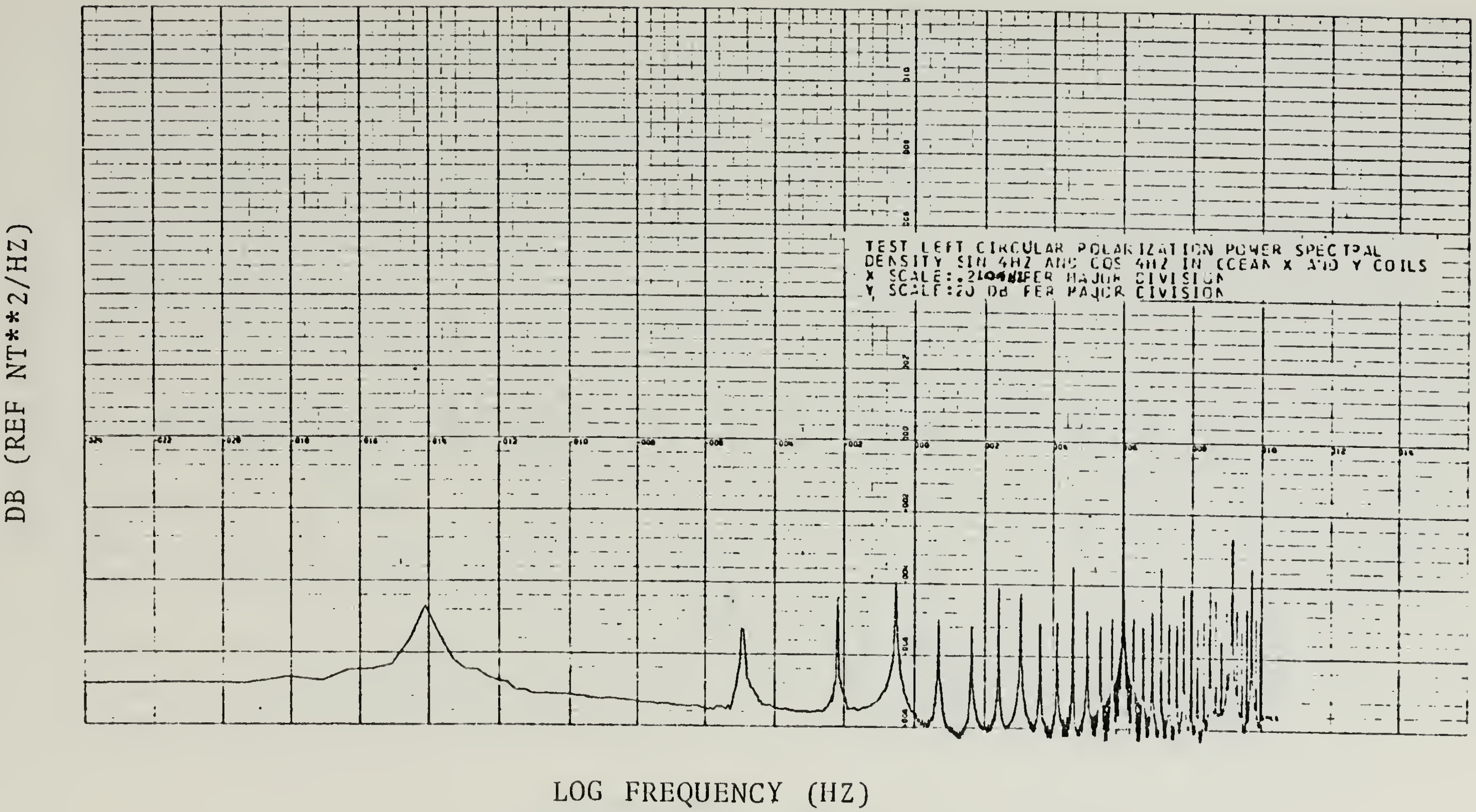

Figure A.10 Test Ocean Left Circular Polarization Power Spectral Density

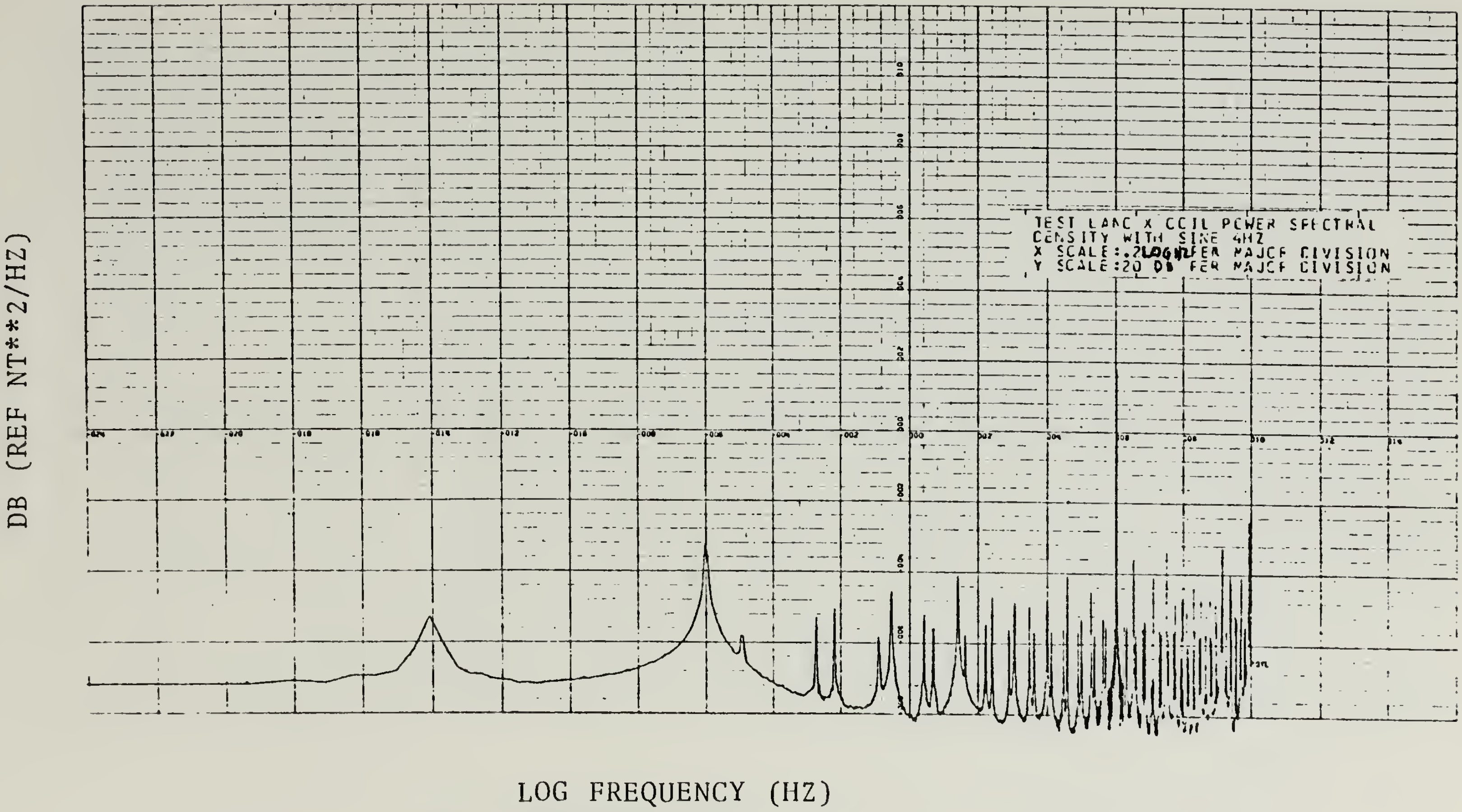

Figure A.11 Test Land x Coil Power Spectral Density

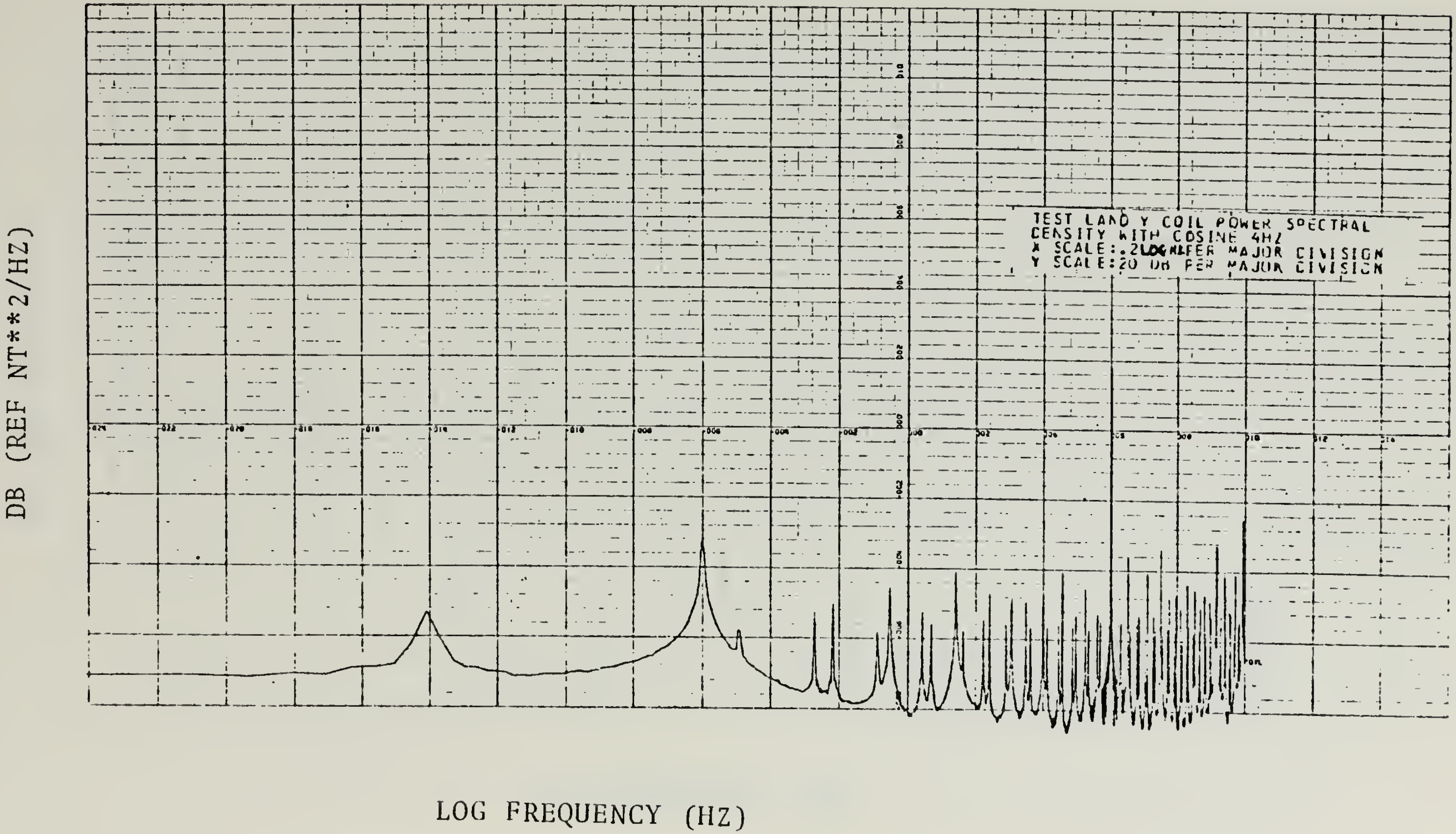

Figure A.12 Test Land y Coil Power Spectral Density

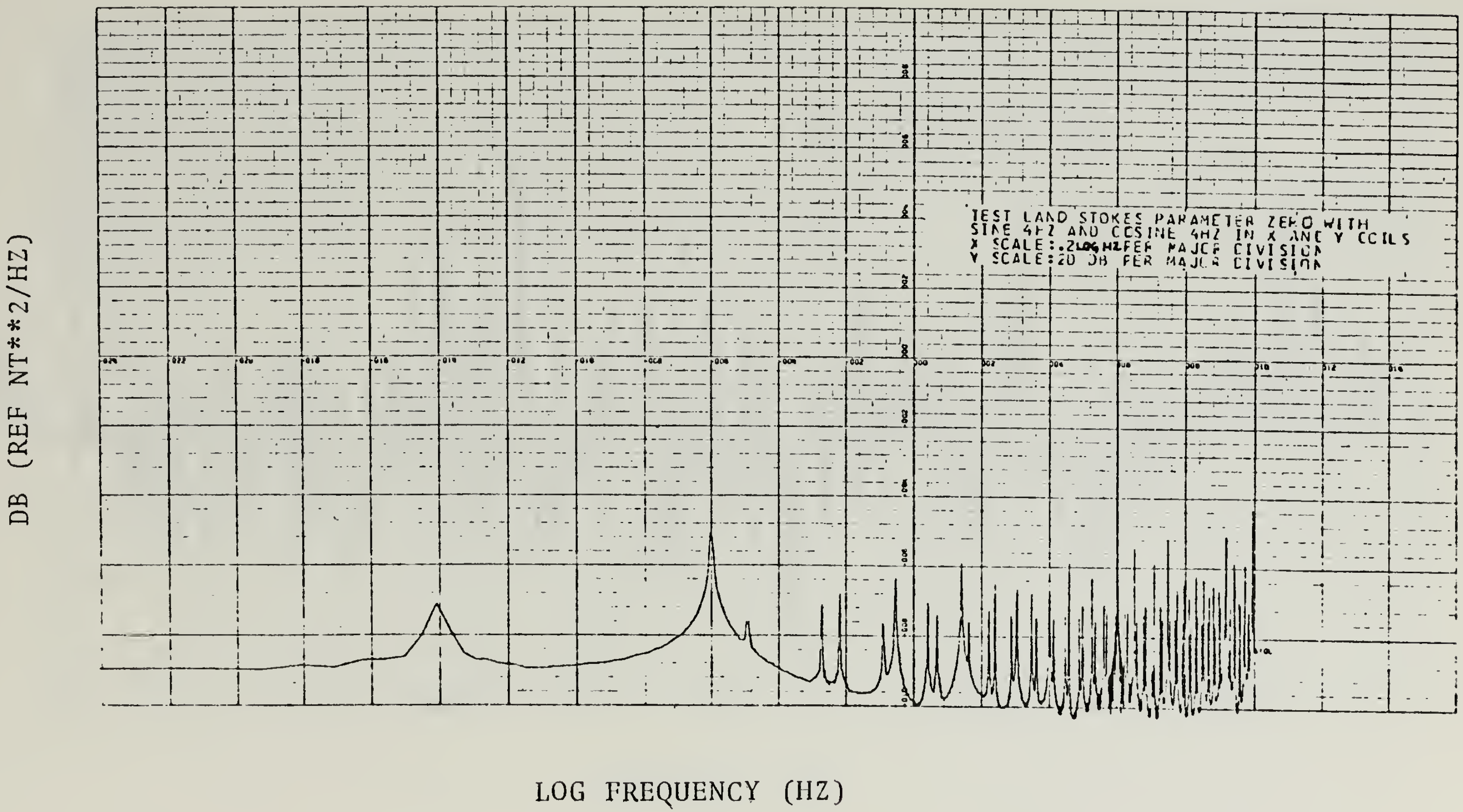

Figure A.13 Test Land Stokes Parameter Zero

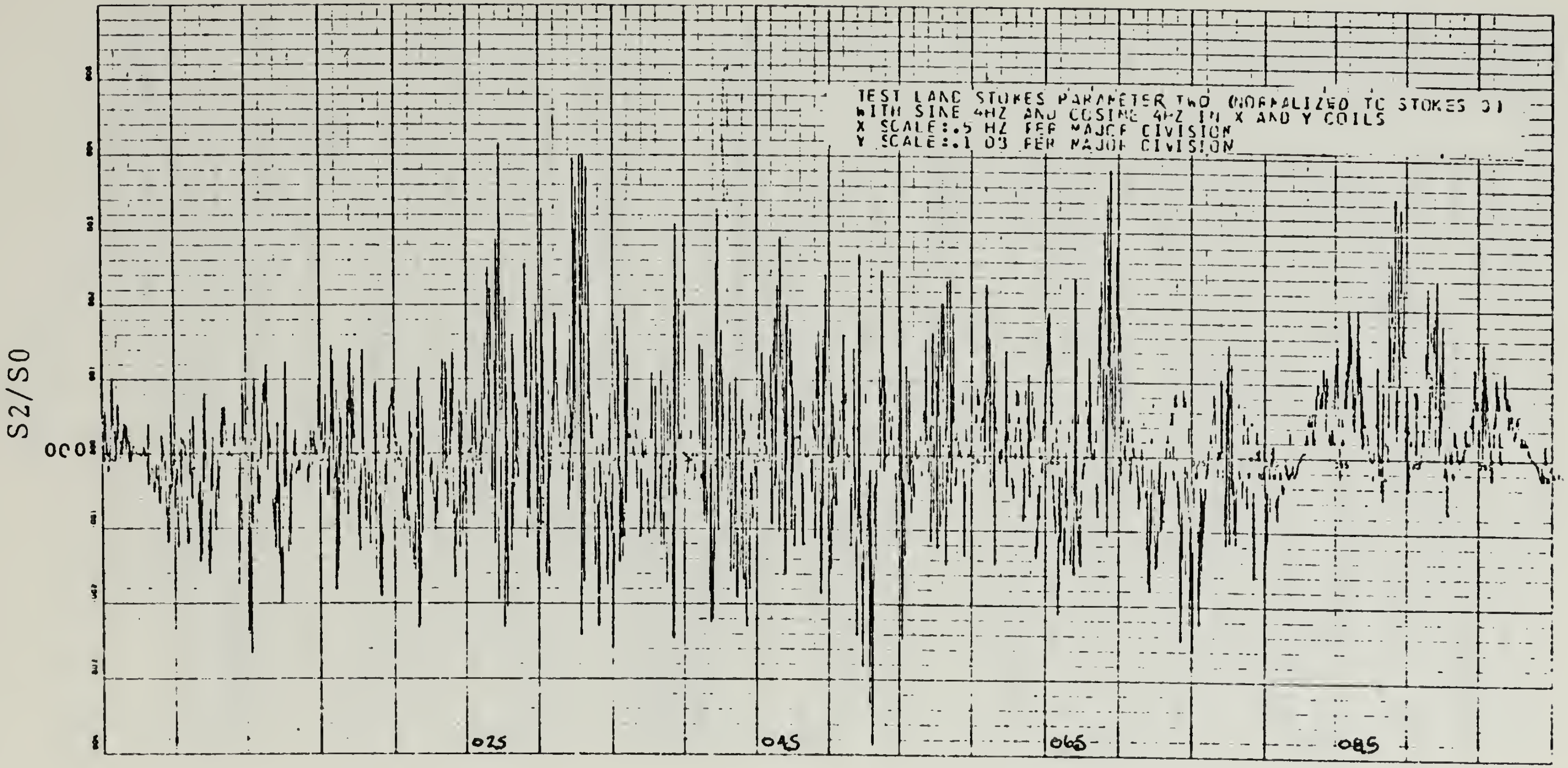

Figure A.14 Test Land Stokes Parameter Two

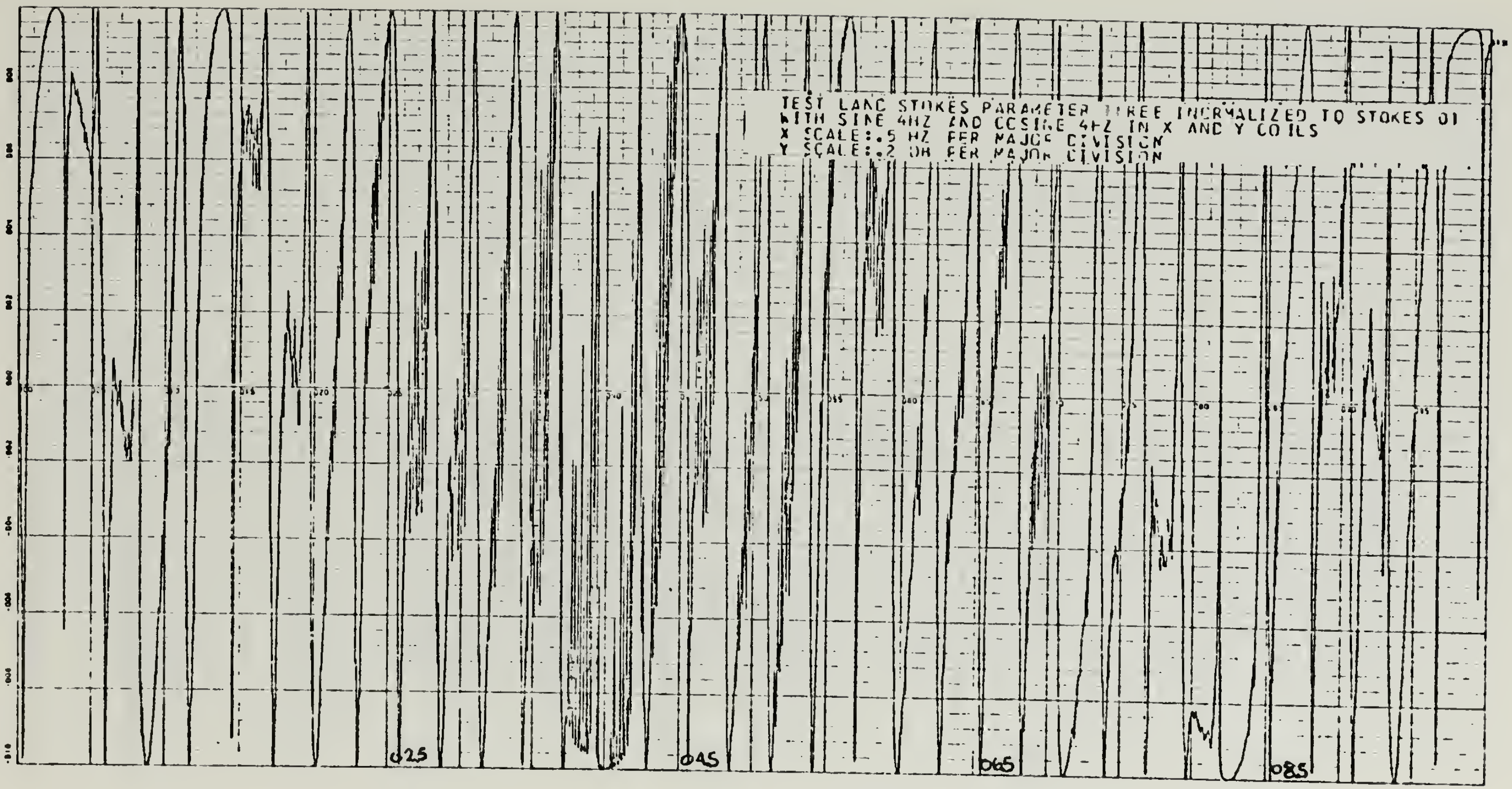

Figure A.15 Test Land Stokes Parameter Three

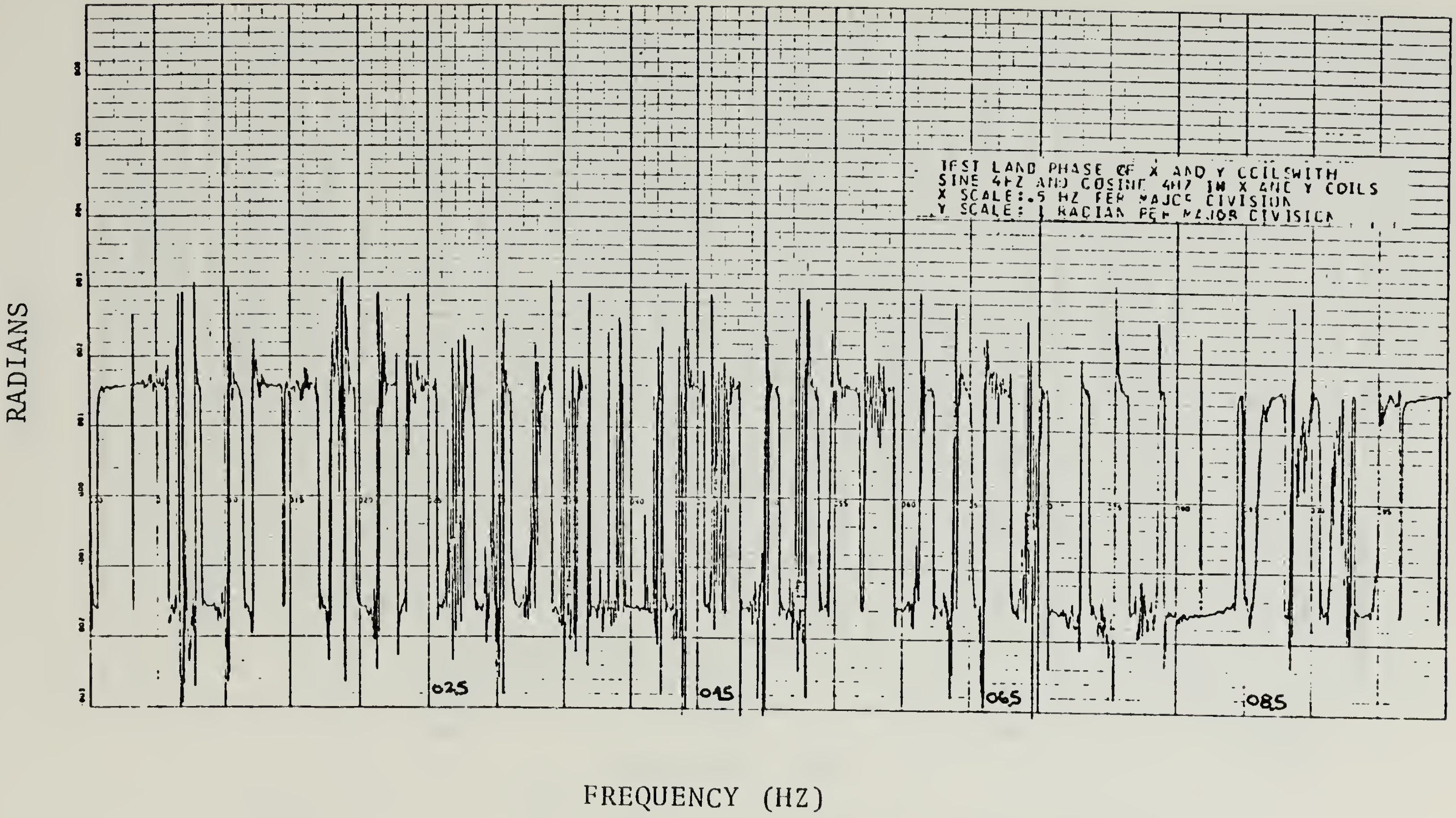

Figure A.16 Test Land Phase of x and y Coils

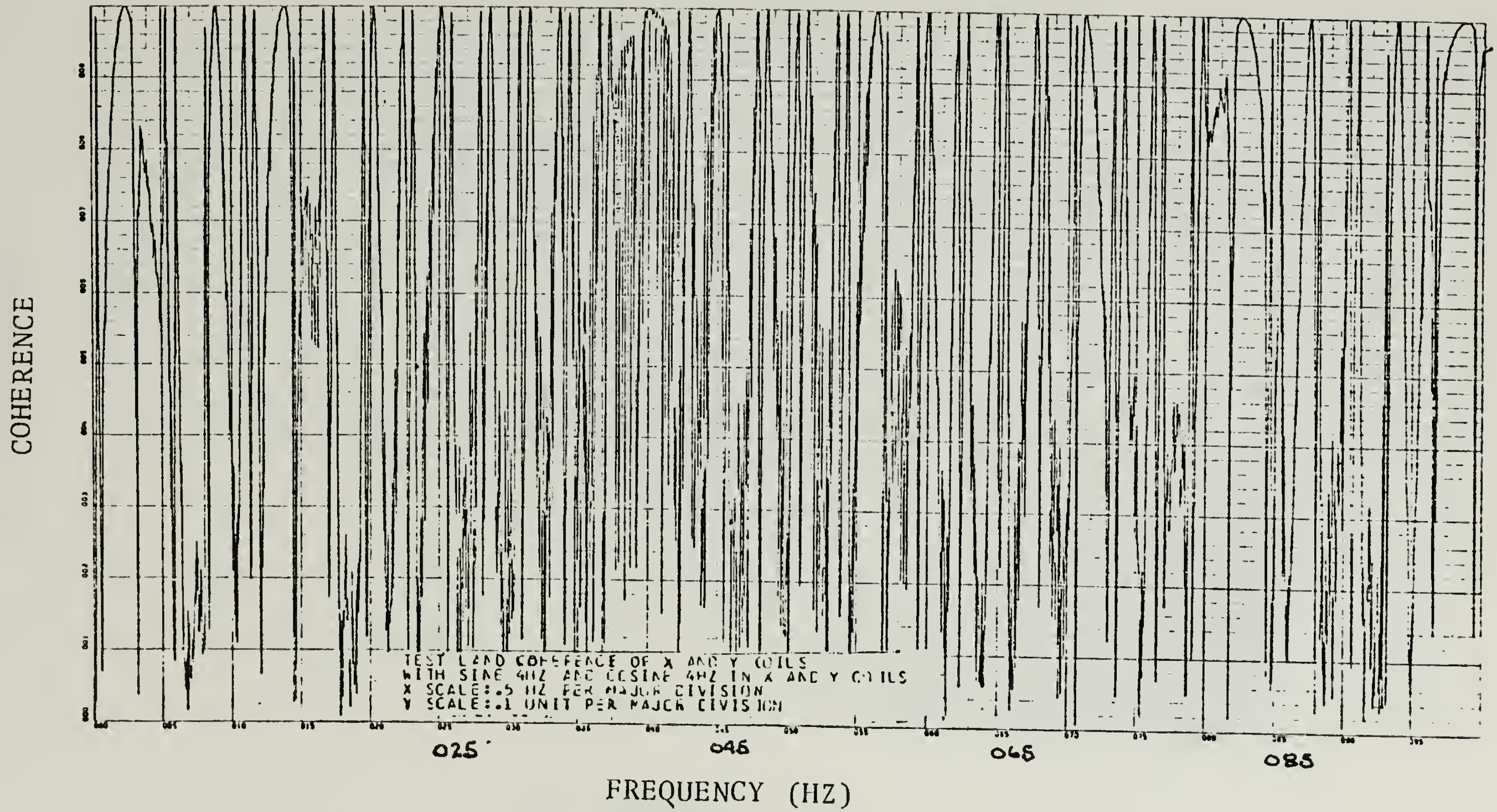

Figure A.17 Test Land Coherence of x and y Coils

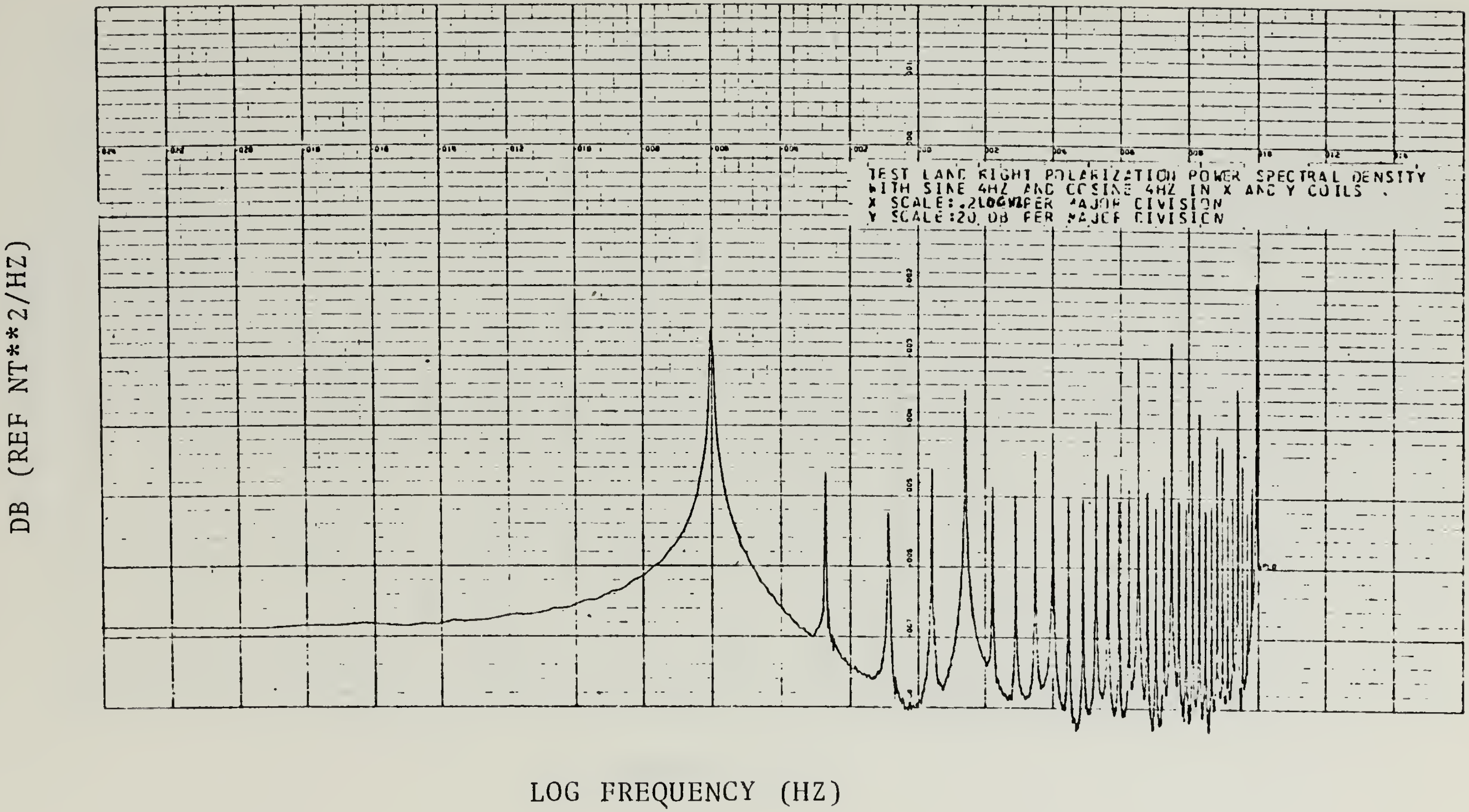

Figure A.18 Test Land Right Polarization Power Spectral Density

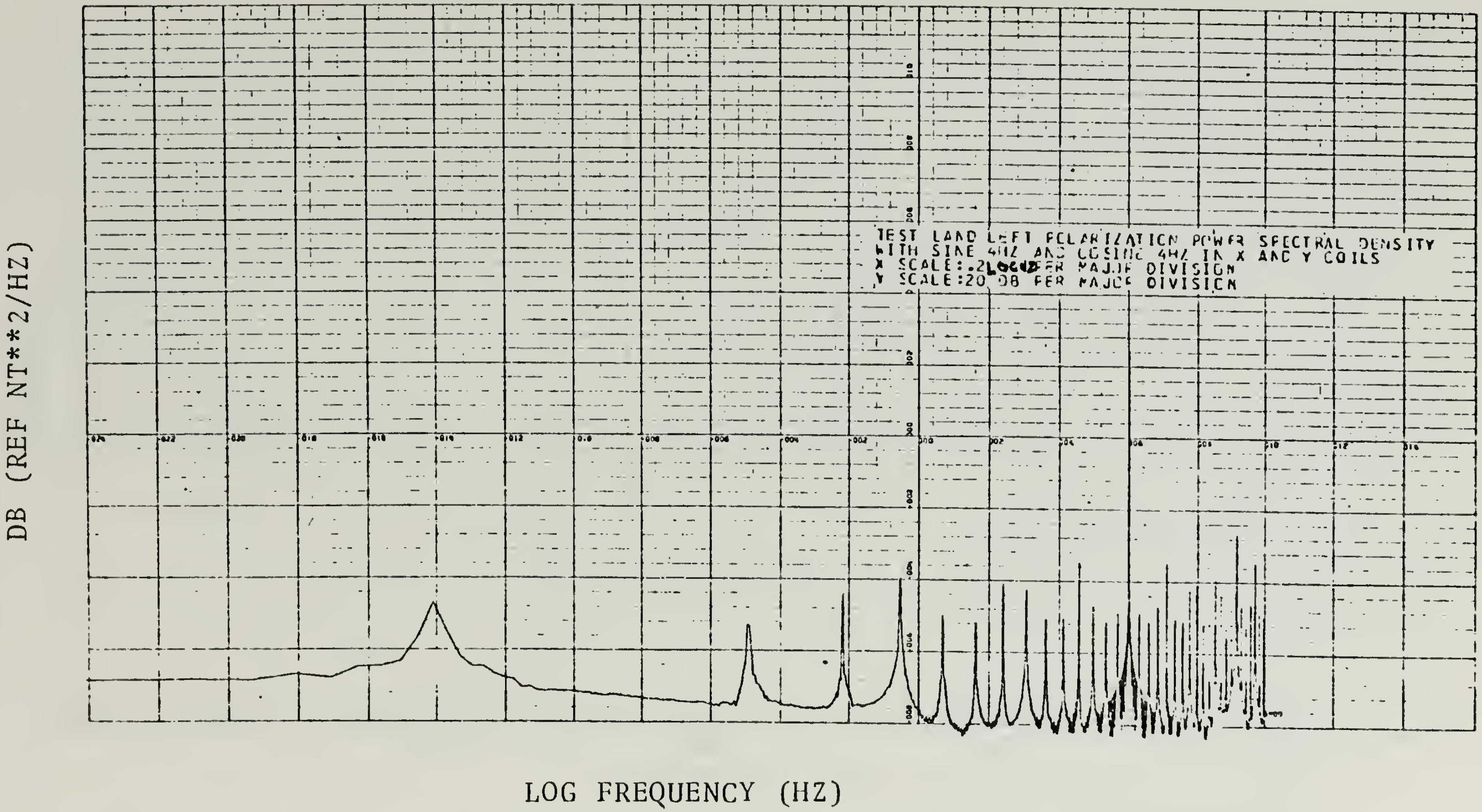

Figure A.19 Test Land Left Polarization Power Spectral Density

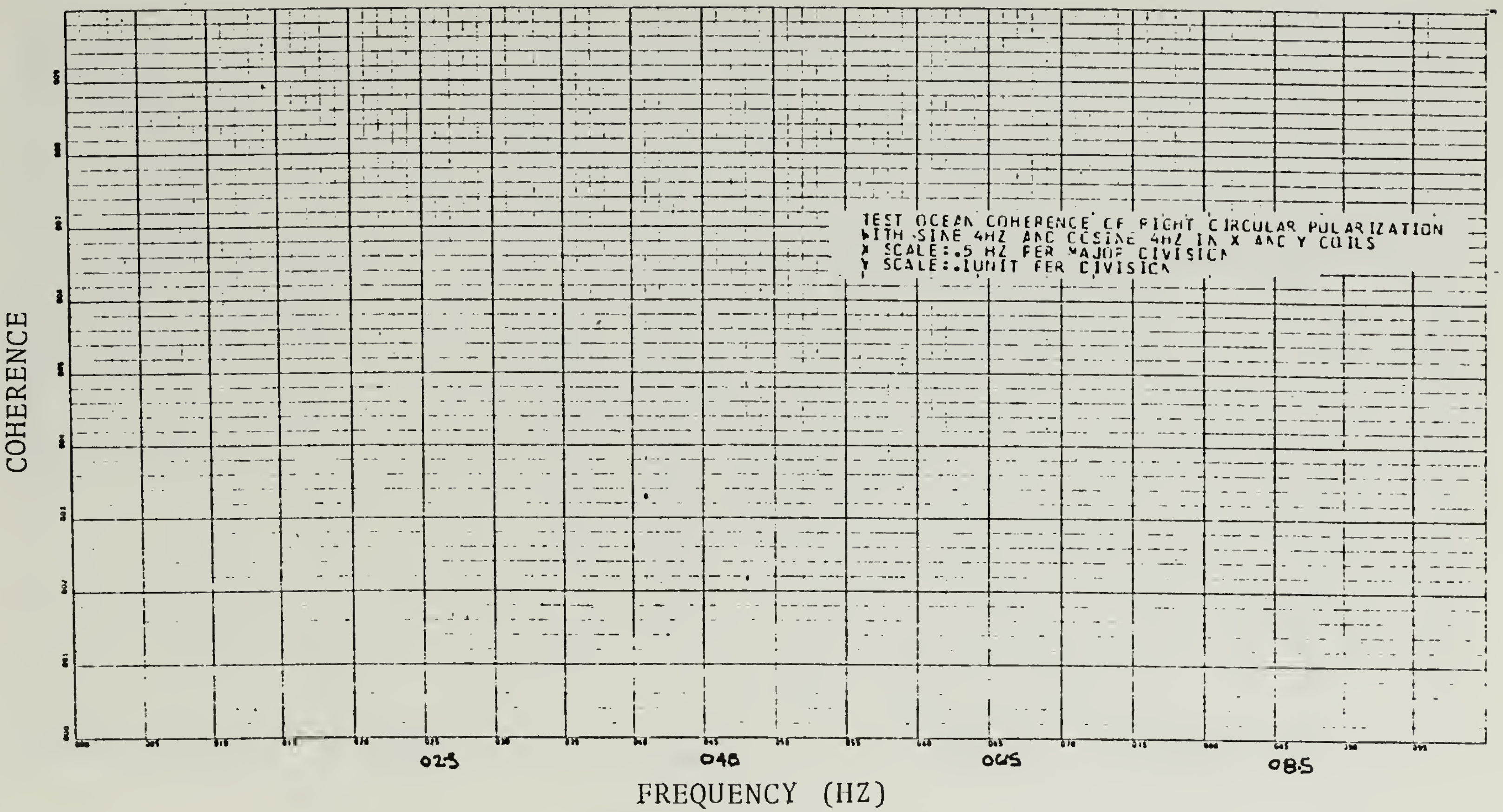

Figure A.20 Test Ocean Coherence of Right Circular Polarization

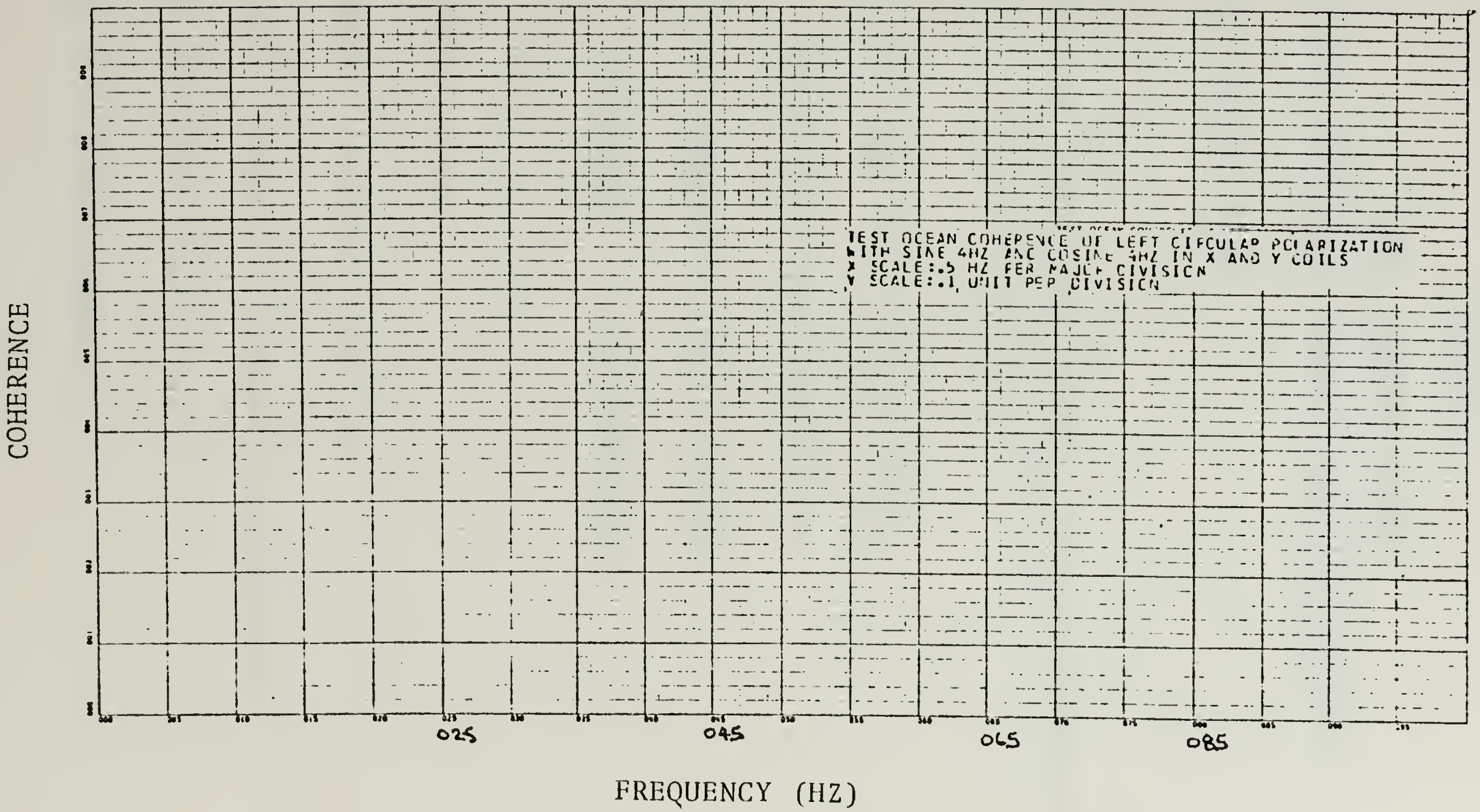

Figure A.21 Test Ocean Coherence of Left Circular Polarization

APPENDIX B

MASS STORAGE PROGRAM

```
//JOEB1MB JOB (1592,0129),'FISHER SMC.1399',CLASS=F
//*MAIN ORG=NPGVM1.1592P
// EXEC FORTXCLG
//FORT.SYSIN DD DSN=MSS.SYS3.NONIMSL.SOURCE(FOURT),DISP=SHR
//    DD  *
C          THE ARRAY 'IN' WILL BE USED TO
C          RECEIVE THE DATA PASSED FROM
C          THE SUBROUTINE 'READ' AND THEN
C          TRANSFERRED TO THE APPROPRIATE
C          XXX OR YYY ARRAY.
      INTEGER*2 IN(16)
      COMPLEX*8 XXX(8192),YYY(8192)
      DIMENSION FREQ(8192),TIME(8192),WORK(16384)
      DATA XXX,YYY/16384*(0.0,0.0)/
      DATA TIME,FREQ/16384*0.0/
```

```
C          THE FOLLOWING SECTION READS THE
C          FIRST SIX SECONDS OF COMPUTER TAPE
C          AND DISCARDS THIS DATA.
      ITL=192
      DO 55 JJ=1,ITL
      CALL RD(20,IN,200,IREC,IRR)
   55 CONTINUE
      IFRAME=8192
      NR=20
      FNR=FLOAT(NR)
      DO 70 L1=1,NR
C          THE NEXT LOOP READS THE COMPUTER
C          TAPE USING THE PROGRAM PROVIDED
C          BY MR. TIM STANTON OF NAVAL POST-
C          GRADUATE SCHOOL.
      DO 60 JJ=1,IFRAME
```

```
      CALL RD(20,IN,1000,IREC,IRR)
      XXX(JJ)=IN(2)
      YYY(JJ)=IN(3)
   60 CONTINUE
      N=8192
      FN=FLOAT(N)
      DELTAT=1./32.
      T=FN*DELTAT
      DELTAF=1./T
      DO 20 J=1,N
      TIME(J)=DELTAT*FLOAT(J)
      FREQ(J)=DELTAF*FLOAT(J)
C           THE NEXT 4 STEPS CONVERT THE
C           DATA TO VOLTAGE AND ENSURES THAT
C           NO ERRONEOUS DATA HAS BEEN INTRODUCED
C           INTO THE ARRAYS.
```

```
      XXX(J)=(XXX(J)-2045.5)*10./2045.5
      XXX(J)=REAL(XXX(J))
      YYY(J)=(YYY(J)-2045.5)*10./2045.5
      YYY(J)=REAL(YYY(J))
   20 CONTINUE
      CALL FOURT(XXX,N,1,-1,0,WORK)
      CALL FOURT(YYY,N,1,-1,0,WORK)
      DO 40 K4=1,N
      XXX(K4)=XXX(K4)/FN
      YYY(K4)=YYY(K4)/FN
   40 CONTINUE
C           THE NEXT LOOP APPLIES THE SYSTEM
C           TRANSFER FUNCTION TO THE TRANSFORMED
C           FREQUENCY DOMAIN DATA. THE TRANSFER
C           FUNCTION CONVERTS VOLTS TO NANOTESLAS.
      DO 9 L=1,N
```

```
  FRQ=FREQ(L)
1 IF(FRQ.LE.15.)GO TO 2
  XXX(L)=XXX(L)/(105.5-3.14*FRQ)
  YYY(L)=YYY(L)/(181.32-7.588*FRQ)
  GO TO 8
2 IF(FRQ.LE.10.)GO TO 3
  XXX(L)=XXX(L)/(5.958*FRQ-30.97)
  YYY(L)=YYY(L)/(7.166*FRQ-39.99)
  GO TO 8
3 IF(FRQ.LE.7.5)GO TO 4
  XXX(L)=XXX(L)/(3.492*FRQ-6.31)
  YYY(L)=YYY(L)/(4.252*FRQ-10.85)
  GO TO 8
4 IF(FRQ.LE.5.)GO TO 5
  XXX(L)=XXX(L)/(2.6311*FRQ+0.14667)
  YYY(L)=YYY(L)/(3.012*FRQ-1.55)
```

```
      GO TO 8
    5 IF (FRQ.LE.3.)GO TO 6
      XXX(L)=XXX(L)/(2.6311*FRQ+0.14667)
    7 YYY(L)=YYY(L)/(2.702*FRQ)
      GO TO 8
    6 XXX(L)=XXX(L)/(2.72*FRQ)
      GO TO 7
    8 CONTINUE
    9 CONTINUE
C          THE NEXT WRITE STATEMENTS SEND
C          THE CONVERTED DATA TO MSS
C          FOR FUTURE MANIPULATION AND RECALL.
C          THIS NEXT SET OF STATEMENTS ALSO
C          PROVIDES THE USER A DIAGNOSTIC.
      WRITE(21)XXX
      WRITE(6,*)XXX(1),XXX(8192)
```

```
      WRITE(21) YYY
      WRITE(6,*) YYY(1),YYY(8192)
   70 CONTINUE
      ENDFILE 21
      STOP
      END
       SUBROUTINE RD(IUN,IO,IRS,IREC,IRQ)
C
C         THIS PROCEDURE FURNISHED BY MR. TIM STANTON,
C         DEPARTMENT OF OCEANOGRAPHY.
C
C              READ DATA FROM IUN, ALLIGN , CHECK & RETURN
C
C       IUN=TAPE NUMBER, EG 20
C       IO=INTEGER*2 ARRAY, 16 LONG,
C       (VALUES 0-4095 , SUBTRACT 2048)*5/2028. GIVES VOLTAGE
```

```
C        IRS= NUMBER OF RESINCS ALLOWED (ERRORS)
C        IREC= COUNTER OF RECORDS (FRAMES OF DATA)
C            BLOCK 512 BITS,   32 BITS = RECORD
C            800 BPI TAPE UNLABLED
C        IRQ= NUMBER OF ACTUAL RESINCS (ERRORS)
C
C
      INTEGER * 2 IO(16),IP(16)
      DATA IRR /0/
      IF (IREC.EQ.0) IS=0
      IER=0
 20   FORMAT (16A2)
      IF (IS.NE.0) GO TO 50
      READ (IUN,20,END=900) IP
      IREC=IREC+1
 40   IS=IS+1
```

```
       IF (IS.LT.17) GO TO 50
       READ (IUN,20,END=900) IP
      IS=1
      IREC=IREC+1
 50   ICH=IMASK(IP(IS),3,0)+1
C      WRITE (6,55) ICH,IS,IUN,IREC
 55    FORMAT ('  RESYNCING ICH,IS,IUN,IREC ',4I8)
C
      IF (ICH.NE.1) GO TO 40
      DO 100 I=1,16
       IO(I)=ISHIFT(IP(IS),4)
      ICH=IMASK(IP(IS),3,0)+1
      IF (ICH.EQ.I) GO TO 80
      IER=IER+1
      WRITE (6,70)  IUN,IREC,I,ICH,IER
 70    FORMAT ('UNIT',I3,'RECORD',I6,'CHAN & DATA CH ',2I4,
```

```
      'ERRORS ',I7)
 80   IS=IS+1
      IF (IS.LT.17) GO TO 100
      READ (IUN,20,END=900) IP
      IS=1
      IREC=IREC+1
 100  CONTINUE
C
      IF (IER.EQ.0) GO TO 150
      IRR=IRR+1
      IF (IRR.LT.IRS) GO TO 120
      WRITE (6,110)
 110  FORMAT ('1 STOPPED IN SUB RD BECAUSE
     C OF IRR.GT.',I6,' AT L110')
      IRQ=IRR
      STOP
```

```
120   CONTINUE
      WRITE (6,130) IREC,IRR
130   FORMAT ('RESYNC AT FRAME',I6,'WITH TOTAL ERRORS',I7)
      IER=0
      IRQ=IRR
      GO TO 50
150   CONTINUE
      RETURN
900   WRITE (6,910) IUN,IREC
910   FORMAT ('1   END OF UNIT ',I3,' AT REC ',I7)
      STOP
      END
      FUNCTION ISHIFT (IN,NPLC)
C                RETURNS SHIFTED VALUE OF I*2 WORD IN
C                -VE LEFT,+VE RIGHT SHIFT
C
```

```
      INTEGER * 2 IN
      IP=IN
      IF (IP.LT.0) IP=IP+65536
      IF (NPLC.LT.0)  GO TO 30
      ISHIFT=IP/(2**IABS(NPLC))
      RETURN
 30   ISHIFT=IP*(2**IABS(NPLC))
      IF (ISHIFT.GT.65535) ISHIFT=MOD(ISHIFT,65536)
      RETURN
      END
      FUNCTION IMASK (IN,IBL,IBR)
C                MASK I*2 WORD IN OUTSIDE BITS IBL & IBR
C
      INTEGER * 2 IN,IO
      IO=IN
      IF (IBR.EQ.0) GO TO 50
```

```
      IT=ISHIFT(IN,IBR)
      IO=IT
 50   IP=ISHIFT(IO,IBL-15-IBR)
      IO=IP
      IMASK=ISHIFT(IO,15-IBL)
      RETURN
      END
/*
//GO.FT21F001 DD UNIT=3330V,MSVGP=PUB4A,DISP=(NEW,CATLG),
//             DSN=MSS.S1592.GMDT1A,
//             DCB=(RECFM=VBS,BLKSIZE=4096,LRECL=4092),
//             SPACE=(CYL,(8,8))
//GO.FT20F001 DD UNIT=3400-4,VOL=SER=GMDT1A,DISP=(OLD,PASS),
//             LABEL=(1,NL,,IN),
//             DCB=(RECFM=FB,LRECL=32,BLKSIZE=512,DEN=2)
//
```

APPENDIX C

MAIN PROGRAM

```
//JOEK1MB JOB (1592,0129),'FISHER SMC.1399',CLASS=F
//*MAIN ORG=NPGVM1.1592P,LINES=(60)
//*FORMAT PR,DDNAME=PLOT.SYSVECTR,DEST=LOCAL
// EXEC FRTXCLGP,PARM.LKED='LIST,MAP,XREF',REGION.GO=2700K
//SYSUT1   DD  UNIT=SYSDA,SPACE=(CYL,(8,8))
//SYSUT2   DD  UNIT=SYSDA,SPACE=(CYL,(8,8))
//SYSLIN   DD  SPACE=(6080,(80,30)),UNIT=SYSDA
//FORT.SYSIN DD DSN=MSS.SYS3.NONIMSL.SOURCE(FOURT),DISP=SHR
//     DD  *
C           DETAILED DESCRIPTIONS OF THE
C           VARIOUS STEPS AND LOOPS ARE
C           CONTAINED IN APPENDICES A AND B.
      INTEGER*2 IN(16)
      COMPLEX*8 XX0(8192),YY0(8192),
     C CS0(8192),CO0(8192),ZX0(8192),
```

```
C CRO(8192),CTO(8192),CUO(8192),
C CVO(8192),CWO(8192),CPO(8192),
C ZYO(8192),COMOL(8192),COL(8192),
C CUL(8192),CVL(8192),CWL(8192),
C COPOL(8192),XXX(8192),YYY(8192),
C XXL(8192),YYL(8192),ZXL(8192),
C ZYL(8192),CSL(8192),BPO(8192),
C BMO(8192),BPL(8192),BML(8192),
C SPOL(8192),SMOL(8192),SPO(8192),
C SPL(8192),SMO(8192),CTL(8192),
C CPL(8192),CRL(8192),SML(8192)
  DIMENSION TIME(8192),FREQ(8192),
C WORK(16384),FRQ2(8192)
  INTEGER*4 ITB(12)/12*0/
  REAL*4    RTB(28)/28*0.0/,CROO(16384),
C CPOO(16384),CUOO(16384),
```

```
C COOO(16384),CTOO(16384),CVOO(16384),
C CWOO(16384),CTLL(16384),
C CPLL(16384),CRLL(16384),COLL(16384),
C CULL(16384),CVLL(16384),
C CWLL(16384),COMOLL(16384),COPOLL(16384),
C SPOO(16384),SPLL(16384),
C SMOO(16384),SMLL(16384)
  REAL ALAB(22)/'PDXO','PDYO','ST1O',
C 'ST2O','ST3O','STOO','PHAO',
C 'GAMO','PDXL','PDYL','ST1L','ST2L',
C 'ST3L','STOL','PHAL','GAML',
C 'SPLO','SPLL','SMOO','SMLL','CPOL','CMOL'/
  REAL*8 TITLE(12)
  EQUIVALENCE(TITLE(1),RTB(5)),(CROO(1),
C CRO(1)),(CPOO(1),CPO(1)),
C  (COOO(1),COO(1)),(CTOO(1),CTO(1)),(CUOO(1),CUO(1)),
```

```
C (CWOO(1),CWO(1)),(CVOO(1),CVO(1)),(CTLL(1),CTL(1)),
C (CPLL(1),CPL(1)),(CRLL(1),CRL(1)),(COLL(1),COL(1)),
C (CULL(1),CUL(1)),(CVLL(1),CVL(1)),(CWLL(1),CWL(1)),
C (COPOLL(1),COPOL(1)),(COMOLL(1),
C COMOL(1)),(SPOO(1),SPO(1)),
C (SPLL(1),SPL(1)),(SMOO(1),SMO(1)),(SMLL(1),SML(1))
  DATA XXO,YYO,CSO,COO,ZXO,ZYO,CRO,
C CTO,CUO,CVO,CWO,XXX,YYY,
C XXL,YYL,ZXL,ZYL,CSL,BPO,BMO,BPL,
C BML,SPOL,SMOL,SPO,SPL,SMO,
C SML,CTL,CRL,COL,CVL,COPOL,CWL,COPOL,
C COMOL/294912*(0.0,0.0)/
  DATA TIME,FREQ,FRQ2/24575*0.0/
  ITL=192
  DO 55 JJ=1,ITL
  CALL RD(20,IN,200,IREC,IRR)
```

```
   55 CONTINUE
      IFRAME=8192
      NR=20
      FNR=FLOAT(NR)
C           THE FIRST STATEMENTS OF LOOP 70
C           RECALLS DATA PREVIOUSLY STORED IN
C           THE IBM 3033 MASS STORAGE SYSTEM.
      DO 70 L1=1,NR
      READ(21) XXX
      READ(21) YYY
      DO 43 II=1,IFRAME
      XXL(II)=XXX(II)
      YYL(II)=YYY(II)
   43 CONTINUE
      DO 60 JJ=1,IFRAME
      CALL RD(20,IN,1000,IREC,IRR)
```

```
      XXO(JJ)=IN(2)

      YYO(JJ)=IN(3)

60    CONTINUE

      N=8192

      FN=FLOAT(N)

      DELTAT=1./32.

      T=FN*DELTAT

      DELTAF=1./T

      DO 20 J=1,N

      TIME(J)=DELTAT*FLOAT(J)

      FREQ(J)=DELTAF*FLOAT(J)

      FRQ2(J)=ALOG10(FREQ(J))

      XXO(J)=(XXO(J)-2045.5)*5./2045.5

      XXO(J)=REAL(XXO(J))

      YYO(J)=(YYO(J)-2045.5)*5./2045.5

      YYO(J)=REAL(YYO(J))
```

```
20   CONTINUE
     CALL FOURT(XXO,N,1,-1,0,WORK)
     CALL FOURT(YYO,N,1,-1,0,WORK)
     DO 40 K4=1,N
     XXO(K4)=XXO(K4)/FN
     YYO(K4)=YYO(K4)/FN
40   CONTINUE
     DO 9 L=1,N
     FRQ=FREQ(L)
 1   IF(FRQ.LE.15.)GO TO 2
     XXO(L)=XXO(L)/(-81.36 +17.066*FRQ - 0.5389*FRQ*FRQ)
     YYO(L)=YYO(L)/(-63.435 +11.7106*FRQ-0.23279*FRQ*FRQ)
     GO TO 8
 2   IF(FRQ.LE.10.)GO TO 3
     XXO(L)=XXO(L)/(-18.486 + 4.9029*FRQ)
     YYO(L)=YYO(L)/(-63.435 +11.7106*FRQ -0.23279*FRQ*FRQ)
```

```
      GO TO 8
    3 IF(FRQ.LE.7.5)GO TO 4
      XXO(L)=XXO(L)/(3.947*FRQ-9.368)
      YYO(L)=YYO(L)/(4.295*FRQ-11.837)
      GO TO 8
    4 IF(FRQ.LE.5.)GO TO 5
      XXO(L)=XXO(L)/(2.8105*FRQ-0.5657)
      YYO(L)=YYO(L)/(2.800*FRQ-.50)
      GO TO 8
    5 XXO(L)=XXO(L)/(2.723*FRQ)
      YYO(L)=YYO(L)/(2.717*FRQ)
      GO TO 8
    8 CONTINUE
    9 CONTINUE
      DO 30 II=1,N
      ZXO(II)=ZXO(II)+(XXO(II)*CONJG(XXO(II)))
```

```
      ZYO(II)=ZYO(II)+(YYO(II)*CONJG(YYO(II)))

      CSO(II)=CSO(II)+(XXO(II)*CONJG(YYO(II)))

      ZXL(II)=ZXL(II)+(XXL(II)*CONJG(XXL(II)))

      ZYL(II)=ZYL(II)+(YYL(II)*CONJG(YYL(II)))

      CSL(II)=CSL(II)+(XXL(II)*CONJG(YYL(II)))

      BPO(II)=XXO(II)+((0.,1.)*YYO(II))

      BMO(II)=XXO(II)-((0.,1.)*YYO(II))

      BPL(II)=XXL(II)+((0.,1.)*YYL(II))

      BML(II)=XXL(II)-((0.,1.)*YYL(II))

      SPOL(II)=SPOL(II)+(BPO(II)*CONJG(BPL(II)))

      SMOL(II)=SMOL(II)+(BMO(II)*CONJG(BML(II)))

      SPO(II)=SPO(II)+(BPO(II)*CONJG(BPO(II)))

      SPL(II)=SPL(II)+(BPL(II)*CONJG(BPL(II)))

      SMO(II)=SMO(II)+(BMO(II)*CONJG(BMO(II)))

      SML(II)=SML(II)+(BML(II)*CONJG(BML(II)))

30    CONTINUE
```

```
70   CONTINUE
     DO 33 I3=1,N
     ZXO(I3)=ZXO(I3)*T/FNR
     ZYO(I3)=ZYO(I3)*T/FNR
     CSO(I3)=CSO(I3)*T/FNR
     ZXL(I3)=ZXL(I3)*T/FNR
     ZYL(I3)=ZYL(I3)*T/FNR
     CSL(I3)=CSL(I3)*T/FNR
     SPOL(I3)=SPOL(I3)*T/FNR
     SPO(I3)=SPO(I3)*T/FNR
     SPL(I3)=SPL(I3)*T/FNR
     SMO(I3)=SMO(I3)*T/FNR
     SML(I3)=SML(I3)*T/FNR
     SMOL(I3)=SMOL(I3)*T/FNR
33   CONTINUE
     DO 44 I4=1,N
```

```
CTO(I4)=(ZXO(I4)+ZYO(I4))*2./T

CPO(I4)=(ZXO(I4)-ZYO(I4))*2./(T*CTO(I4))

CRO(I4)=(4*CSO(I4))/(CTO(I4)*T)

COO(I4)=CSO(I4)/(CSQRT(ZXO(I4))*CSQRT(ZYO(I4)))

CWO(I4)=ATAN2(AIMAG(COO(I4)),REAL(COO(I4)))

COO(I4)=CSQRT(COO(I4)*CONJG(COO(I4)))

CTO(I4)=4.3429448*CLOG(CTO(I4))

CUO(I4)=4.3429448*CLOG(ZXO(I4))

CVO(I4)=4.3429448*CLOG(ZYO(I4))

CTL(I4)=(ZXL(I4)+ZYL(I4))*2./T

CPL(I4)=(ZXL(I4)-ZYL(I4))*2./(T*CTL(I4))

CRL(I4)=(4*CSL(I4))/(CTL(I4)*T)

COL(I4)=CSL(I4)/(CSQRT(ZXL(I4))*CSQRT(ZYL(I4)))

CTL(I4)=4.3429448*CLOG(CTL(I4))

CUL(I4)=4.3429448*CLOG(ZXL(I4))

CVL(I4)=4.3429448*CLOG(ZYL(I4))
```

```
      CWL(I4)=ATAN2(AIMAG(COL(I4)),REAL(COL(I4)))

      COL(I4)=CSQRT(COL(I4)*CONJG(COL(I4)))

      COPOL(I4)=SPOL(I4)/(CSQRT(SPO(I4))*CSQRT(SPL(I4)))

      COPOL(I4)=CSQRT (COPOL(I4)*CONJG(COPOL(I4)))

      COMOL(I4)=SMOL(I4)/(CSQRT(SMO(I4))*CSQRT(SML(I4)))

      COMOL(I4)=CSQRT (COMOL(I4)*CONJG(COMOL(I4)))

      SPO(I4)=4.3429448*CLOG(SPO(I4))

      SPL(I4)=4.3429448*CLOG(SPL(I4))

      SMO(I4)=4.3429448*CLOG(SMO(I4))

      SML(I4)=4.3429448*CLOG(SML(I4))

 44   CONTINUE

      NPTS=10./DELTAF+1.

      ITB(2)=0

      ITB(3)=20

      ITB(4)=10

      ITB(6)=1
```

```
ITB(7)=1

ITB(12)=1

RTB(1)=0

RTB(2)=0

RTB(3)=ALAB(1)

READ(5,3000) TITLE

CALL DRAWP(NPTS,FRQ2,CUOD,ITB,RTB)

ITB(6)=1

RTB(3)=ALAB(2)

READ(5,3000) TITLE

CALL DRAWP(NPTS,FRQ2,CVOD,ITB,RTB)

ITB(6)=1

RTB(3)=ALAB(3)

READ(5,3000) TITLE

CALL DRAWP(NPTS,FREQ,CPOD,ITB,RTB)

ITB(6)=1
```

```
RTB(3)=ALAB(4)

READ(5,3000) TITLE

CALL DRAWP(NPTS,FREQ,CROD,ITB,RTB)

ITB(6)=1

RTB(3)=ALAB(5)

READ(5,3000) TITLE

CALL DRAWP(NPTS,FREQ,CROD(2),ITB,RTB)

ITB(6)=1

RTB(3)=ALAB(6)

READ(5,3000) TITLE

CALL DRAWP(NPTS,FRQ2,CTOD,ITB,RTB)

ITB(6)=1

RTB(3)=ALAB(7)

READ(5,3000) TITLE

CALL DRAWP(NPTS,FREQ,CWOD,ITB,RTB)

ITB(6)=1
```

```
RTB(3)=ALAB(8)

READ(5,3000)TITLE

CALL DRAWP(NPTS,FREQ,COOD,ITB,RTB)

ITB(6)=1

RTB(3)=ALAB(9)

READ(5,3000)TITLE

CALL DRAWP(NPTS,FRQ2,CULL,ITB,RTB)

ITB(6)=1

RTB(3)=ALAB(10)

READ(5,3000)TITLE

CALL DRAWP(NPTS,FRQ2,CVLL,ITB,RTB)

ITB(6)=1

RTB(3)=ALAB(11)

READ(5,3000)TITLE

CALL DRAWP(NPTS,FREQ,CPLL,ITB,RTB)

ITB(6)=1
```

```
RTB(3)=ALAB(12)
READ(5,3000)TITLE
CALL DRAWP(NPTS,FREQ,CRLL,ITB,RTB)
ITB(6)=1
RTB(3)=ALAB(13)
READ(5,3000)TITLE
CALL DRAWP(NPTS,FREQ,CRLL(2),ITB,RTB)
ITB(6)=1
RTB(3)=ALAB(14)
READ(5,3000)TITLE
CALL DRAWP(NPTS,FRQ2,CTLL,ITB,RTB)
ITB(6)=1
RTB(3)=ALAB(15)
READ(5,3000)TITLE
CALL DRAWP(NPTS,FREQ,CWLL,ITB,RTB)
ITB(6)=1
```

```
RTB(3)=ALAB(16)

READ(5,3000)TITLE

CALL DRAWP(NPTS,FREQ,COLL,ITB,RTB)

ITB(6)=1

RTB(3)=ALAB(17)

READ(5,3000)TITLE

CALL DRAWP(NPTS,FRQ2,SPOD,ITB,RTB)

ITB(6)=1

RTB(3)=ALAB(18)

READ(5,3000)TITLE

CALL DRAWP(NPTS,FRQ2,SPLL,ITB,RTB)

ITB(6)=1

RTB(3)=ALAB(19)

READ(5,3000)TITLE

CALL DRAWP(NPTS,FRQ2,SMOD,ITB,RTB)

ITB(6)=1
```

```
      RTB(3)=ALAB(20)

      READ(5,3000)TITLE

      CALL DRAWP(NPTS,FRQ2,SMLL,ITB,RTB)

      ITB(6)=1

      RTB(3)=ALAB(21)

      READ(5,3000)TITLE

      CALL DRAWP(NPTS,FREQ,COPOLL,ITB,RTB)

      ITB(6)=1

      RTB(3)=ALAB(22)

      READ(5,3000)TITLE

      CALL DRAWP(NPTS,FREQ,COMOLL,ITB,RTB)

 3000 FORMAT(6A8)

      STOP

      END

      SUBROUTINE RD(IUN,IO,IRS,IREC,IRQ)

C
```

```
C          THIS PROCEDURE FURNISHED BY MR. TIM STANTON,
C          DEPARTMENT OF OCEANOGRAPHY.
C
C               READ DATA FROM IUN, ALLIGN , CHECK & RETURN
C
C        IUN=TAPE NUMBER, EG 20
C        IO=INTEGER*2 ARRAY, 16 LONG,
C        (VALUES 0-4095 , SUBTRACT 2048)*5/2028. GIVES VOLTAGE
C        IRS= NUMBER OF RESINCS ALLOWED (ERRORS)
C        IREC= COUNTER OF RECORDS (FRAMES OF DATA)
C            BLOCK 512 BITS,   32 BITS = RECORD
C            800 BPI TAPE UNLABLED
C        IRQ= NUMBER OF ACTUAL RESINCS (ERRORS)
C
C
      INTEGER * 2 IO(16),IP(16)
```

```
       DATA IRR /0/
       IF (IREC.EQ.0) IS=0
       IER=0
 20    FORMAT (16A2)
       IF (IS.NE.0) GO TO 50
       READ (IUN,20,END=900) IP
       IREC=IREC+1
 40    IS=IS+1
       IF (IS.LT.17) GO TO 50
       READ (IUN,20,END=900) IP
      IS=1
      IREC=IREC+1
 50   ICH=IMASK(IP(IS),3,0)+1
C      WRITE (6,55) ICH,IS,IUN,IREC
 55    FORMAT ('  RESYNCING ICH,IS,IUN,IREC ',4I8)
C
```

```
      IF (ICH.NE.1) GO TO 40
      DO 100 I=1,16
       IO(I)=ISHIFT(IP(IS),4)
      ICH=IMASK(IP(IS),3,0)+1
      IF (ICH.EQ.I) GO TO 80
      IER=IER+1
      WRITE (6,70)  IUN,IREC,I,ICH,IER
 70    FORMAT ('UNIT',I3,'RECORD',I6,'CHAN & DATA CH ',2I4,
       'ERRORS ',I7)
 80    IS=IS+1
       IF (IS.LT.17) GO TO 100
       READ (IUN,20,END=900) IP
       IS=1
       IREC=IREC+1
 100   CONTINUE
C
```

```
      IF (IER.EQ.0) GO TO 150
      IRR=IRR+1
      IF (IRR.LT.IRS) GO TO 120
      WRITE (6,110)
110   FORMAT ('1 STOPPED IN SUB RD BECAUSE
     C OF IRR.GT.',I6,' AT L110')
      IRQ=IRR
      STOP
120   CONTINUE
      WRITE (6,130) IREC,IRR
130   FORMAT ('RESYNC AT FRAME',I6,'WITH TOTAL ERRORS',I7)
      IER=0
      IRQ=IRR
      GO TO 50
150   CONTINUE
      RETURN
```

```
 900    WRITE (6,910) IUN,IREC
 910    FORMAT ('1   END OF UNIT ',I3,' AT REC ',I7)
        STOP
        END
        FUNCTION ISHIFT (IN,NPLC)
C                RETURNS SHIFTED VALUE OF I*2 WORD IN
C                -VE LEFT,+VE RIGHT SHIFT
C
        INTEGER * 2 IN
        IP=IN
        IF (IP.LT.0) IP=IP+65536
        IF (NPLC.LT.0) GO TO 30
        ISHIFT=IP/(2**IABS(NPLC))
        RETURN
  30    ISHIFT=IP*(2**IABS(NPLC))
        IF (ISHIFT.GT.65535) ISHIFT=MOD(ISHIFT,65536)
```

```
      RETURN
      END
      FUNCTION IMASK (IN,IBL,IBR)
C                 MASK I*2 WORD IN OUTSIDE BITS IBL & IBR
C
      INTEGER * 2 IN,IO
      IO=IN
      IF (IBR.EQ.0) GO TO 50
      IT=ISHIFT(IN,IBR)
      IO=IT
 50   IP=ISHIFT(IO,IBL-15-IBR)
      IO=IP
      IMASK=ISHIFT(IO,15-IBL)
      RETURN
      END
/*
```

```
//GO.FT20F001 DD UNIT=3400-4,VOL=SER=GMDT1B,DISP=(OLD,PASS),
//              LABEL=(1,NL,,IN),
//              DCB=(RECFM=FB,LRECL=32,BLKSIZE=512,DEN=2)
//GO.FT21F001 DD UNIT=3330V,MSVGP=PUB4A,DISP=(OLD,KEEP),
//              DSN=MSS.S1592.GMDT1A,
//              DCB=(RECFM=VBS,BLKSIZE=4096,LRECL=4092)
//GO.SYSDUMP DD SYSOUT=A
//GO.SYSIN  DD *
X COIL PSD, MTRY BAY,1122-1254 LOCAL,17AUG82,
20 AVGS, 32S/SEC,5VOLT, (DB NT**2 VS LOG FREQ)
Y COIL PSD, MTRY BAY,1122-1254 LOCAL,17AUG82,
20 AVGS, 32S/SEC,5VOLT, (DB NT**2 VS LOG FREQ)
STOKES NO. ONE, MTRY BAY, 1122-1254
LOCAL, 17AUG82, 20 AVGS, 32S/SEC, 5VOLT
STOKES NO. TWO, MTRY BAY, 1122-1254
LOCAL, 17AUG82, 20 AVGS, 32S/SEC, 5VOLT
```

STOKES NO. THREE, MTRY BAY, 1122-1254 LOCAL, 17AUG82, 20 AVGS, 32S/SEC, 5VOLT

STOKES NO. ZERO, MTRY BAY, 1122-1254 LOCAL, 17AUG82, 20 AVGS, 32S/SEC, 5VOLT, (LOG VS LOG)

PHASE OF X AND Y, MTRY BAY 1122-1254 LOCAL, 17AUG82, 20 AVGS, 32S/SEC, 5VOLT

COHER OF X AND Y COILS, MTRY BAY, 1122-1254 LOCAL, 17AUG82, 20 AVGS, 32S/SEC, 5VOLT

X COIL PSD, LA MESA,1122-12545LOCAL,17AUG82, 20 AVGS, 32S/SEC,10VOLT, (DB NT**2 VS LOG FREQ)

Y COIL PSD, LA MESA,1122-1254 LOCAL,17AUG82, 20 AVGS, 32S/SEC,10VOLT, (DB NT**2 VS LOG FREQ)

STOKES NO. ONE, LA MESA, 112201254 LOCAL, 17AUG82, 20 AVGS, 32S/SEC, 10VOLT

STOKES NO. TWO, LA MESA, 1122-1254 LOCAL, 17AUG82, 20 AVGS, 32S/SEC, 10VOLT

STOKES NO. THREE, LA MESA, 1122-1254

LOCAL, 17AUG82, 20 AVGS, 32S/SEC, 10VOLT

STOKES NO. ZERO, LA MESA, 1122-1254 LOCAL,

17AUG82, 20 AVGS, 32S/SEC, 10VOLT, (LOG VS LOG)

PHASE OF X AND Y, LA MESA, 1122-1254

LOCAL, 17AUG82, 20 AVGS, 32S/SEC, 10VOLT

COHER OF X AND Y COILS, LA MESA, 1122-1254

LOCAL, 17AUG82, 20 AVGS, 32S/SEC, 10VOLT

RT CIRC POLARIZATION PSD,MTRY BAY,1122-1254

LOCAL,17AUG82,20 AVGS,32S/SEC,5VOLT,(DB VS LOG)

RT CIRC POLARIZATION PSD, LA MESA, 1122-1254

LOCAL,17AUG82,20 AVGS,32S/SEC,10VOLT,(DB VS LOG)

LEFT CIRC POLARIZATION PSD, MTRY BAY,1122-1254

LOCAL,17AUG82, 20 AVGS,32S/SEC,5VOLT,(DB VS LOG)

LEFT CIRC POLARIZATION PSD, LA MESA, 1122-1254

LOCAL,17AUG82,20 AVGS,32S/SEC,10VOLT,(DB VS LOG)

```
COHER RT CIRC POLARIZATION MTRY BAY/LA MESA,

1122-1254 LOCAL, 17AUG82, 20 AVGS, 32S/SEC

COHER LEFT CIRC POLARIZATION MTRY BAY/LA MESA,

1122-1254 LOCAL, 17AUG82, 20 AVGS, 32S/SEC

/*

//
```

APPENDIX D

DATA CURVES

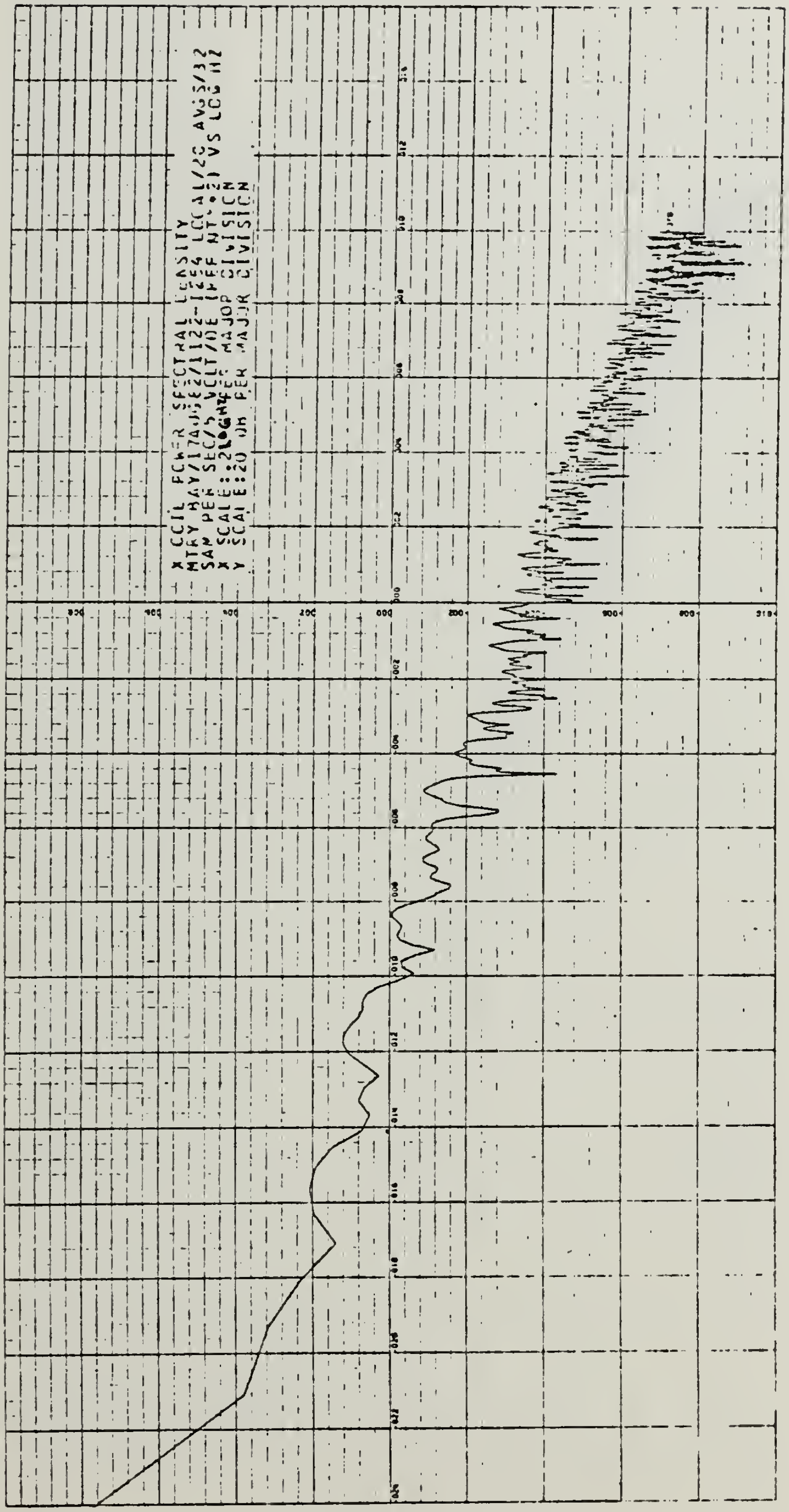

Figure D.1 x Coil Power Spectral Density, Mtry Bay, 17 Aug. 82, 1122-1254 Local

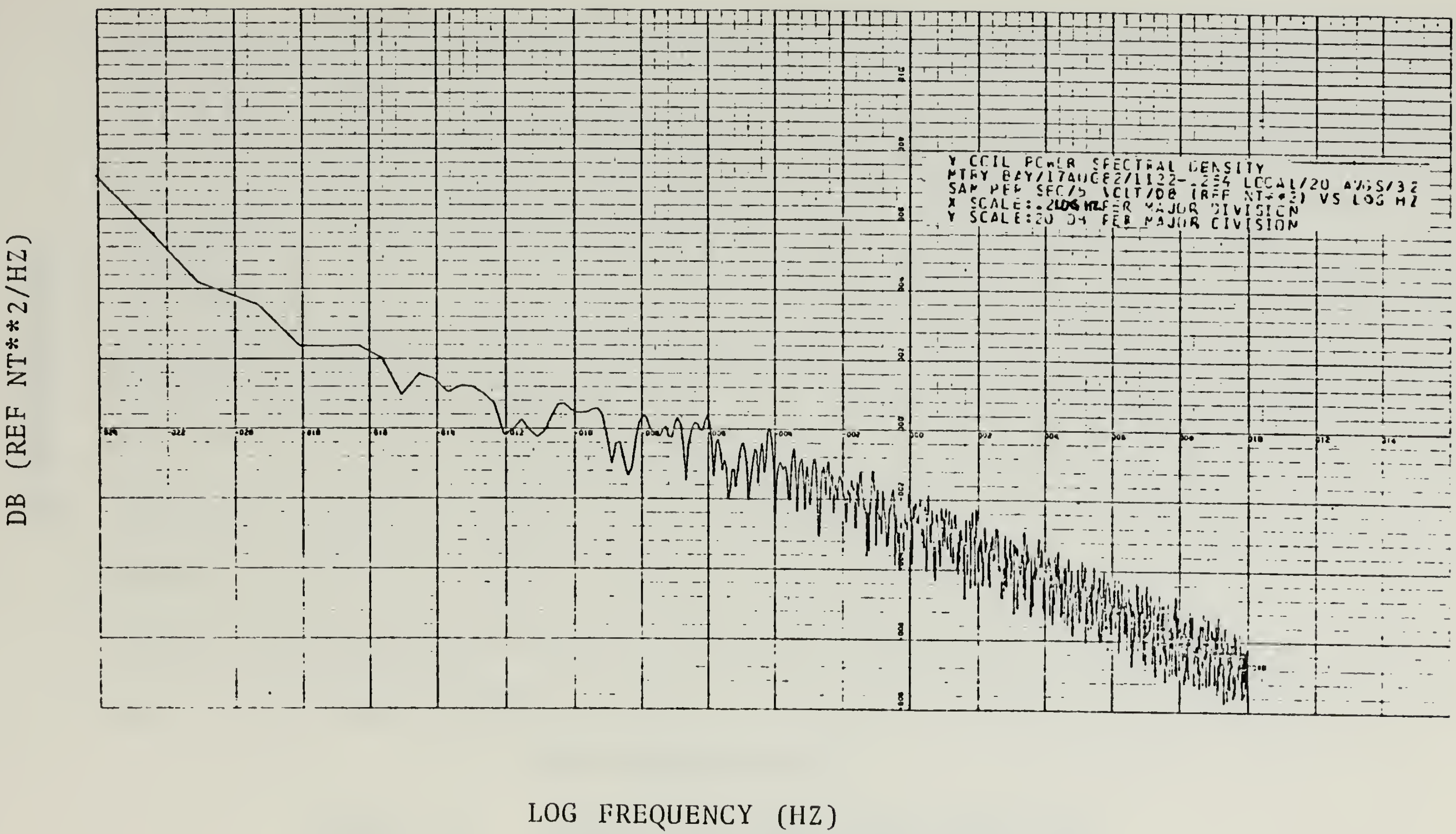

Figure D.2 y Coil Power Spectral Density, Mtry Bay, 17 Aug. 82, 1122-1254 Local

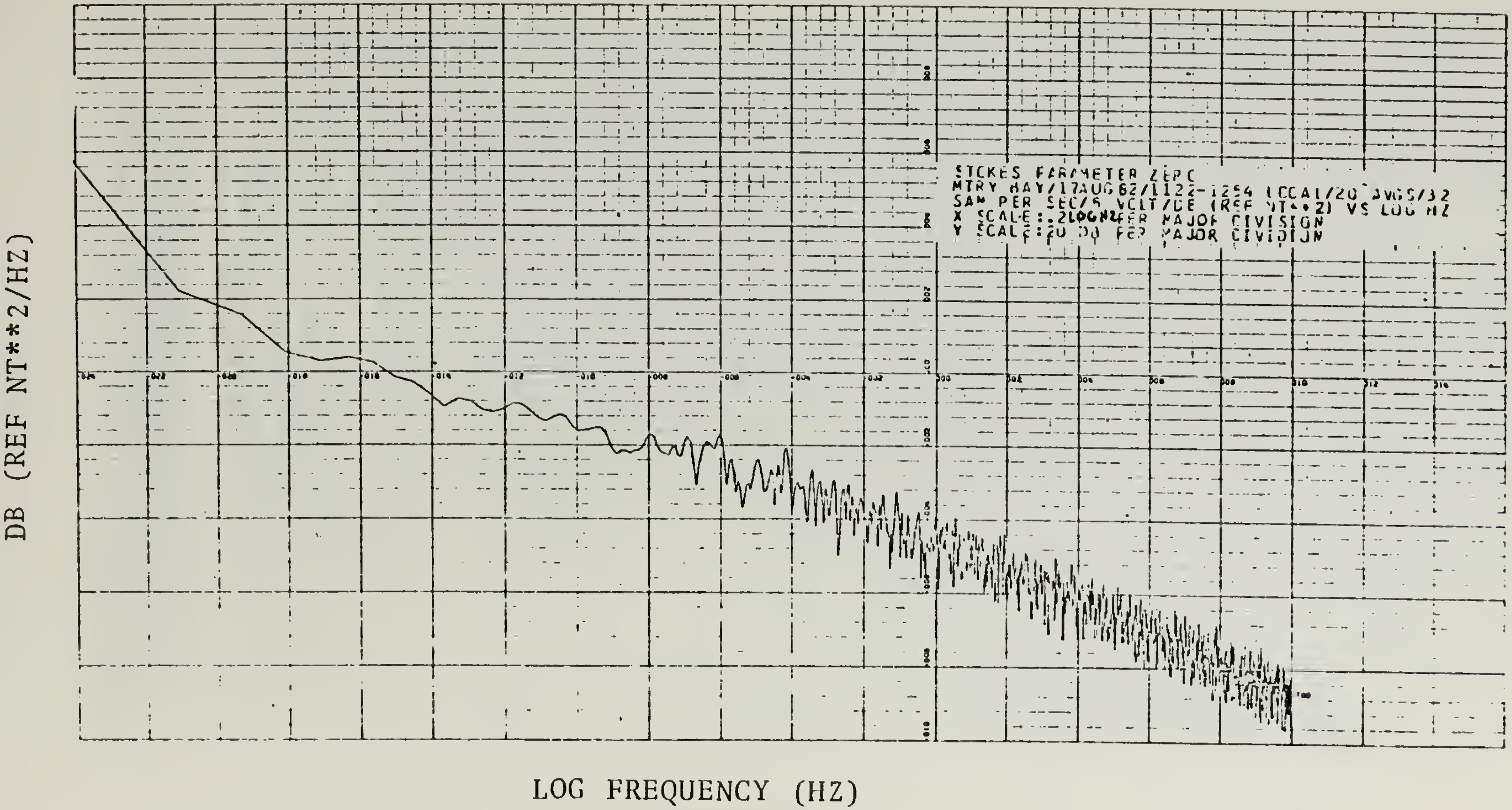

Figure D.3 Stokes Parameter Zero, Mtry Bay, 17 Aug. 82, 1122-1254 Local

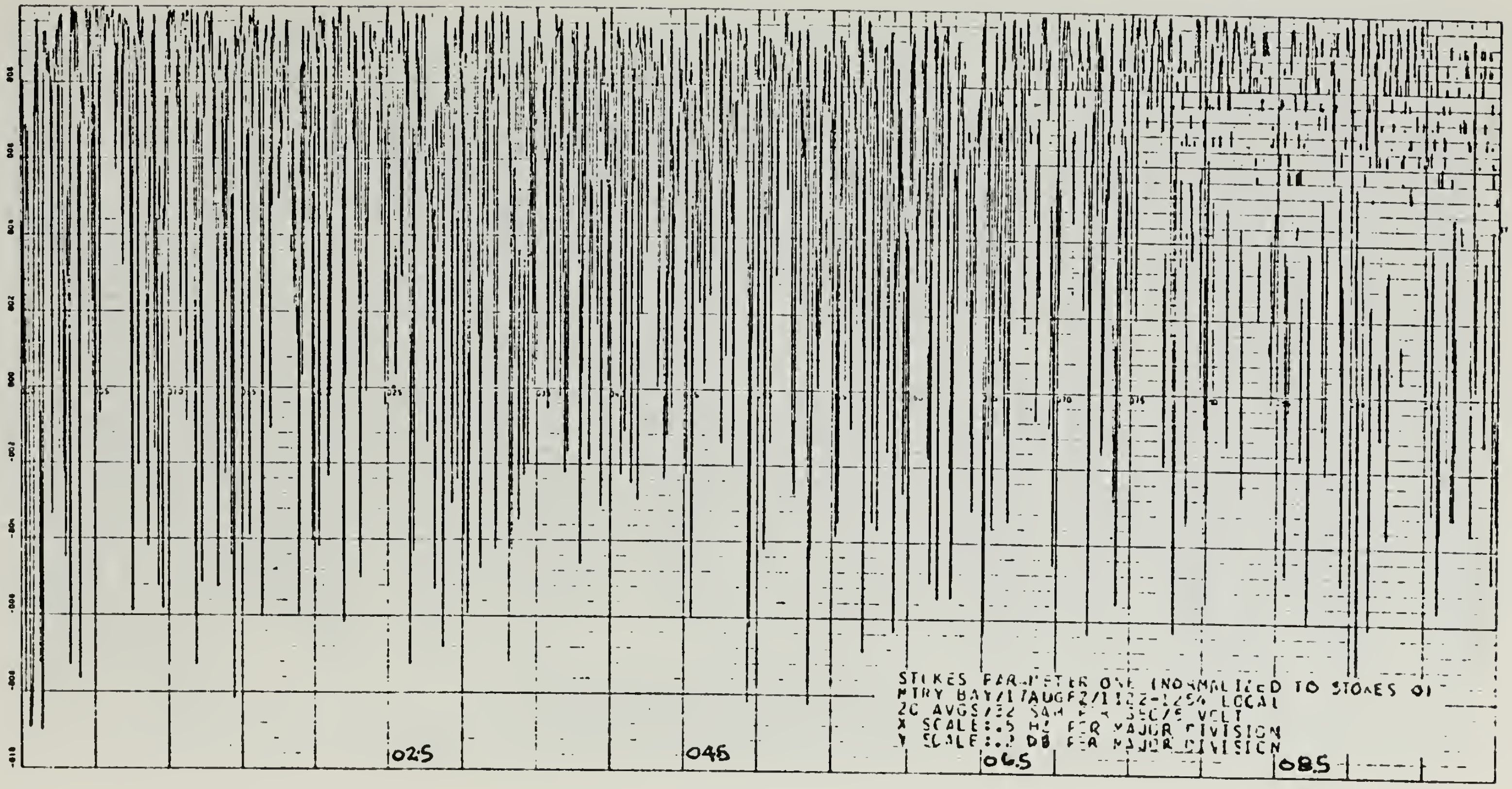

Figure D.4 Stokes Parameter One, Mtry Bay, 17 Aug. 82, 1122-1254 Local

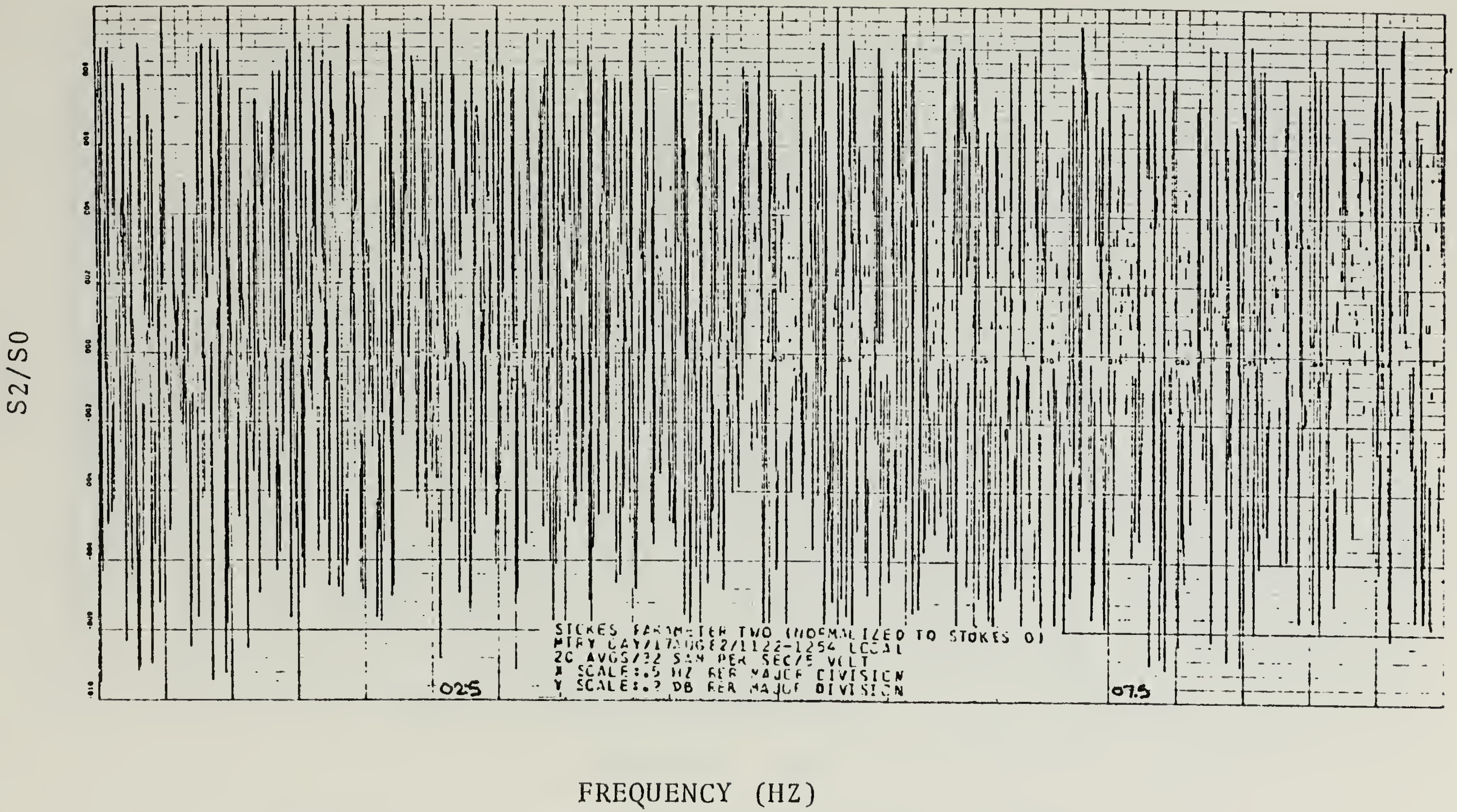

Figure D.5 Stokes Parameter Two, Mtry Bay, 17 Aug. 82, 1122-1254 Local

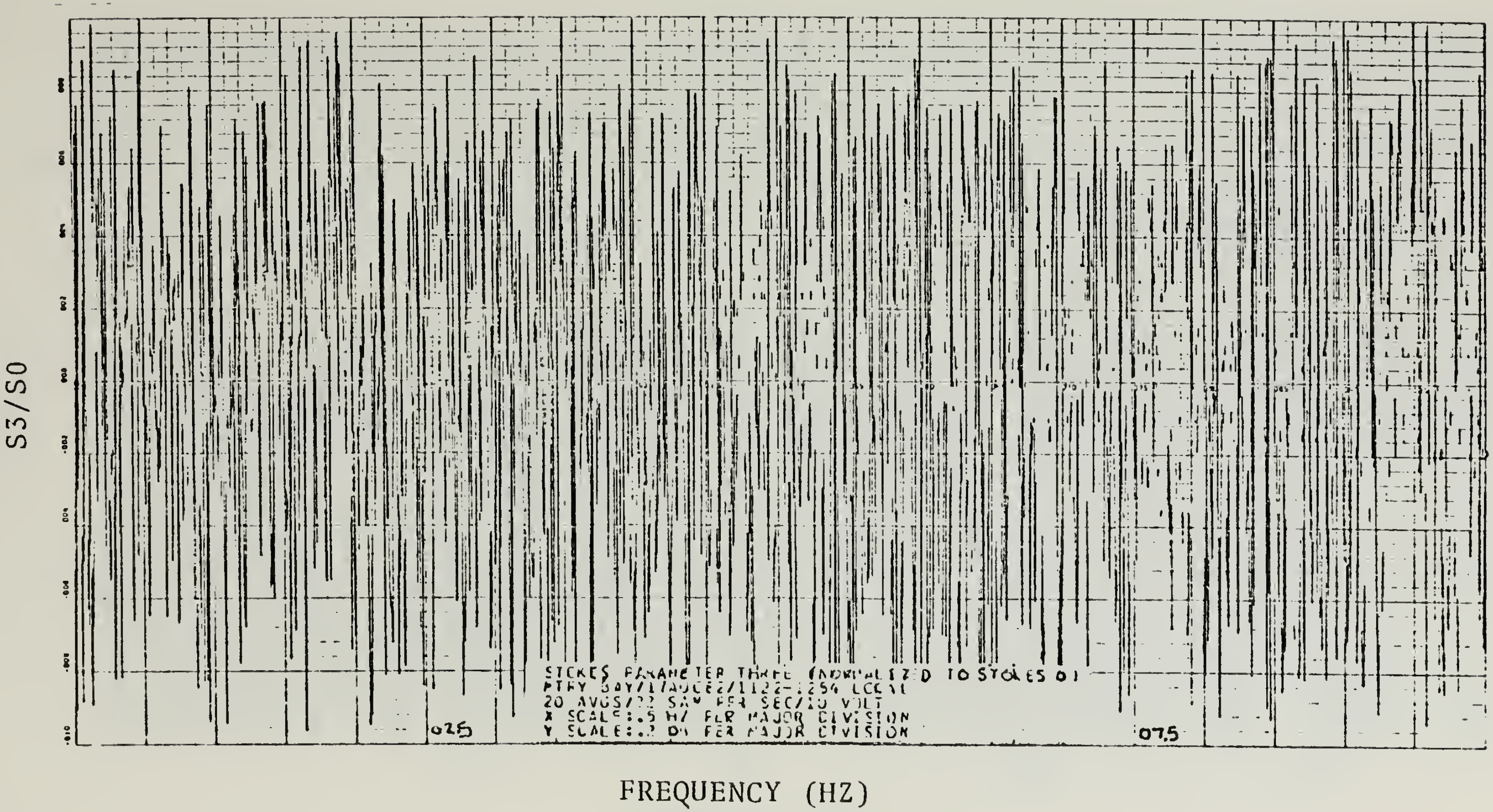

Figure D.6 Stokes Parameter Three, Mtry Bay, 17 Aug. 82, 1122-1254 Local

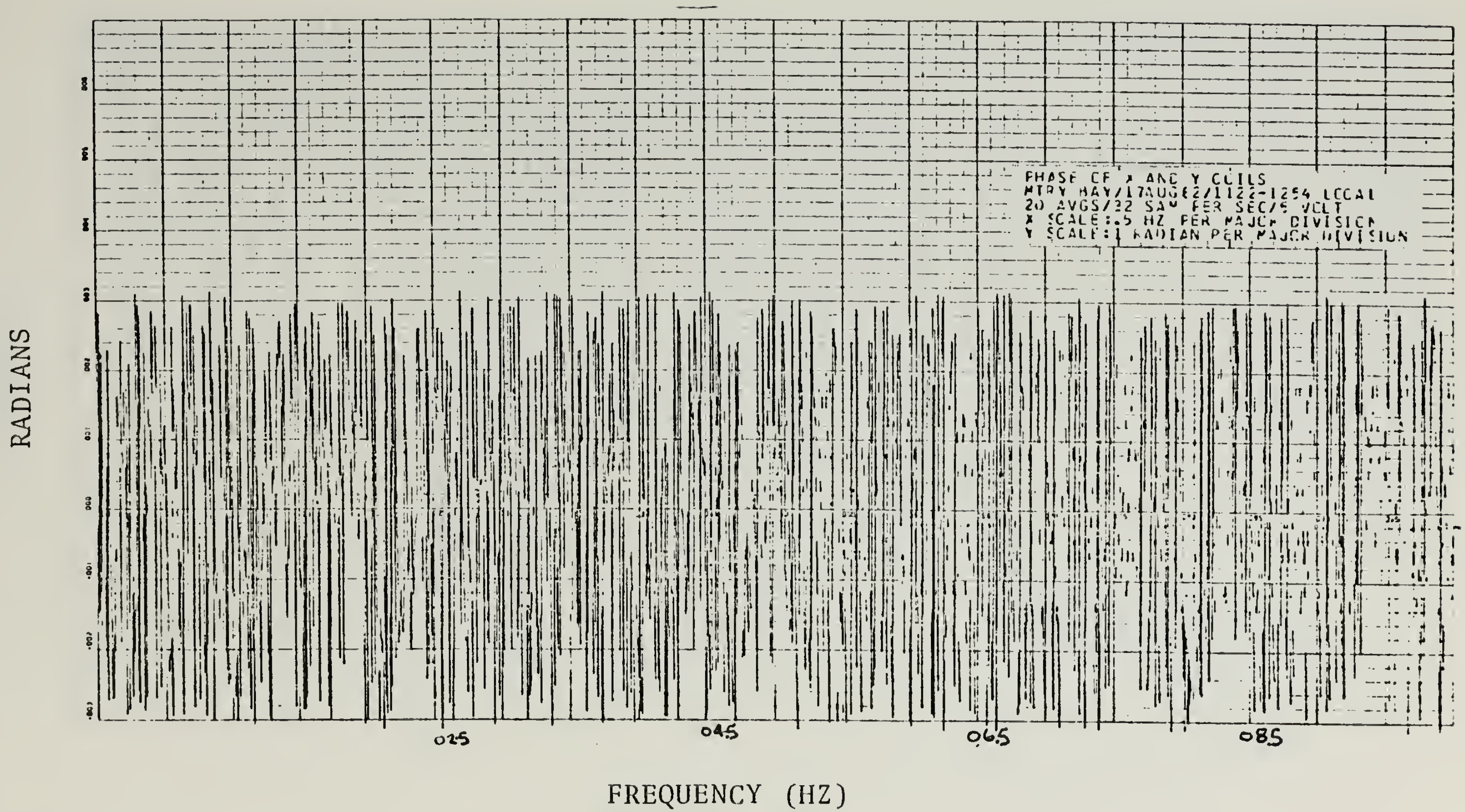

Figure D.7 Phase of x and y Coils, Mtry Bay, 17 Aug. 82, 1122-1254 Local

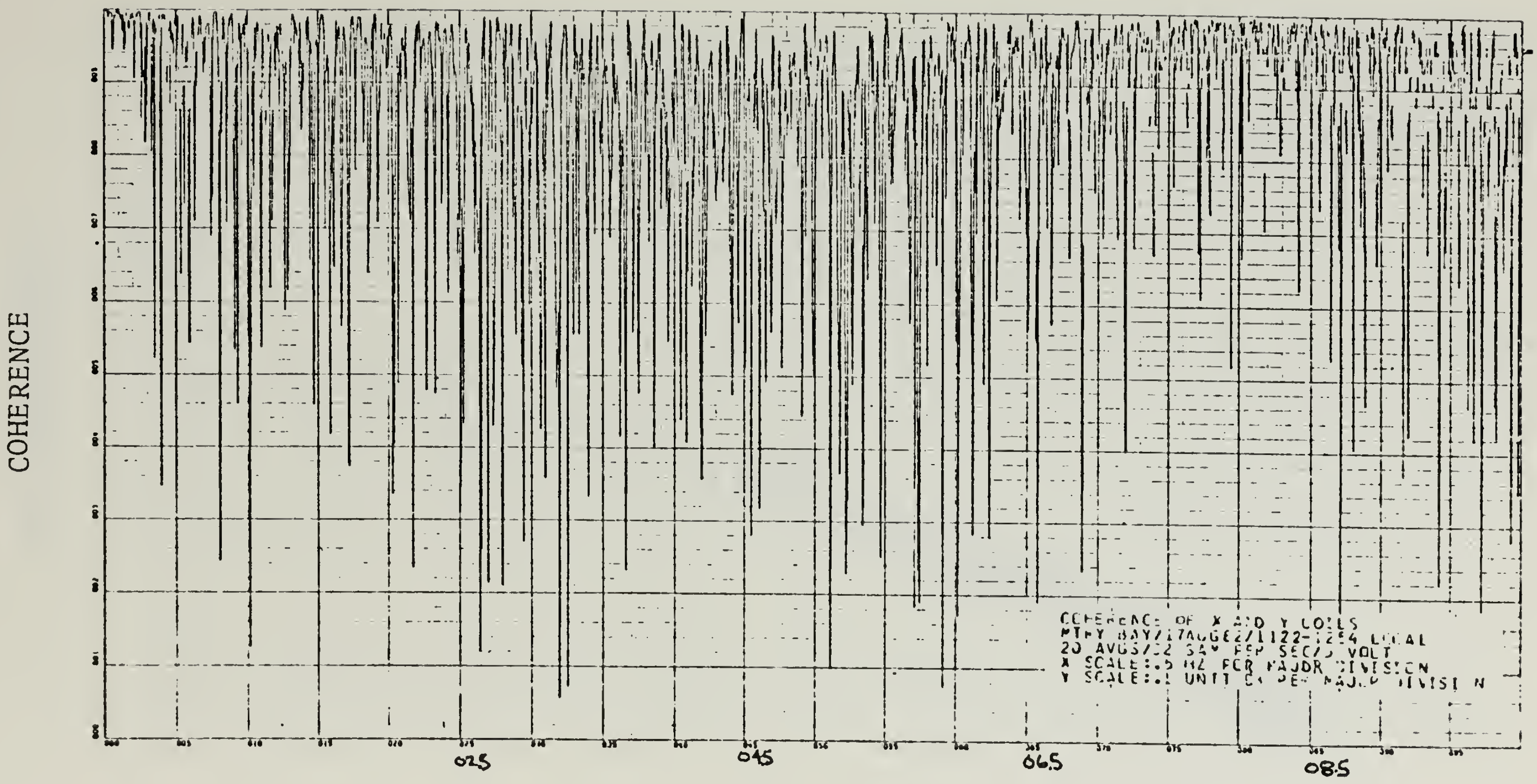

Figure D.8 Coherence of x and y Coils, Mtry Bay, 17 Aug. 82, 1122-1254 Local

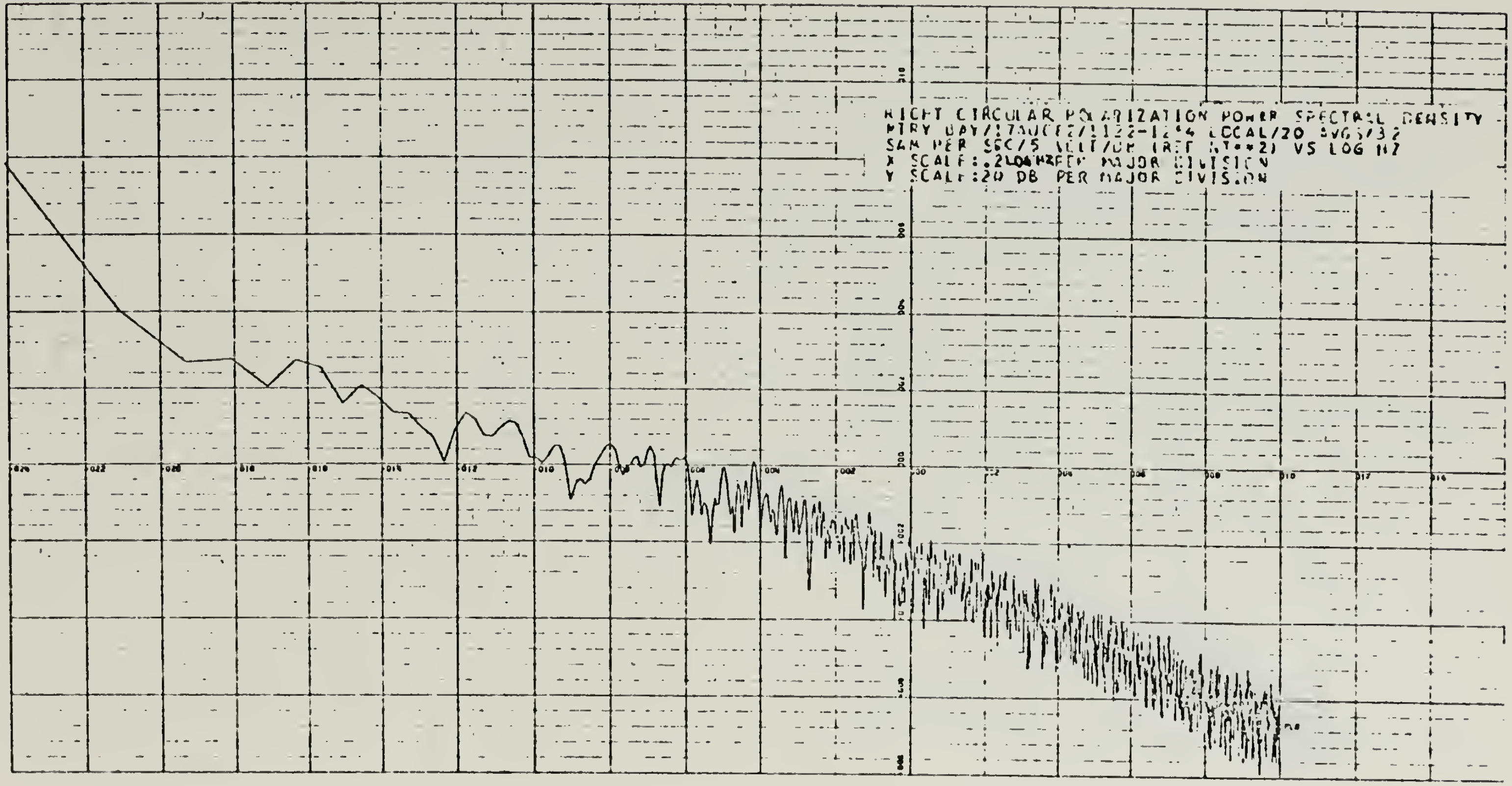

Figure D.9 Right Circular Polarization Power Spectral Density, Mtry Bay, 17 Aug. 82, 1122-1254 Local

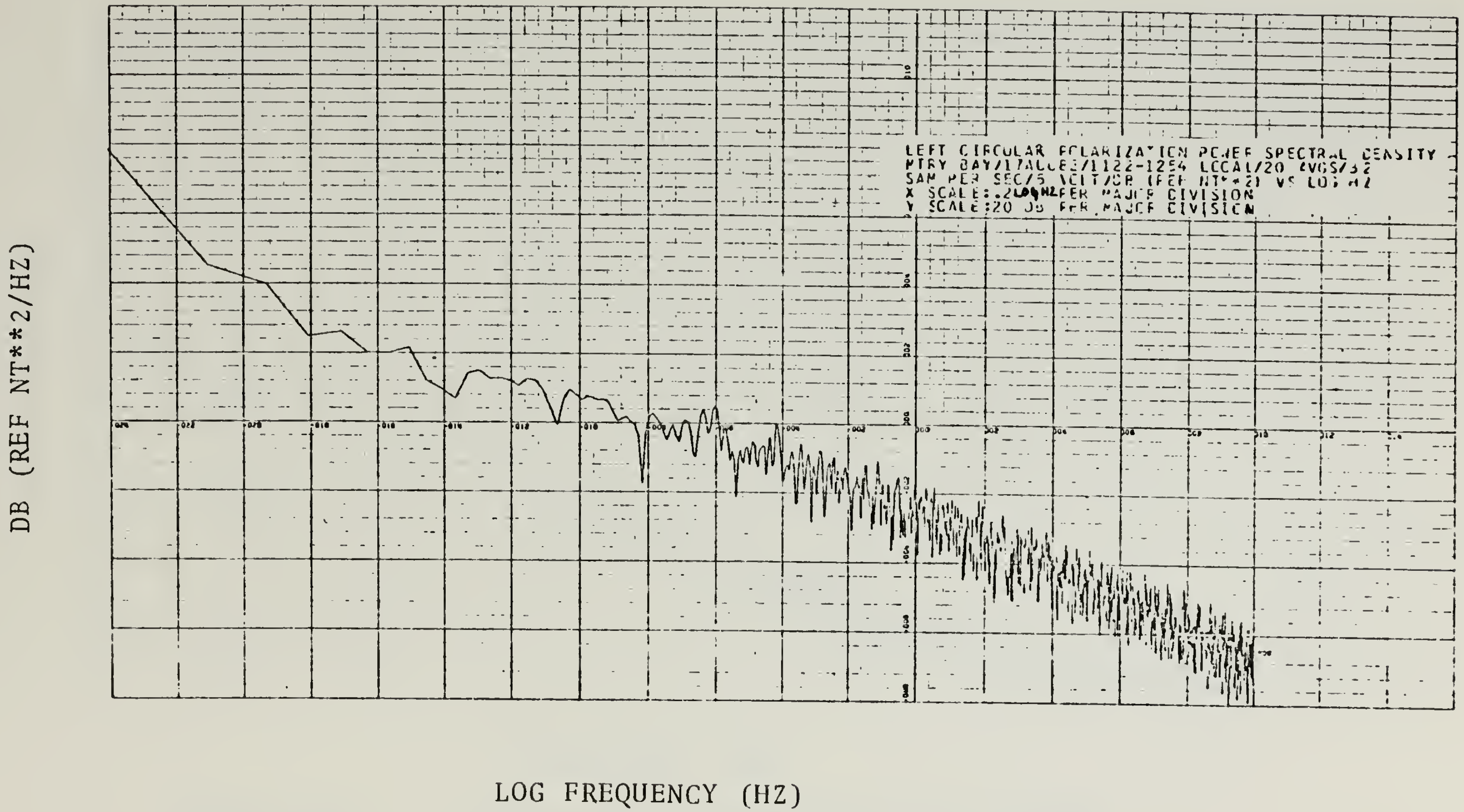

Figure D.10 Left Circular Polarization Power Spectral Density, Mtry Bay, 17 Aug. 82, 1122-1254 Local

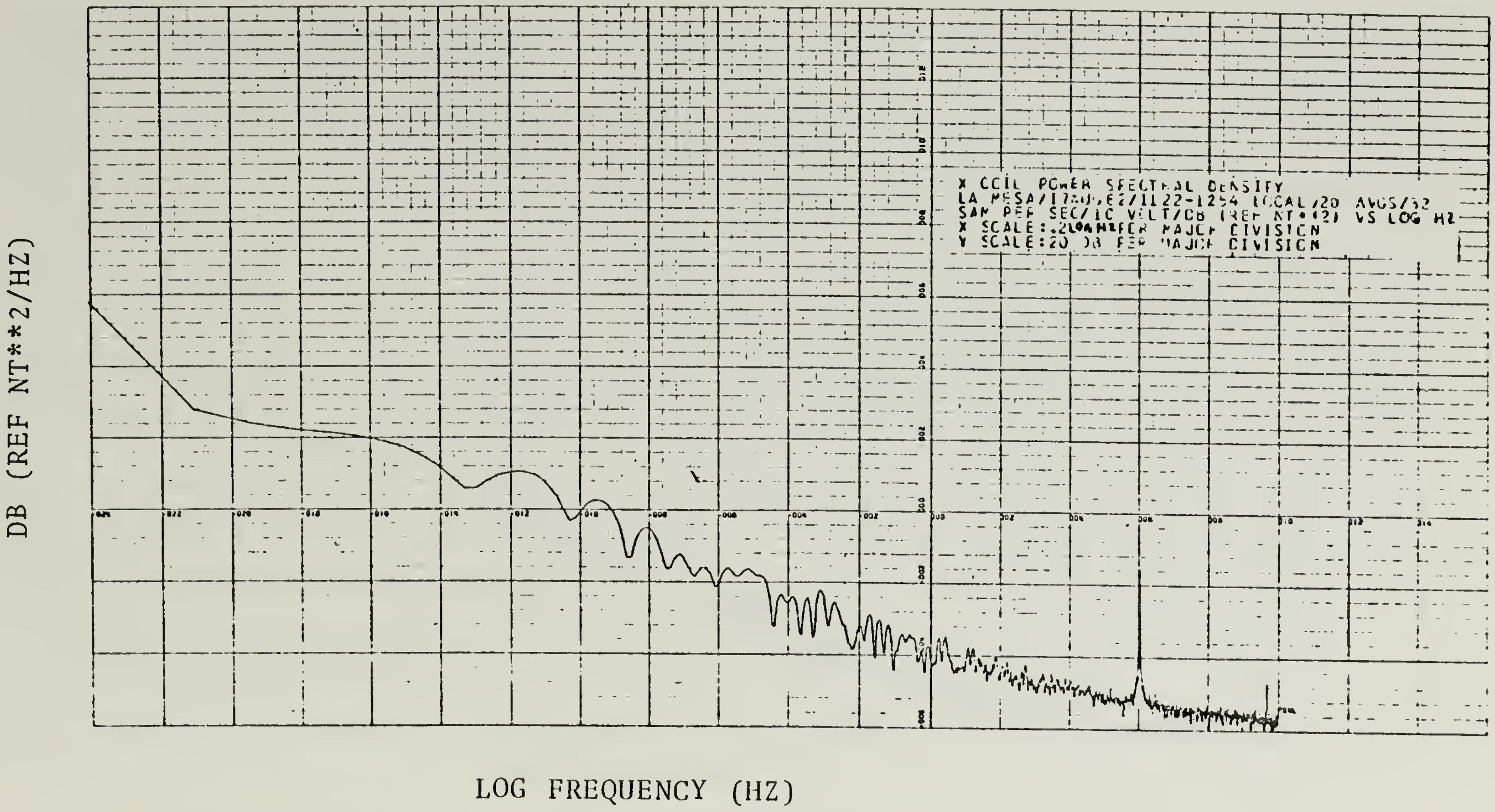

Figure D.11 x Coil Power Spectral Density, La Mesa, 17 Aug. 82, 1122-1254 Local

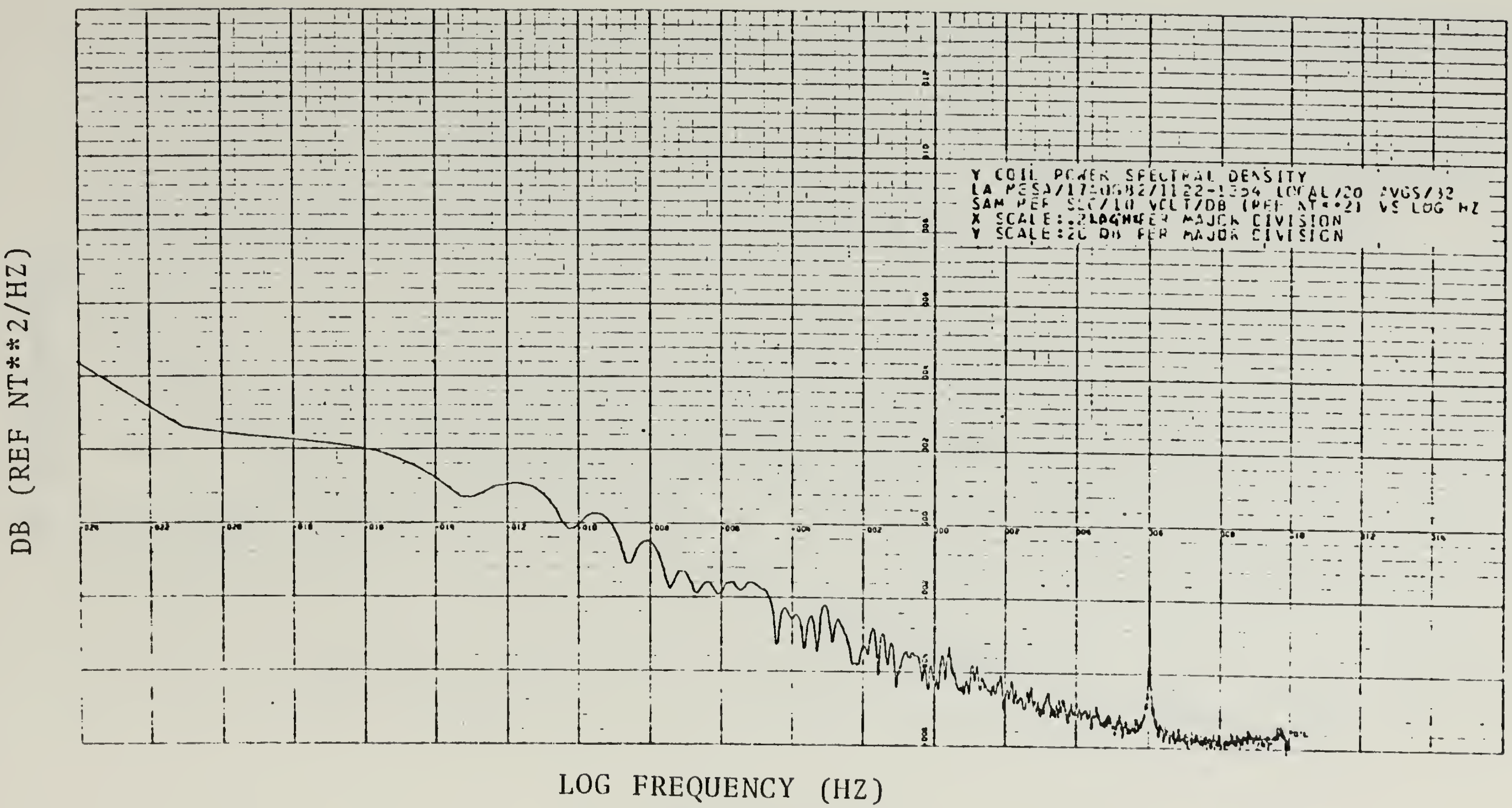

Figure D.12 y Coil Power Spectral Density, La Mesa, 17 Aug. 82, 1122-1254 Local

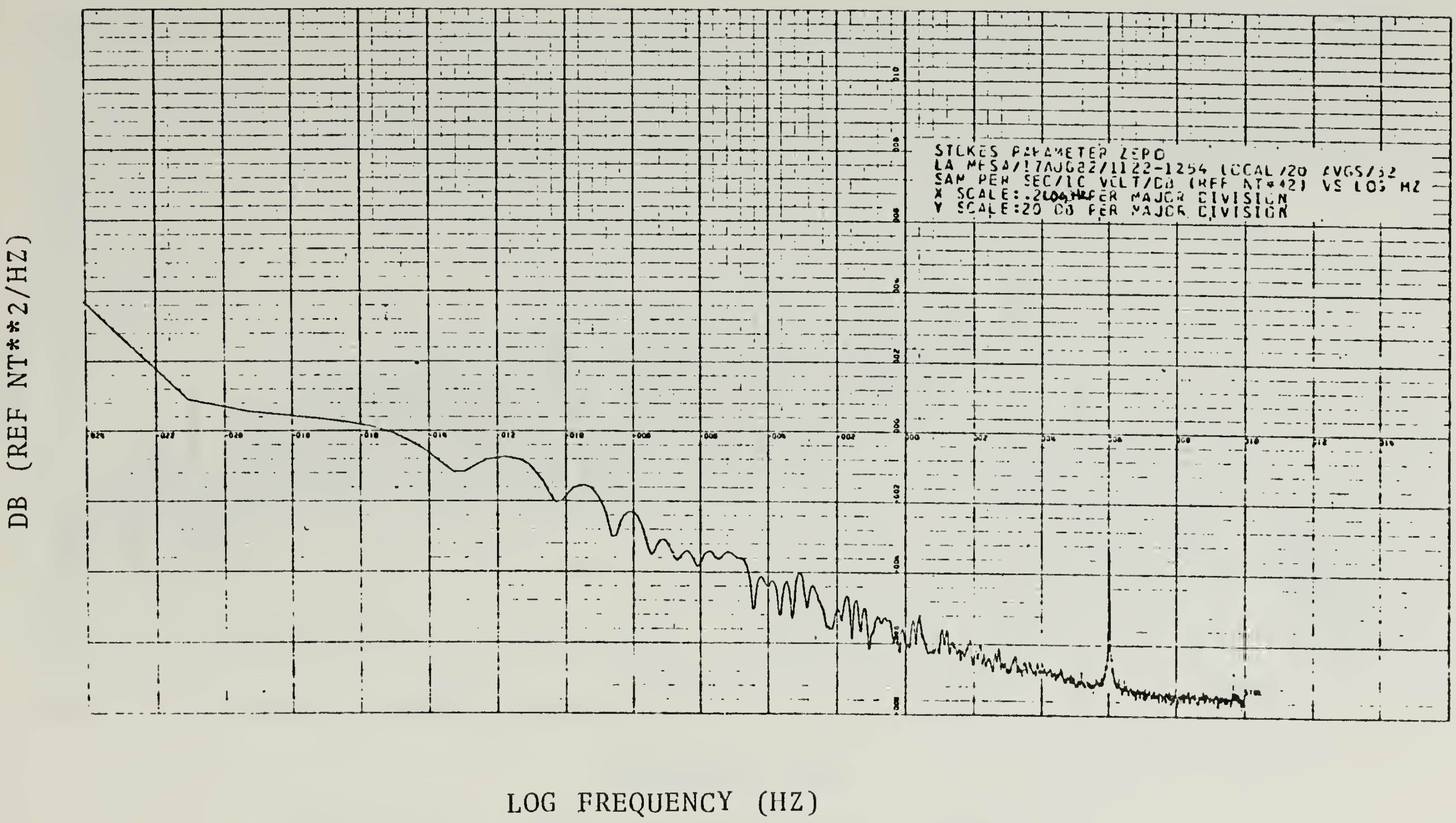

Figure D.13 Stokes Parameter Zero, La Mesa, 17 Aug. 82, 1122-1254 Local

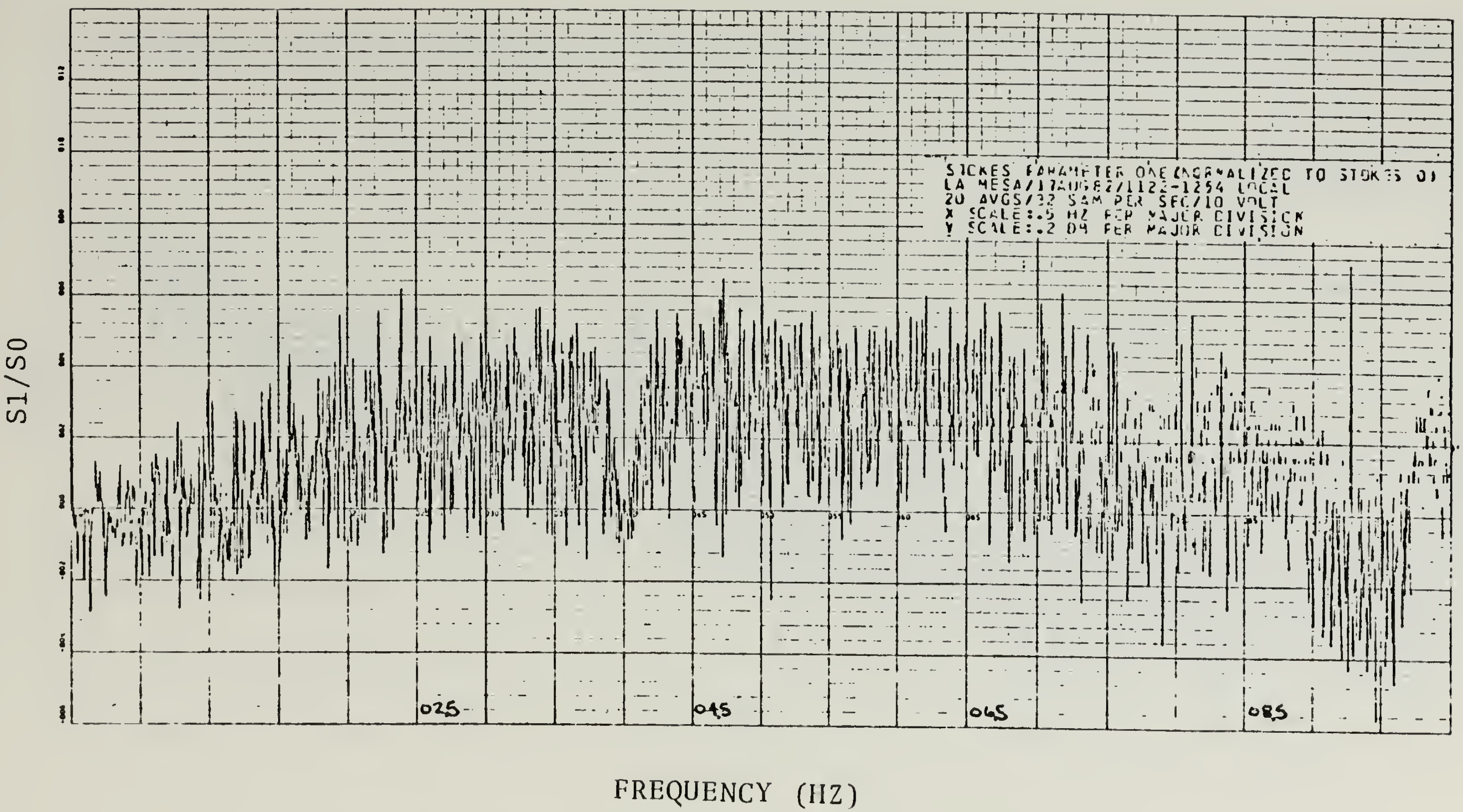

Figure D.14 Stokes Parameter One, La Mesa, 17 Aug. 82, 1122-1254 Local

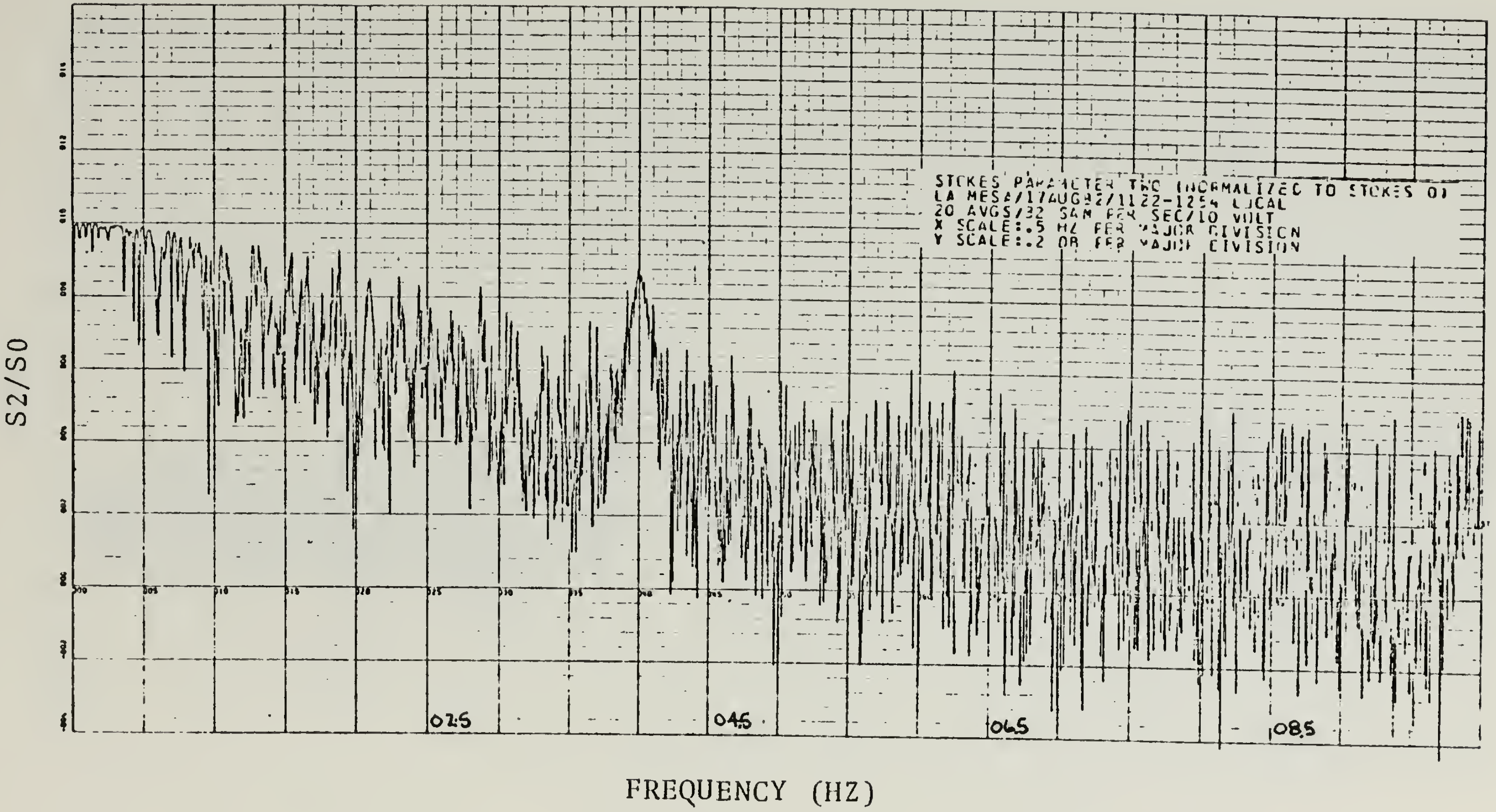

Figure D.15 Stokes Parameter Two, La Mesa, 17 Aug. 82, 1122-1254 Local

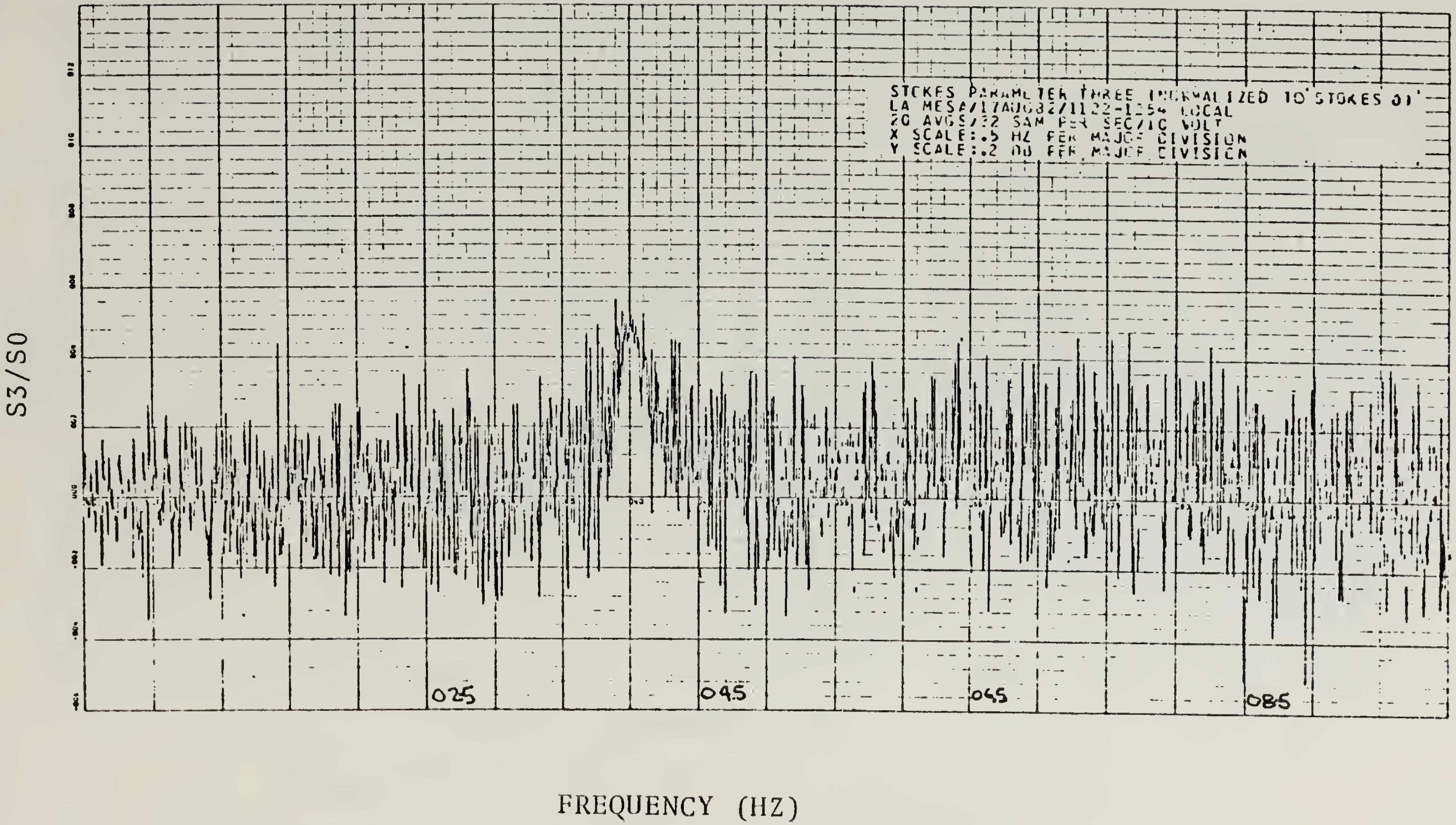

Figure D.16 Stokes Parameter Three, La Mesa, 17 Aug. 82, 1122-1254 Local

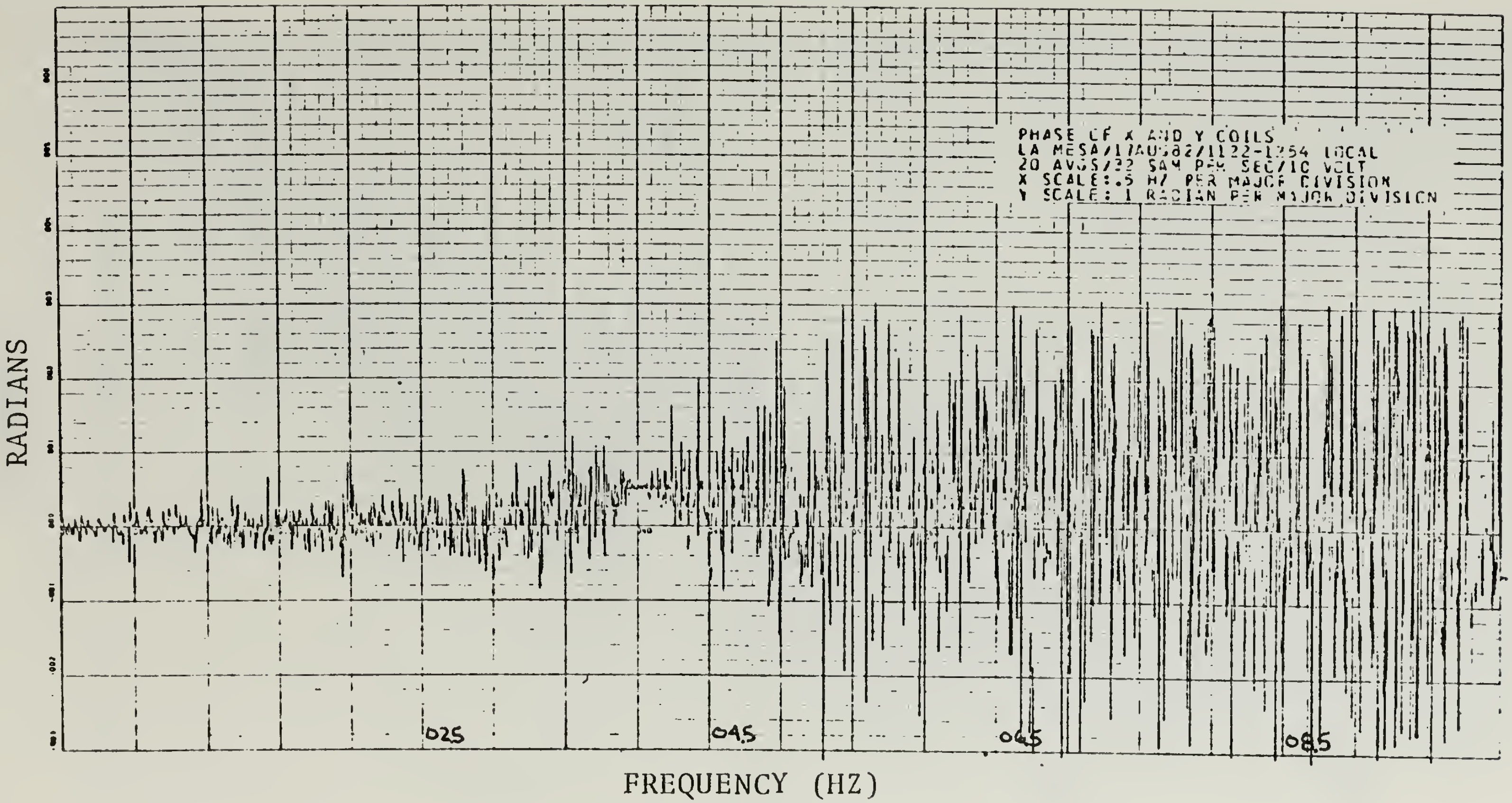

Figure D.17 Phase of x and y Coils, La Mesa, 17 Aug. 82, 1122-1254 Local

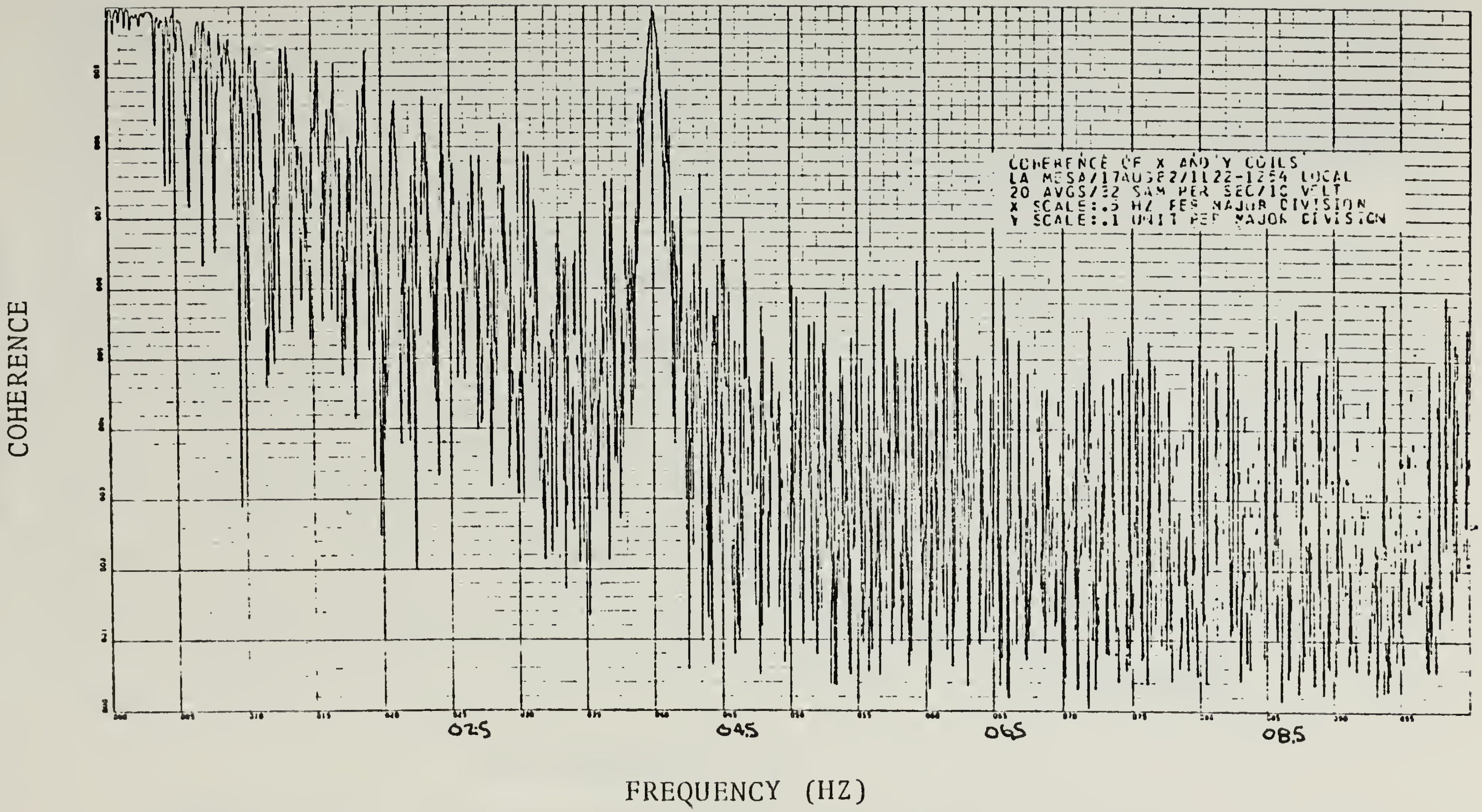

Figure D.18 Coherence of x and y Coils, La Mesa, 17 Aug. 82, 1122-1254 Local

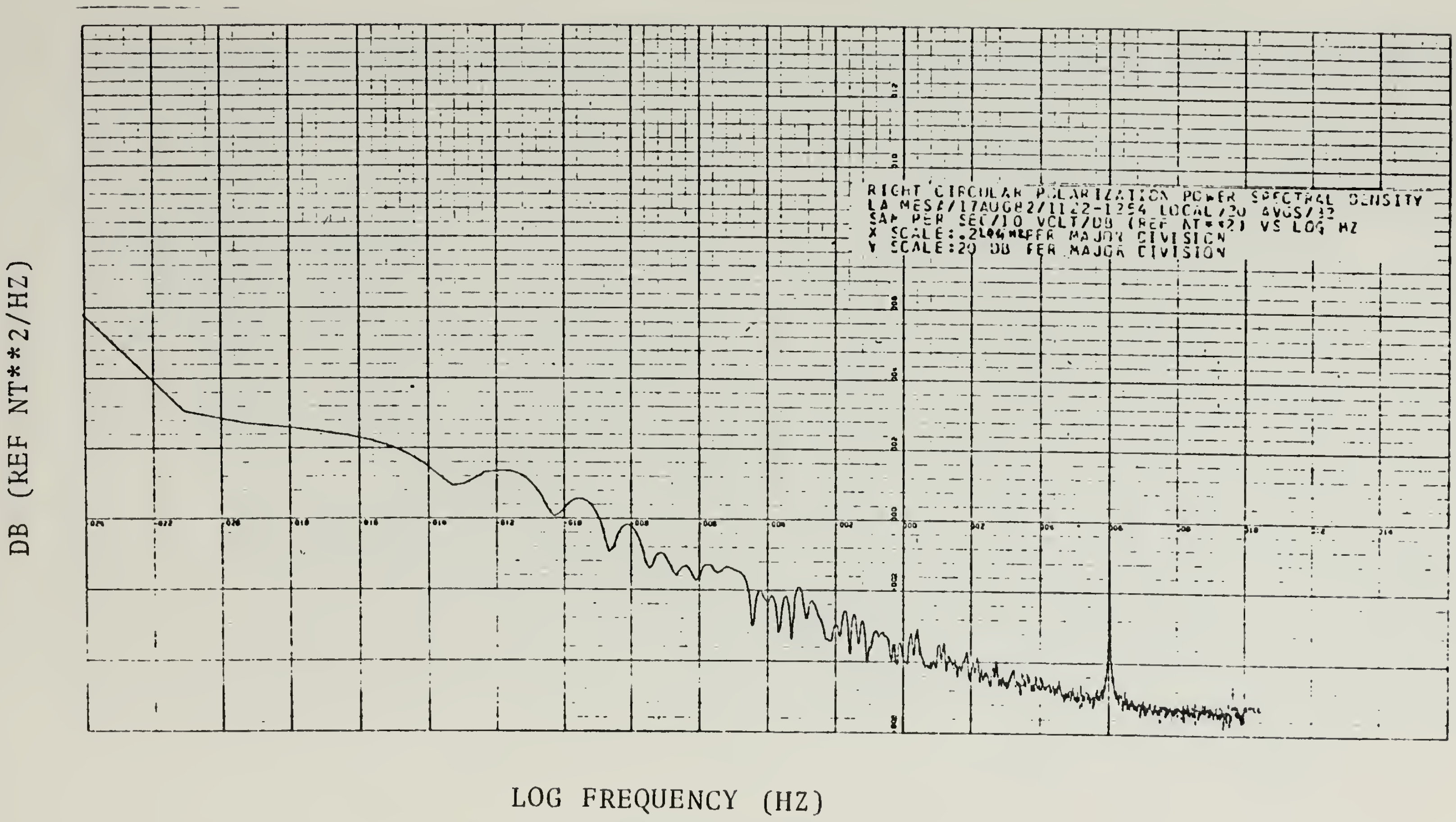

Figure D.19 Right Circular Polarization Power Spectral Density, La Mesa, 17 Aug. 82, 1122-1254 Local

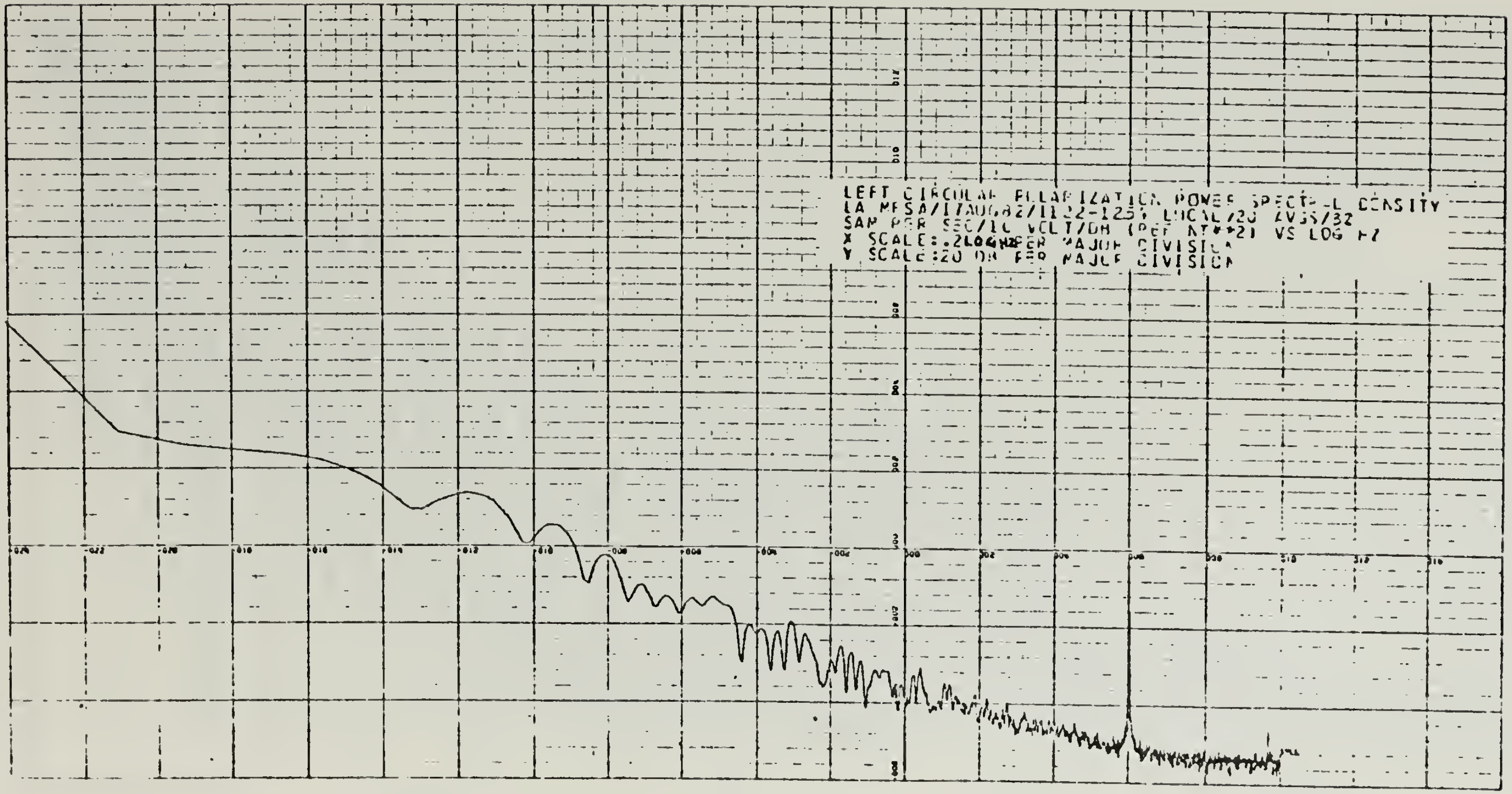

Figure D.20 Left Circular Polarization Power Spectral Density, La Mesa, 17 Aug. 82, 1122-1254 Local

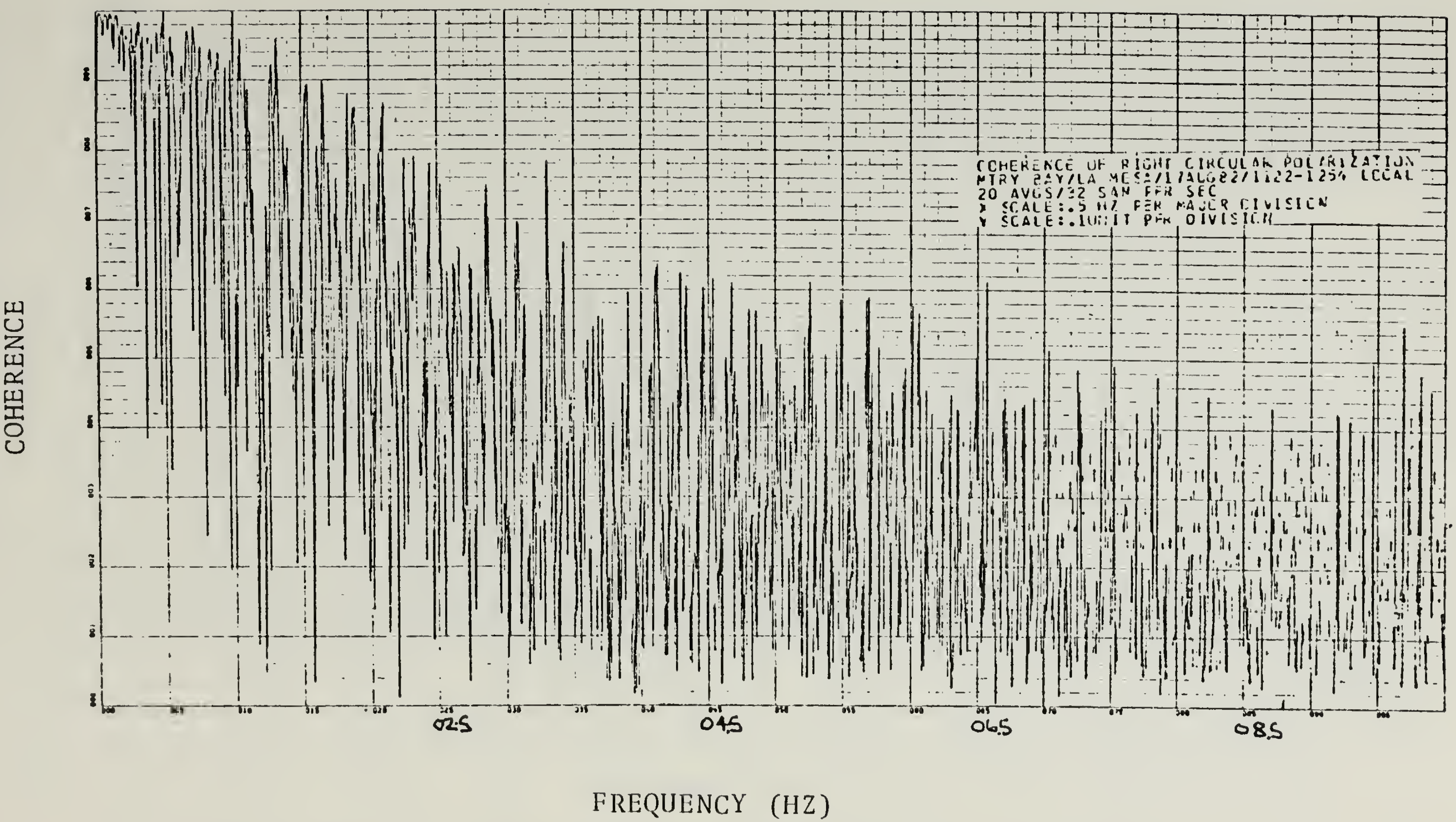

Figure D.21 Coherence of Right Circular Polarization, Mtry Bay/La Mesa, 17 Aug. 82, 1122-1254 Local

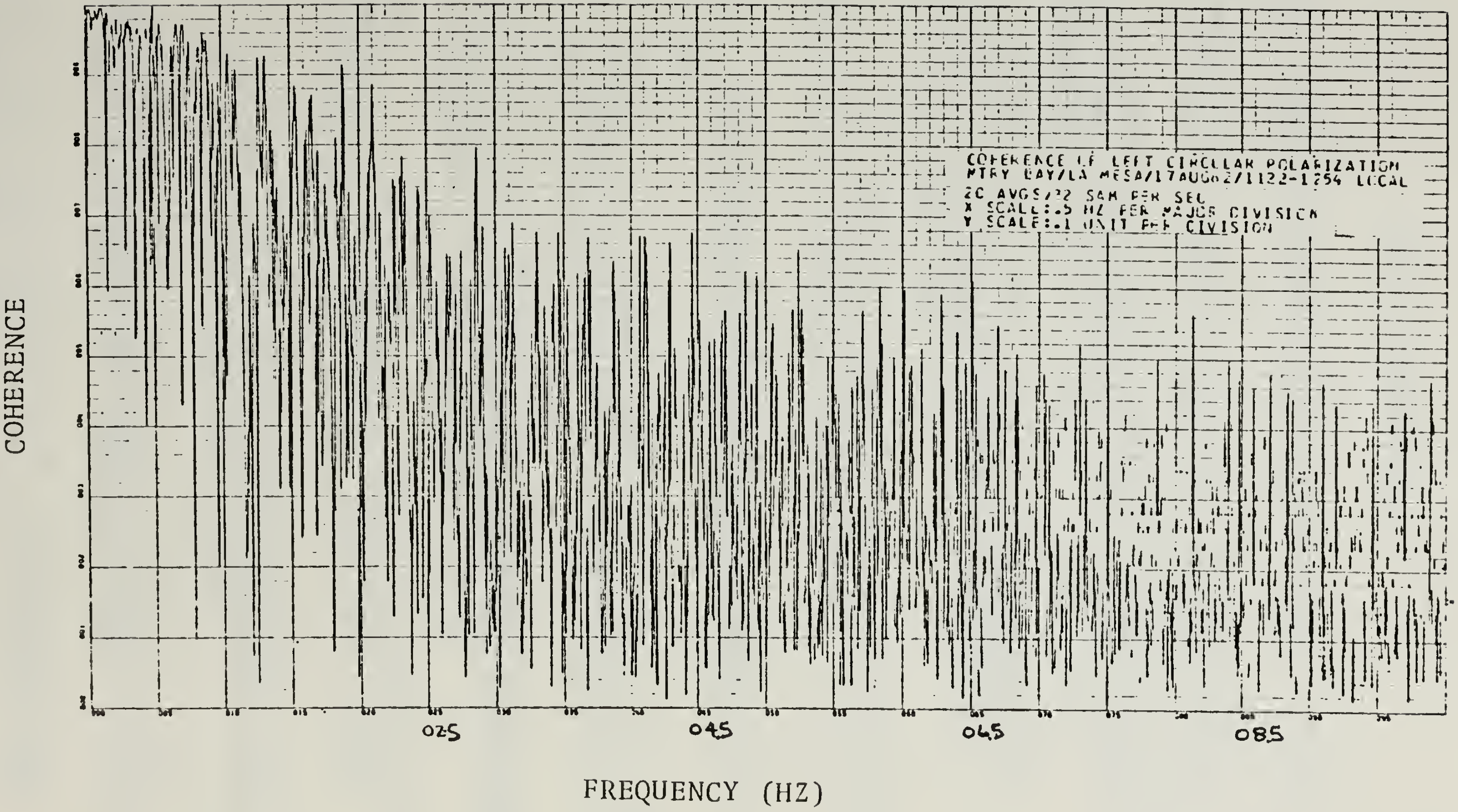

Figure D.22 Coherence of Left Circular Polarization, Monterey Bay/La Mesa, 17 Aug. 82, 1122-1254 Local

LIST OF REFERENCES

1. Jacobs, J. A., *Geomagnetic Micropulsations*, Springer, New York, 1970.

2. Carrigan, C. R., Gubbiner, D., "The Source of the Earth's Magnetic Field," *Scientific American*, Feb. 1979.

3. Air Force Cambridge Research Laboratories, L. G. Hanscom Field, Bedford, Massachusetts, Report AFCRL-72-0570, *The Geomagnetic Field*, by David J. Knecht, 1972.

4. Nagata, Takesi, and Ozina, Minoru, *Paleomagnetism*, pp. 103-180 in *Physics of Geomagnetic Phenomena*, Matmshita, S., and Campbell, W. H., editors, Academic Press, New York, 1967.

5. Inglis, D. R., "Dynamic Theory of the Earth's Varying Magnetic Field," *Review of Modern Physics*, V. 53, p. 481, July 1981.

6. Jacobs, J. A., *Physics and Chemistry in Space*, Vol. I, Roederer, Denver and Zahringer, Springer-Verlag, New York, 1970.

7. Fraser-Smith, A. C., "Short-Term Prediction and a New Method of Classification of PC 1 Pulsation Occurrences," *Planet Space Science*, V. 28, pp. 739-747, 1980.

8. Chaffee, E. J., *Low Frequency Geomagnetic Fluctuations (0.1 to 3 Hz) on the Floor of Monterey Bay*, M.S. Thesis, Naval Postgraduate School, Monterey, 1979.

9. Schumann, W. D. and Konig, H., "Ueber die Beobachtung von Atmospherics bei geringsten Frequenzen," *Natur-wissen-schafflen*, V. 41, p. 183, 1954.

10. Weaver, J. T., "Magnetic Variations Associated with Ocean Waves and Swell," *Journal of Geophysical Research*, V. 70, No. 8, pp. 1921-1929, April 1965.

11. U. S. Navy Mine Defense Laboratory Report No. 2743, *A Study of the Electric and Magnetic Fields of Ocean Waves*, by J. Wynn and H. W. Trantham, 1968.

12. Johnson, R. B. and Gritzke, A. R., *Ocean Floor Geomagnetic Data Collection System*, M.S. Thesis, Naval Postgraduate School, Monterey, 1982.

13. Jackson, J. A., Classical Electrodynamics, Wiley, New York, 1975.

14. Born, M., Wolf, E., Principles of Optics, Pergamon Press, New York, 1970.

15. Brigham E. O., The Fast Fourier Transform, Prentice-Hall, Englewood Cliffs, 1974.

16. Clayton, F. W., Power Spectra of Geomagnetic Fluctuations between .4 and 40 Hz, M.S. Thesis, Naval Postgraduate School, Monterey, 1979.

INITIAL DISTRIBUTION LIST

		No. Copies
1.	Defense Technical Information Center Cameron Station Alexandria, Virginia 22314	2
2.	Library, Code 0142 Naval Postgraduate School Monterey, California 93940	2
3.	Dr. Otto Heinz, Code 61 Hz Department of Physics Naval Postgraduate School Monterey, California 93940	2
4.	Dr. Andrew R. Ochadlick, Jr., Code 610c Department of Physics Naval Postgraduate School Monterey, California 93940	2
5.	Dr. Paul Moose, Code 62Me Department of Electrical Engineering Naval Postgraduate School Monterey, California 93940	1
6.	Dr. Michael Thomas, Code 61 Department of Physics Naval Postgraduate School Monterey, California 93940	1
7.	Dr. John Powers, Code 62Po Department of Electrical Engineering Naval Postgraduate School Monterey, California 93940	1
8.	Dr. A. C. Fraser-Smith Radio Science Laboratory Stanford Electronics Laboratories Stanford University Palo Alto, California 94305	1
9.	Dr. David M. Bubenik Assistant Director Electromagnetic Sciences Laboratory SRI International 333 Ravenswood Avenue Menlo Park, California 94025	1

10.	Dr. Robert N. McDonough, 8-368 The Johns Hopkins University Applied Physics Laboratory Johns Hopkins Road Laurel, Maryland 20801	2
11.	Chief of Naval Research, Code 100C1 Department of the Navy 800 North Quincy Street Arlington, Virginia 22217	1
12.	Chief of Naval Research, Code 414 Department of the Navy 800 North Quincy Street Arlington, Virginia 22217	1
13.	Chief of Naval Research, Code 420 Department of the Navy 800 North Quincy Street Arlington, Virginia 22217	1
14.	Mr. William Andahazy Naval Ship Research and Development Center Annapolis Laboratory Annapolis, Maryland 21402	1
15.	LCDR Joseph Timothy Fisher USS Towers (DDG-9) FPO San Francisco 96601	1